MECHANICAL PROPERTIES OF DENTAL RESIN COMPOSITE CAD/CAM BLOCKS

by

Ian Thornton

B.Sc., The University of Ottawa, 1996
D.D.S., The University of Western Ontario, 2005

A THESIS SUBMITTED IN PARTIAL FULFILLMENT OF

THE REQUIREMENTS FOR THE DEGREE OF

MASTER OF SCIENCE

in

THE FACULTY OF GRADUATE AND POSTDOCTORAL STUDIES

(Craniofacial Science)

THE UNIVERSITY OF BRITISH COLUMBIA

(Vancouver)

August 2014

Abstract

Objective: The goal of this study was to determine the flexural strength (σ_f), flexural modulus (E_f) and fracture toughness (K_{IC}) of two new commercially available nano-ceramic resin composite CAD/CAM blocks (Lava Ultimate CAD and Enamic CAD) and compare them to those of a widely-used ceramic CAD/CAM block (IPS e.max CAD), that served as a control, in order to evaluate the clinical suitability of the former.

Materials and Methods: Fifty bars of Lava Ultimate and Enamic and 25 bars of e.max were made for 3-point bending testing (to determine σ_f and E_f). Testing was completed on an Instron machine whereby a force was applied at a constant crosshead speed of 1 mm/min until failure occurred. Twenty-four 6x6x6x12 mm equilateral triangular prisms were fabricated from Lava Ultimate and >Enamic and 12 from e.max and fracture toughness (K_{IC}) was determined using the notchless triangular prism specimen (NTP) K_{IC} test. Half of the prepared Lava Ultimate and Enamic samples were stored in 37°C water for 30 days prior to testing, to analyze the effect of aging. Weibull statistics were used to evaluate the characteristic strength and the reliability of each material. Two-way ANOVA followed, if warranted, by multiple means Scheffé comparisons was used to further analyze the results.

Results: The σ_f, E_f and K_{IC} of Lava Ultimate and Enamic were considerably lower than that of IPS e.max CAD. Additionally, aging of Lava Ultimate and Enamic samples lowered the σ_f by 27 % and 12 % but increased the K_{IC} by 10 % and 40 %, respectively. Aging also significantly lowered E_f of both Lava Ultimate and Enamic samples. The σ_f of Enamic was statistically

significantly lower than that of Lava Ultimate, while the E_f of Enamic was statistically significantly higher. Only in the aged samples were significant differences between K_{IC} detected.

Conclusion: When compared to conventional resin composites, the presence of ceramic nano-particles in Lava Ultimate and Enamic did not greatly improve σ_f or K_{IC} of these materials. However, the flexural modulus of Enamic was greatly improved to levels not seen before in dental resin composites. Even so, although this finding necessitates future research, the mechanical properties of these materials do not approach the values seen those of dental ceramics. Therefore, based on the mechanical testing results obtained in this study, their consideration and clinical use should be similar to that of conventional dental resin composites.

Preface

This project was researched, all samples were prepared and the dissertation was written without collaboration, apart from the help obtained from my supervisor, Dr N.D. Ruse. He provided his expertise with the testing of the samples in addition to the statistical analysis. This research project did not require ethics board approval.

Table of Contents

List of Tables

List of Figures

List of Equations

List of Abbreviations

σ_f - Flexural strength

E_f - Flexural modulus

K_{IC} – Fracture toughness

PICN – Polymer infiltrated ceramic network

NCRC – Nano-ceramic resin composite

CAD – Computer aided design

CAM – Computer aided manufacturing

CEREC - Chairside economical restorations of esthetic ceramics

SEM – Scanning electron microscope

NTP – Notchless triangular prism specimen

SENB – Single edged notched beam

CNSR – Chevron notched short rod

Acknowledgements

This project is the culmination of my student academic career and it would not have been possible without the kind support and help of many individuals. I would like to extend my sincere thanks to all of them.

To Paul Sills, former Professor Emeritus at the Schulich School of Dentistry, mentor and friend. I express my gratitude for both instilling in me a passion for prosthodontics but also having the confidence in me that I would be successful if I chose to follow your path. You have always been a role model as a clinician and a teacher whose attributes and career I strive to emulate. You are truly missed.

To Dr. N. Dorin Ruse, Professor and Chair of the Department of Biomaterials, University of British Columbia, my teacher, supervisor and friend. I am indebted to you for your guidance, wisdom and passion that were integral in the completion of this project. Your office door was always open and with that, you had the innate ability to be able to provide a sympathetic ear, a motivational speech or simply a friendly conversation as needed to keep this project on track. As a result of your unwavering support, I have memories that will last a lifetime. It was truly my privilege to complete this project under your supervision.

To Dr. Caroline Nguyen, Assistant Professor and Dr. Ricardo Carvalho, Professor, Department of Oral Health Sciences, University of British Columbia, and members of my research committee. I thank you for your support and direction in the planning and establishment of the direction of this project.

To the Royal Canadian Dental Corps, my sponsors for my post graduate education. I thank you for both your financial support but also having the confidence in my success. I am honoured to serve alongside each and every one of you.

To my family and my wife's family. Your enduring love, help and support through the years have allowed me to follow my academic dreams. I am truly blessed to have such a wonderful family. You are my support structure and continue to guide my success. I deeply appreciate your generosity, thoughtful words and sound advice and I could not have made it through all these years of school without your encouragement.

To my dearest wife and soul mate, Erin Thornton. This project and these past three years would not have been possible without you. You provided me with the space when I needed to work, the assistance as required as I struggled through aspects of this project and my program that are not your area of expertise and an unending love throughout this journey. The long hours/days while attending classes/clinics were truly difficult and you kept the foundation of our family strong. You have been with me throughout all these years and have truly made them the best years of my life. I owe you everything.

Dedication

This thesis and my accomplishments over the past three years of graduate training are dedicated to my family and specifically, my wife and adorable children, Sykora, Alyssa and Noah. Your smiling faces and unconditional love gave me something to look forward to at the end of each and every long day and constantly inspire me to be a better person. You are my life.

Chapter 1: Introduction

The art and science of dentistry is always evolving, allowing for multiple treatment options being available to satisfy patient demands. In many offices (and even countries), dental amalgam has become taboo and the shifting standard towards resin composite restorations combined with patients' desires for natural looking restorations, even in the posterior region of the mouth, has led to the growth of aesthetic dentistry (Miyazaki et al, 2009; Manhart et al, 2000; Rekow and Thompson, 2005; Yin et al, 2006; Nguyen et al, 2012). New materials development over the years has had to evolve with this dental paradigm shift to ensure that, when utilized intraorally, these materials are able to withstand the functional demands placed upon them. Additionally, the emerging treatment philosophy of minimally invasive dentistry, which aims to preserve as much tooth structure as possible, has further challenged the mechanical limits of restorative dental materials.

Throughout dental history, materials science and dental processing technology have been closely related to intraoral restorations and dental prostheses fabrication. As the level of innovation in material development continues, the quest to develop next-generation materials that outperform their predecessors can ideally only benefit the profession and, ultimately, the patient. Concomitantly, the evolution of computer aided design and manufacturing (CAD/CAM) over the past thirty years has seen an unprecedented development of new materials, treatment modalities and prosthesis manufacturing processes. At the current rate of expansion, reliable and time-tested systems such as the lost wax technique, used in the traditional manufacturing of crowns and bridges, may truly become lost. CAD/CAM technology has advanced to a point where it provides dentists with a wide range of versatile restorative options both chair-side and via a traditional dental laboratory. This technology has become predictable and effective in

compensating for changes in dimensions that come with milling different materials with known processing shrinkages to obtain ideal and precise fit of crowns and fixed partial dentures to abutment teeth (Miyazki et al, 2009). Commercial chair-side dental CAD/CAM systems have expanded and improved their accuracy and precision to allow the ability for a dentist to provide esthetic all-ceramic restorations in one short appointment. Furthermore, the use of resin composites has expanded from simply a direct restorative material to industrialized composite blocks that can be milled in CAD/CAM systems for the fabrication of indirect restorations (Miyazaki et al, 2009). However, in general, resin composites have inferior mechanical properties when compared to traditional dental ceramics (Nguyen et al, 2012), yet the machinability of dental ceramics is not ideal as they tend to chip during the milling process and the propagation of machining-induced damage shortens the lifetime of the prosthesis remarkably (Rekow and Thompson, 2005; Yin et al, 2006). As becomes evident, the lack of a universal restorative material, one that can aesthetically match the tooth structure being replaced, possesses mechanical properties similar to both enamel and dentin as required, and withstands the harsh oral environment, still prevails.

Lava Ultimate, a recently introduced nano-ceramic resin composite (NCRC) from 3M ESPE and Enamic, a similarly classified NCRC from Vita, claim to bridge these deficiencies effectively. 3M ESPE claims that "like a composite, this material is not brittle, it is fracture resistant and like a glass ceramic, has excellent polish retention for lasting esthetics" (3M ESPE product sheet, 2012). However, prior to in-vivo use, the material properties must be confirmed and compared to the properties of materials that have been shown to produce effective and durable restorations. This can then serve as the foundation for one's evidence-based material selection when treating the demands of aesthetically driven patients.

1.1 Computer Aided Design/Computer Aided Manufacturing

Computer aided design/computer aided manufacturing (CAD/CAM) has evolved into dentistry from its revolutionary introduction in the machining industry in the 1960's. Initially developed for the aviation and automotive industries, it began to make its way into dentistry in the 1970s (McLaren, 2011). Both in other industries and dentistry, the advent and improvements noted via the implementation of CAD/CAM methodologies have both reduced material costs and technical time while at the same time, dramatically improving productivity.

Myazaki et al outlined that the development of dental CAD/CAM systems had to overcome four limitations that did not necessarily exist in other manufacturing industries. These were that the operation time/manipulation of these systems had to be at least as productive, practical and of equal and/or higher quality than established systems; morphology of adjacent teeth, abutment teeth (especially the delicate margins) and opposing teeth must be accurately digitized prior to restoration fabrication; numerical representation of the shape of crowns and FPDs is complex and cannot be simply expressed via functional equations; and accurate processing and mechanical milling of sharp corners and narrow margins was difficult (Myazaki et al, 2009). Nonetheless, through the perseverance of some visionary practitioners, a new era of digital prosthodontics was launched.

1.1.1 History

The pioneer of dental CAD/CAM was François Duret who built an optical scanner that would make a digital impression of an abutment tooth, which was then transferred to a computer to design an appropriately contoured crown, which was then milled on a numerically controlled

machine. From his original work, he developed the Sopha system, a precursor and inspiration for future CAD/CAM systems (Myazaki et al, 2009).

Subsequently, following the path blazed by Dr. Duret, Werner Mormann and Marco Brandestini further improved the capabilities of the two dimensional optical impression to the point where a chairside optical impression was taken and a linked chairside milling machine would produce a ceramic restoration in a single visit. Named CEREC, an acronym for Chairside Economical Restorations of Esthetic Ceramics (Mormann, 2006), the innovative system revolutionized dentistry and once it was announced as being available for consumer use, it rapidly spread CAD/CAM to the dental profession (Davidowicz and Kotick, 2011).

The initial iteration of CEREC only permitted the same-day manufacturing of inlays and although this reduced both chairside and laboratory time, the anatomic morphology and occlusal contours were less than desirable (Mormann et al, 1989). Overcoming the difficulties of an intra-oral impression, subsequent generations of CAD/CAM systems "regressed" to utilizing a conventional impression and then either the subsequent stone cast or the impression itself was scanned to allow continuation of the digital workflow, as pioneered by the Procera system. Presently, the current CEREC system is in its fourth generation and although many improvements have been made as technology had advanced, it is still limited to essentially the fabrication of individual restorations. Figure 1 outlines the currently available workflows for dental CAD/CAM.

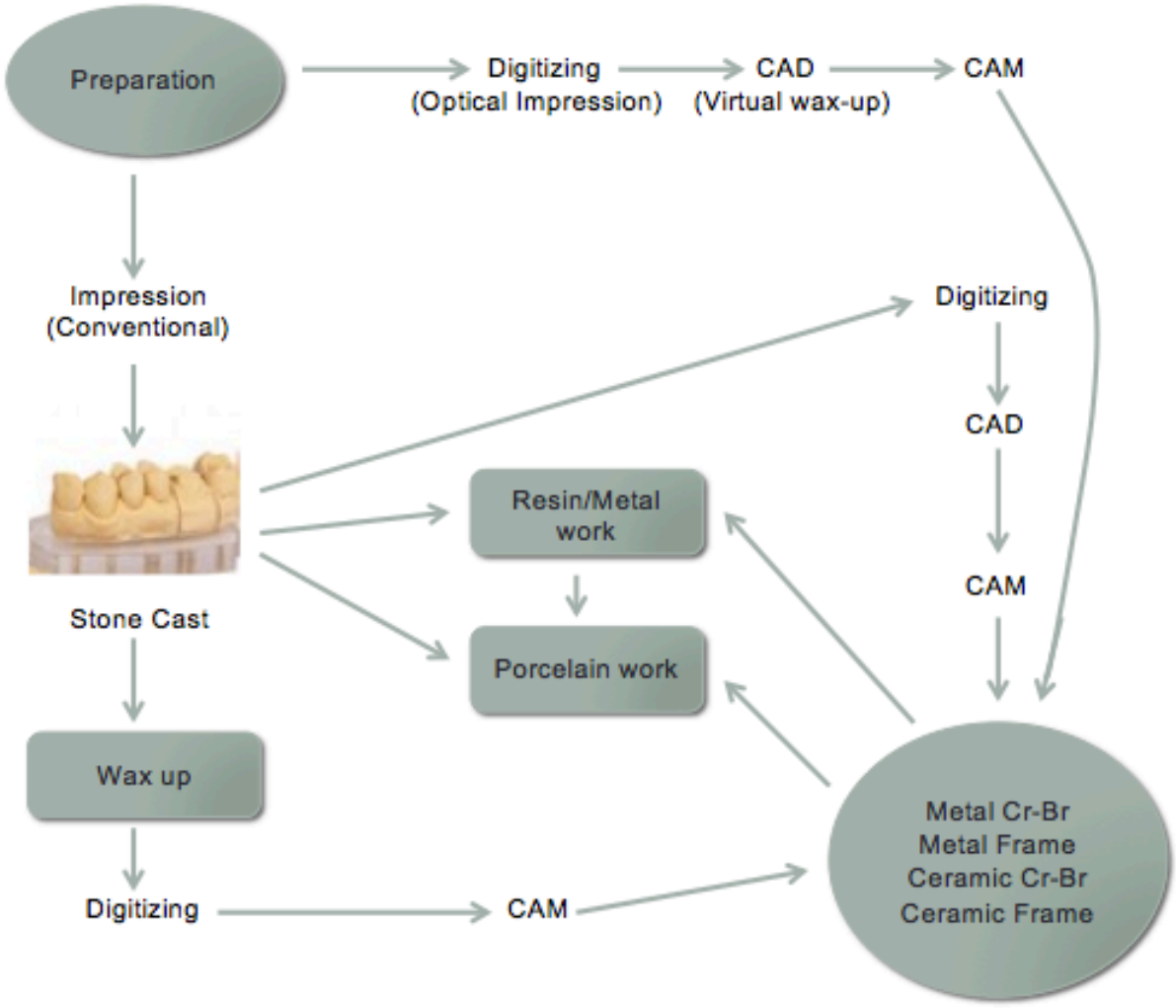

Figure 1: Digital CAD/CAM workflow (Miyazaki et al, 2009)

Much of the advancements of CEREC and other systems are entrenched in either the optical capture of the preparation/teeth and/or the milling process itself. In terms of optical capture, CEREC Blue Cam utilizes an LED blue light camera from which, via triangulation, a three dimensional reconstruction is made (Galhano et al, 2012). The iTero system (Align Technologies) utilizes parallel confocal imaging technology via the projection of 100000 beams of parallel red laser light and the reflection of these lasers is then converted into an optical image

(Galhano et al, 2012). Finally, Lava Chairside Oral Scanner (LAVA COS) utilizes 192 LEDs and 22 lens systems along with active wavefront sampling to capture the necessary information in video format (Davidowicz and Kotick, 2011). Typical accuracies of these systems have been reported in the 17 - 50 μm range depending on the investigation and the system being investigated (Ender and Mehl, 2010; Mehl et al, 2009; Galhano et al, 2012). This precision is easily comparable to the accuracies reported from conventional impressions. Presently, their limitations are related to operator ability/comfort with the intraoral scanner and the necessary use, in almost all systems, of titanium dioxide powder, which provides an excellent reflective optical coating, due to its high refractive index, but requires a steep learning curve with its use. Over-powdering or under-powdering of the preparation yields an inaccurate scan and thus, a less than ideal fitting prosthesis.

The advancements made in the milling realm specifically relate to the number of axes of milling. All chairside milling machines are limited to three axes (X, Y and Z) milling thus limiting the accuracy and precision of the restorations. Five axes milling systems are able to adjust the tension bridge as well as being able to rotate the milling spindle which, in addition to the aforementioned axes, permit the ability of milling more complex structures with increased accuracy, fit and precision (Khng, 2013).

These technological advancements, combined with the desires of many dentists to be able to provide advanced prosthetic solutions to their patients faster, has given rise to 30000 dentists worldwide having chairside milling units and, since the initial CEREC restoration in 1971, more than 15 million CEREC restorations being placed worldwide, with unknown numbers of others being developed fully or in part via the digital CAD/CAM process (Sirona internal data, 2008).

1.1.2 Material Options

With the expanding use of both in-office milling machines and in-lab digital design/manufacturing of prostheses, material development for these processes has had to progress concurrently. The initial restorations, as aforementioned, were limited to feldspathic porcelain inlays while currently, dental restorations are millable from many different ceramics, resin composites and metal materials. These newer CAD/CAM material options are thought to be advantageous due to their industrial production whereby they are manufactured in a standardized and tightly controlled environment thus producing a more dense and reliable structure than can be produced conventionally (Giordano, 2006).

1.1.2.1 Conventional Materials for Prosthetic Dentistry

Feldspathic porcelains are still used in the chairside CAD/CAM milling machines but their use is declining as materials with better mechanical properties have been developed. These include leucite-reinforced porcelains and lithium disilicate reinforced porcelains, which collectively, make up the biggest proportion of all chairside milled restorations (Giordano, 2006). Additionally, resin composite blocks have been available for use as definitive restorations. Initially, only Paradigm MZ-100, a 3M ESPE product that is essentially a polymerized block of their successful direct restorative resin composite Z-100, was the only available option. More recently, Trinia, a Bicon Implants product, has been introduced to the market. Fabricated via the multi-directional interlacing of fiberglass and resin composite into several layers, Trinia to this point, has been predominantly used on Bicon short implants with very limited case reports to substantiate its clinical use and success. A new "class" of nano-ceramic resin composite (NCRC) blocks has very recently been introduced by both 3M ESPE

(Lava Ultimate) and by VITA (Enamic). These materials, although from the same class of material and both with a resin matrix and ceramic fillers, are manufactured differently and therefore likely behave differently intraorally. Lastly, highly cross-linked polymethylmethacrylate blocks exist for provisional crown and bridge use, namely Telio CAD (Ivoclar Vivadent) and Vita CAD-Temp (VITA).

Laboratory milling systems tend to be more industrial, powerful and thus have more material milling options available to them. It allows the dentist to provide both alumina based restorations and zirconia based restorations that cannot be milled chairside due to their hardness (Fasbinder, 2010). Table 1 summarizes most of the available permanent restorative materials for CAD/CAM systems.

PERMANENT CAD/CAM DENTAL RESTORATIVE MATERIALS

ITEM	MATERIAL	MANUFACTURER	CLINICAL/ LAB
CEREC blocks	Feldspathic ceramic	Sirona	Both
Cercon Smart Ceramics	Zirconia based ceramic	DeguDent	Lab
Choron	Chrome cobalt	Straumann	Lab
inCoris Zi	Zirconia	Sirona	Lab
inCoris Al	Zirconium oxide + Aluminum oxide	Sirona	Lab
IPS Empress CAD	Leucite reinforced glass ceramic	Ivoclar Vivadent	Both
IPS Empress CAD Multi	Leucite reinforced glass ceramic	Ivoclar Vivadent	Both

ITEM	MATERIAL	MANUFACTURER	CLINICAL/ LAB
IPS e.max ZirCAD	Zirconia	Ivoclar Vivadent	Lab
IPS e.max CAD	Lithium disilicate	Ivoclar Vivadent	Both
KaVo Everest Zirconium	Zirconia	KaVo	Lab
Lava Crown and Bridge	Zirconia	3M Espe	Lab
Lava Ultimate	NCRC	3M Espe	Both
Paradigm C	Leucite reinforced glass ceramic	3M Espe	Both
Paradigm MZ 100	Resin composite	3M Espe	Both
ProCAD	Leucite reinforced glass ceramic	Ivoclar Vivadent	Lab
Procera	Zirconia oxide (partially sintered)	Nobel Biocare	Lab
TDS Titanium	Titanium	U-Best Dental Tech.	Lab
Vita Enamic	NCRC	Vident	Both
Vita In-Ceram Zirconia	Zirconia	Vident	Lab
Vita In-Ceram 2000 AL	Zirconium oxide + Aluminum oxide	Vident	Lab
Vita In-Ceram Alumina	Aluminous porcelain	Vident	Lab
Vita In-Ceram Spinell	Magnesium oxide	Vident	Lab
Vita Mark II Aesthetic	Feldspathic ceramic	Vident	Both
Vita YZ InVision	Yttria stabilized zirconia	Vident	Lab
VITABLOC Aesthetic Line	Feldspathic ceramic	Vident	Both
VITABLOC Triluxe	Feldspathic ceramic	Vident	Both

Table 1: Available materials for CAD/CAM systems (Giordano, 2009; Fasbinder, 2010)

1.1.2.2 Ceramic-Polymer Blocks

Collectively identified as NCRCs, they allegedly combine the positive characteristics of ceramics and resin composites, for maximum patient benefit. Specifically, it is claimed that the dual network of a ceramic and polymer material provides less brittleness, excellent machinability and edge stability, while maintaining excellent esthetics (Spitznagel et al, 2014).

1.1.2.2.1 Lava Ultimate

Lava Ultimate was introduced into the dental market in 2012 and was the original member of this new class of materials. It contains a blend of individually bonded nano-particles and nano-particles agglomerated in clusters, all embedded in a highly cross-linked polymer matrix. It is a combination of 0.6 – 1.0 μm aggregated zirconia/silica clusters (comprised of 20 nm silica and 4 - 11 nm zirconia particles); non-agglomerated/non-aggregated 20 nm silica nano-particles; and non-agglomerated/non-aggregated 4 to 11 nm zirconia nanoparticles. These are treated with a proprietary silane-coupling agent (in a proprietary process) to bond them chemically to the cross-linked polymer matrix (3M ESPE internal data, 2012). The formulation using both the nanomer and nanocluster fillers gives a total nanoceramic filler content of approximately 80 % by weight (3M ESPE internal data, 2012).

Figure 2, an internal 3M SEM image, shows the ceramic nanocluster formation and Figure 3 shows the Lava Ultimate CAD/CAM block prior to milling.

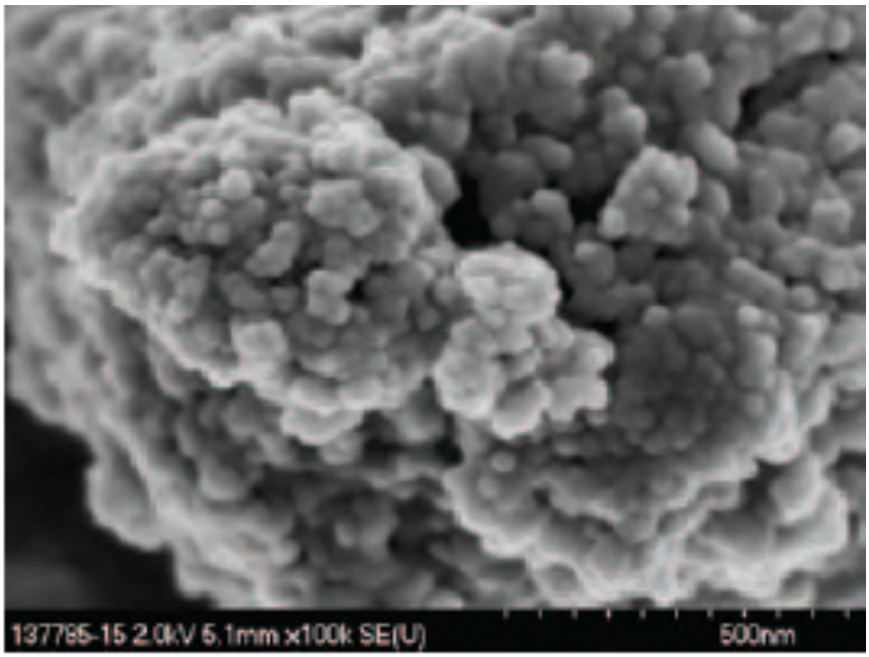

Figure 2: SEM image of Lava Ultimate nanocluster (3M ESPE internal data, 2012)

Figure 3: Lava Ultimate CAD/CAM block (3M ESPE internal data, 2012)

1.1.2.2.2 Enamic

Launched onto the market in 2013, Enamic has been called a "hybrid ceramic" or a polymer-infiltrated-ceramic network (PICN). Manufactured with a dual network structure,

Enamic is composed of a dominant porous ceramic network that is reinforced, via capillary action, with a polymer matrix (VITA internal data, 2013). The so-called double interpenetrating network is essentially a lattice-like feldspar ceramic matrix strengthened by a methacrylate polymer network that ensures both networks fully penetrate and integrate with each other (VITA internal data, 2013). The ceramic structure occupies 86 % by weight (VITA internal data, 2013).

Figure 4 shows an SEM image of the PICN network (Della Bonna et al, 2014) and Figure 5 shows the CAD/CAM block prior to milling.

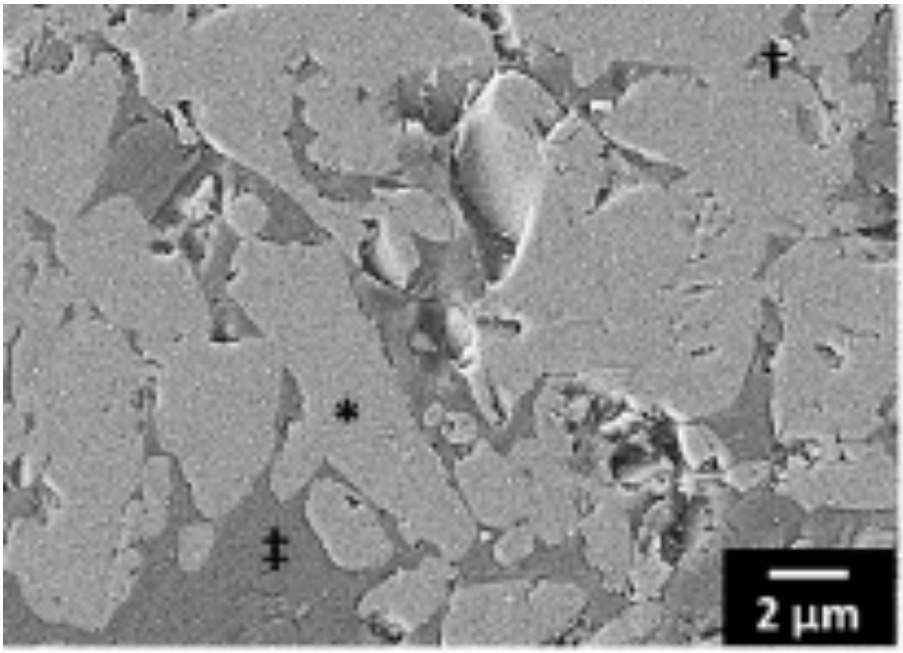

Figure 4: SEM image of Enamic double interpenetrating networks (Della Bona et al, 2014)

Figure 5: Enamic CAD/CAM block (Vita Internal data, 2013)

1.1.2.3 IPS e.max CAD

Ceramics are typically classified according to their fusing temperature, their major crystalline structure or their chemistry (Ho and Matinlinna, 2011). Thus, using the crystalline structure as the guide, IPS e.max CAD is classified as a lithium disilicate reinforced glassy ceramic. In general, aluminosilicates, which contain various amounts of potassium and sodium, are known as feldspars, which are then modified in some way to create the porcelains used in the dental industry. By using various filler particles that integrate into the nucleating precipitate as the glass is forming, improved mechanical properties in the material are achieved (Tysowski, 2009). By using the SiO_2-Li_2O system as crystalline filler, lithium disilicate ($Li_2Si_2O_5$) is formed (Ivoclar internal data, 2005). The unusual microstructure of many small interlocking, randomly oriented plate-like crystals create an impressively homogenous material that vastly improves the mechanical properties of this material when compared to other glassy (feldspathic) and reinforced (leucite) glassy ceramics (Tysowski, 2009; Mohsen, 2011).

IPS e.max CAD is produced via a pressure casting procedure that, according to the manufacturer, uses optimizing processing parameters to prevent the formation of defects (Ivoclar

internal data, 2005). Processed into an intermediate crystalline phase (blue state), the lithium disilicate crystals are precipitated following post-milling crystallization.

The microstructure of the blue state material consists of 40 % lithium metasilicate crystals embedded in a glassy phase and the fully crystallized microstructure consists of approximately 70 % by weight fine grain lithium disilicate crystals (Kelly and Benetti, 2011).

Figure 6 is an SEM image that shows the lithium disilicate microcrystalline structure of IPS e.max CAD while Figure 7 shows the blue state CAD/CAM prior to milling.

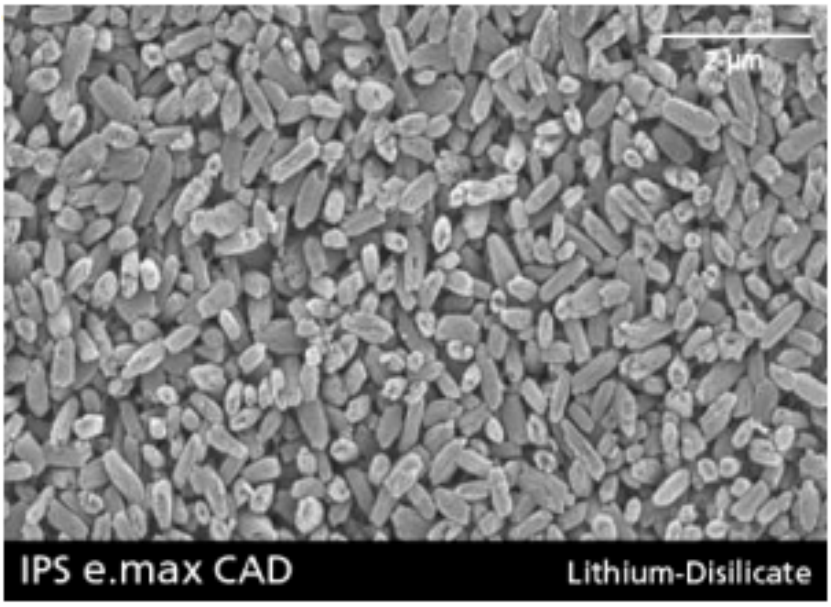

Figure 6: SEM image of e.max CAD lithium disilicate microcrystalline structure (McLaren and Cao, 2009)

Figure 7: IPS e.max CAD/CAM block (http://digital-dental-cadcam.com/ips-e-max-cad/)

1.1.2.4 Additional CAD/CAM Uses

CAD/CAM technology has also been expanded into the use of complete denture fabrication (Goodacre et al, 2012). A recent trial was done to evaluate the accuracy of CAD/CAM fabricated dentures and found that final prosthesis to have only 0.5 mm of error compared to the actual software design (Kanazawa et al, 2011). The company promoting this new technology, Dentca, claims that their advanced 3D software provides increased accuracy, creates more comfortable dentures for patients, and allows one to complete a full denture case 2.5 times faster (Dentca website).

Williams et al reported in 2006 on the first CAD/CAM chromium cobalt removable partial denture and found that the accuracy of the fit of the framework was on par or similar to results obtained by traditional cast processing (Williams et al, 2006). Subsequent authors have had similar success and today, many laboratories utilize CAD/CAM and similar rapid prototyping to design and manufacture such prostheses.

Orthodontic devices and implant superstructures are two additional areas where CAD/CAM has begun to establish itself (Miyazaki et al, 2009). Miyazaki further states that, "the application of CAD/CAM technology is promising in the delivery of high quality devices in all fields of dentistry" (Miyazaki et al, 2009).

1.1.2.5 Experimental CAD/CAM Materials

Nguyen et al have looked at the mechanical properties of various resin composites polymerized under high pressure and high temperature. In multiple studies of commercially available direct resin composites (Nguyen et al, 2013), of experimental UDMA based composite resins (Nguyen et al, 2012) and of resin-infiltrated ceramic networks (Nguyen et al, 2014), the authors found that the mechanical properties (namely fracture strength, hardness and fracture toughness) were significantly improved. They additionally found that fewer and smaller porosities existed which ultimately lead to decreased internal manufacturing flaws and thus a decreased propensity for failure thus producing increased reliability (Nguyen et al, 2013). Prepolymerized blocks of Paradigm MZ-100 have better properties than conventionally cured resin composites, however, when known direct restorative resins were instead polymerized under high temperature and high pressure, they exhibited superior mechanical properties to Paradigm MZ-100. This modified processing technique holds promise for improved resin based CAD/CAM materials that would allow the dentist to utilize the benefits of resin restorations without some of their known and limiting mechanical drawbacks.

1.1.3 CAD/CAM Advantages

Miyazaki lists the advantages of CAD/CAM in dentistry as the application of new materials, reduced labour, cost effectiveness and quality control (Miyazaki et al, 2009). Santos adds minimization of human error and patient satisfaction to this list (Santos et al, 2013). Davidowicz and Kotick, in a summary of the use of CAD/CAM in dentistry, list the purported advantages as speed, ease of use and increase in quality (Davidowicz and Kotick, 2011).

According to Miyazaki, CAD/CAM has allowed the profession to overcome difficulties in processing new materials and succeed in introducing new materials (Miyazaki et al, 2009). For example, utilization of yttria stabilized zirconia before/without CAD/CAM milling and precise control of the processing shrinkage, was impossible (Denry and Kelly, 2008; Denry and Holloway, 2010).

The clinical benefit of the ability to accurately and quickly remake prostheses upon demand, as the milling file is stored electronically, cannot be understated. Clinical complications, even when every precaution is taken, are unavoidable due to the unpredictability of both patients and the materials themselves. The ease of dealing with these complications that CAD/CAM affords is priceless.

Productivity is also increased via CAD/CAM on many accounts. Chairside milling units allow for the convenience of producing indirect restorations for patients in one visit, thus saving precious chair time, laboratory time and patient time (Davidowicz and Kotick, 2011). If lab based CAD/CAM systems are preferred, reduced production time is still possible in addition to the ability of milling multiple works in one machine at one time (Miyazaki et al, 2009). These facets combined vastly improve the productivity of this workflow as a whole.

Almost universal in listed advantages are the quality control of the material themselves, as they are fabricated in a standardized manner under standardized conditions. Furthermore, waste is avoided as errors are often detected in advance and can be immediately corrected prior to milling, thus minimizing the number of remakes (Miyazaki et al, 2009). The combination of improved mechanical properties of the material and improved manufacturing of the restoration with this material leads ideally to restorations with high success and survival (Fasbinder, 2006; Wittneben et al, 2009).

1.1.4 CAD/CAM Disadvantages

There are disadvantages as well with CAD/CAM dentistry. Santos et al list marginal adaptation, postoperative sensitivity and opposing tooth wear as the major concerns (Santos et al, 2013). Problems associated with marginal adaptation are directly related to the milling of a brittle material that has a tendency to chip, especially at the margin, as this area is the most delicate location (Yin et al, 2006). Initial comparisons however of the marginal integrity of crowns with different convergence angles found that there was no statistical difference in the marginal integrity of any group when compared to the conventional method (Nakamura et al, 2003). Additionally, numerous studies evaluated clinically the marginal integrity of some of the initial CEREC inlays. These studies found non-significant small differences versus those fabricated conventionally but still within the realm of what is deemed clinically acceptable (Denissen et al, 2000; Isenberg et al, 1992; Magnuson et al, 1991; Sjogren et al, 1998). Nonetheless, authors have found that material surface damage in the form of chipping occurs due to machining and that these defects can reduce the accuracy of fit and contribute to decreased mechanical properties over time (Tsitrou et al, 2007; Shearer et al, 1993; Frankenberger et al,

1998). Worse yet, in a review article, Denry concluded that milling ceramics with a diamond bur, as done in CAD/CAM machining, is directly correlated to an increase in failure-inducing flaws (Denry, 2013).

Another well-cited disadvantage of both the chairside and lab-based milling systems is the necessary outlay of initial costs. Beuer et al state that the high investment for machines might overextend the budget of smaller laboratories (Beuer et al, 2008). In terms of chairside CAD/CAM units, Mormann et al identify that the prohibitive cost of these units is definitely limiting and that dentists that do not have the necessary production volume will have a hard time both justifying the initial outlay of costs and paying off of these expenses over time (Mormann et al, 1989). Indirectly, in an effort to increase necessary volume and pay off this debt, this results in overtreatment and unnecessary procedures being provided to unsuspecting patients.

Currently, there is not an ideal intra-oral scanner that balances the ease of use with the desired accuracy of fixed prosthodontics. Controlling saliva, the tongue, cheek and lips while working in a limited space environment, utilizing, depending on the system, larger than ideal devices is arduous. The use of, and controlling the appropriate use of, the almost universally necessary titanium dioxide powder requires tact and precision as over-powdering can lead to unwanted distortion and under-powdering can lead to an inaccurate image. Both these scenarios, if not corrected, can lead to ill-fitting fixed restorations (Santos et al, 2013).

Lastly, a monopoly of the CAD/CAM market combined with exorbitant manufacturing costs may have limited the creation, development and affordability of new systems in addition to limiting innovative solutions to the aforementioned problems (de Sousa Muianga, 2009).

1.1.5 Success/Survival Studies

The difficulty in looking at the success and survival of CAD/CAM restorations is that the studies with the longest evaluation period are those with either restorations fabricated with materials that have been vastly improved upon and/or fabricated utilizing CAD/CAM systems that are obsolete. Nonetheless, initial long-term prospective clinical studies on the success/survival of porcelain inlays fabricated employing early generations of the CEREC system are positive (Mormann et al, 1989; Isenberg et al, 1992).

Martin and Jedynakiewicz reported a systematic review of all clinical studies involving intra-coronal CEREC restorations from 1986 to 1997. In fifteen clinical studies, they found a mean survival rate of 97.4 % with the predominant reason for failure being fracture of the supporting tooth and/or fracture of the ceramic (Martin and Jedynakiewicz, 1999). These results were confirmed in a clinical study of 2328 inlays in 794 patients where a survival rate of 95.5 % after nine years was observed (Posselt and Kershbaum, 2003).

Hickel and Manhart reviewed clinical studies in the 1990's decade to determine annual failure rates of all posterior restorations/materials. They found that CAD/CAM ceramic restorations annual failure rate ranged from 0 – 4.4 % (with bulk fracture of the tooth and/or the restoration being the prime culprit in failure) and that these were consistent with other restorative materials (Hickel and Manhart, 2001). It is difficult to make comparisons between restorative materials in a study like this due to the rationale behind the clinical decisions to place these restorations and the associated variability of costs of these different restorations. Teeth that require crowns are more likely to have had multiple and/or larger previous restorations thus necessitating the need for the crown and thus potentially, increasing the overall risk of failure. Furthermore, the cost of crowns may be prohibitive for some patients whose teeth could benefit

from a full coverage restoration such as a crown, but "settle" for a full coverage amalgam which then is more prone for failure and results in a potential skewing of the results. Nonetheless, at face value, CAD/CAM restorations performed as well or better than other posterior restorations.

A recent systematic review looked at the clinical performance of CAD/CAM single tooth restorations of various systems. The authors found that, when analyzing 1957 restorations in sixteen studies, the overall survival rate was 91.6 % after five years with a calculated failure rate of 1.75 % per year (Wittneben et al, 2009). These authors also bemoan the fact that there is an overall lack of (absence of) clinical studies using a randomization protocol and that many of the currently used commercial systems lack any scientific evidence longer than three years (Wittneben et al, 2009). This is the dilemma of biomaterial (and CAD/CAM system) development in that "newer and better" materials are replacing "outdated" products (and systems) that themselves are without a long-term track record supporting their improvements and success/survival.

1.2 Resin Composites

A "composite", in material sciences, occurs when two dissimilar materials are mixed together to form a new material (Ferracane, 1995). A standard premise in material science for composites is that the collective unification of these dissimilar materials yields properties that are different and superior to those of the individual constituents.

1.2.1 History

Although much more prevalent today, the desire and demand for tooth coloured restorations has been omnipresent. Early iterations of this class of restorative filling material

were initially based on silicate cements until direct filling methyl methacrylate appeared in the United States in 1947 (Schulein, 2005). Each of these original materials, although filling the "aesthetic need", had inherent limitations, namely high oral fluid solubility for the cements and excessive polymerization shrinkage (and thus micro-leakage) for the methacrylate resins (Schulein, 2005).

In 1955, Buonocore literally forever changed the face of adhesive dentistry via the introduction of the acid etch technique (Buonocore, 1955). Utilizing ortho-phosphoric acid to adequately precondition the tooth's enamel surface for adhesive bonding of plastic resin, it allowed both improvements in the durability of the restorations themselves (edge adaptation and bond strength) but also paved the way for the boom of resin composite technological development thus spawning the era of esthetic restorative dentistry (Handelman and Shey, 1996).

This development again was paramount in 1962 when Bowen synthesized dimethacrylates (from epoxy resin and methacrylic acid) and incorporated into them, silanized quartz powder to form the first truly successful dental resin composite (Bowen, 1963). Bowen's resin, or bis-phenol A-glycidyl methacrylate (BisGMA) still forms the basis of the vast majority of resin composite products available for direct restorative use today (Garcia et al, 2006).

The next true revolution that occurred, in 1973, was the utilization of ultra violet light to activate the polymerization reaction that then allowed predictable esthetic restorations to be made for fractured and/or carious anterior teeth (Garcia et al, 2006). Five years later, resin composite curing was accomplished via visible light activation of camphoroquinone, which lead to improved setting time and colour stability while avoiding the known eye dangers associated with ultraviolet radiation (Rueggeberg, 2002).

In the 1980's, new classes of resin composites, based on filler size, appeared on the market. Initially microfilled composites replaced the original macrofilled ones which allowed for improved polishability. Later on, a "best of both world" solution, the "hybrid" composite was introduced, whereby utilizing various micro and macro filler sizes, the clinical/mechanical advantages of both aforementioned classes was maximized (Schulein, 2005).

In recent years, and mirroring many other manufacturing industries, the goal of "smaller is better" has prevailed. Nanocomposites and nanohybrids, to also be used universally, each with even more miniscule fillers than their microfilled counterparts, have enjoyed increased commercial use. By definition, nanotechnology is the development of functional materials/structure in the realm of 0.1 to 100 nanometers (Kirk, in Mitra et al, 2003). The development of dental nano-resin composites was founded upon the idea of finding a material that had satisfied the esthetic demand of cosmetic restorations but also possessed the requisite mechanical properties for posterior restorations (Mitra et al, 2003). Clinical studies with nano-resin composites have shown good initial results with comparable outcomes to other resin composite classes (Ernst et al, 2006; Kramer et al, 2009). However, Ilie and Hickel, in their comprehensive review of resin composites on the market, found that nano-resin composites as a group had lower modulus of elasticity and increased water sorption, thus leading the authors to question the viability of using this class of restorative material in stress-bearing areas (Ilie and Hickel, 2009).

A summary of the evolution of dental composites is given in Figure 8.

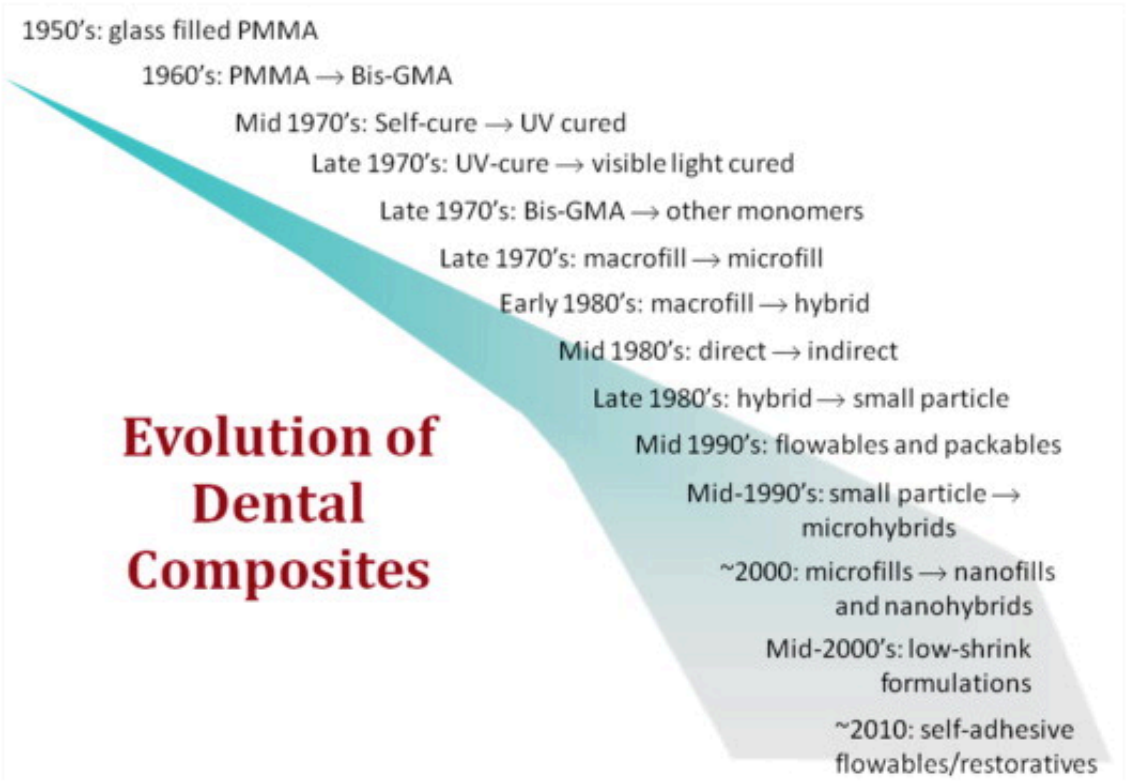

Figure 8: Evolution of dental composites (Ferracane, 2010)

1.2.2 Composition

Dental composites are essentially made up of four major components, namely, an organic polymer matrix, inorganic filler particles, organosilane coupling agents and the initiator system. Each individual component is integral in allowing the realization of the best mechanical properties possible and thus achieving clinical success when used restoratively.

1.2.2.1 Organic Polymer Matrix

In reality, not much has changed over the past fifty years in regards to the matrix component. In an update of the status of the resin composites that are available on the market, it

was concluded that the most prevalent used monomer is still BisGMA (Chen, 2010). Glycol dimethacrylate, urethane dimethacrylate (UEDMA), triethyleneglycol dimethacrylate (TEGDMA), urethane dimethacrylateethoxylated bisphenol-A-dimethacrylate (Bis-EMA), decanediol dimethacrylate (D3MA) are also often used today as monomers/co-monomers in various proportions (Chen, 2010). Although the monomer BisGMA is still heavily used, the recent public fears of the negative side effects caused by Bisphenol-A has resulted in other (Bisphenol-A-free) monomer/combinations of monomer alternatives to become increasingly developed and researched (Cramer et al, 2011).

The chemical structures of the common monomer molecules are given in Figure 9.

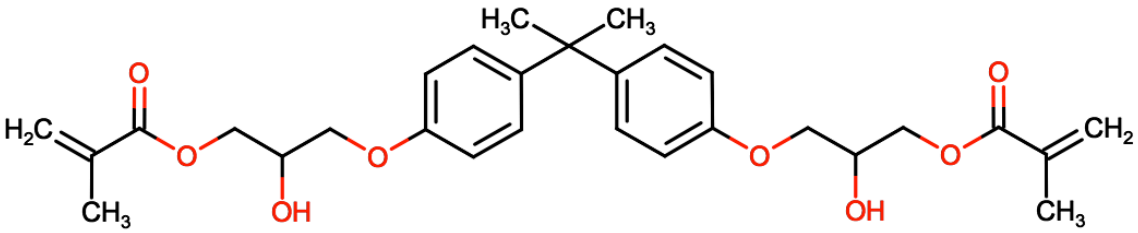

BisGMA

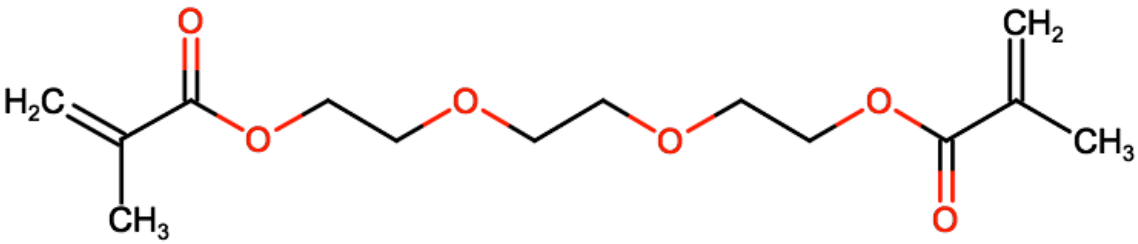

TEGDMA

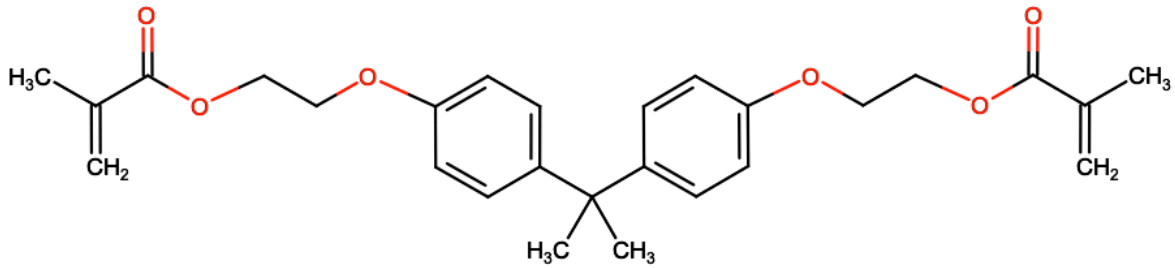

BisEMA

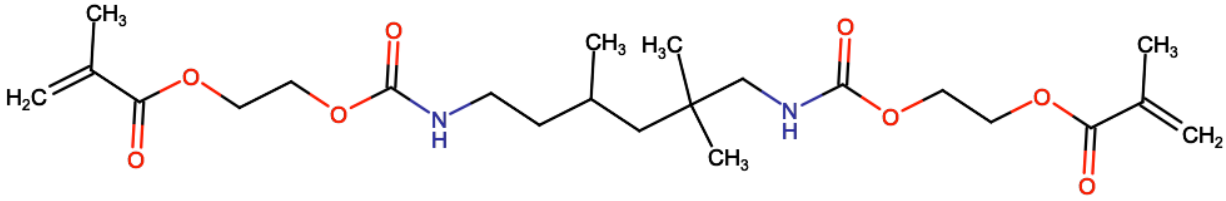

UEDMA

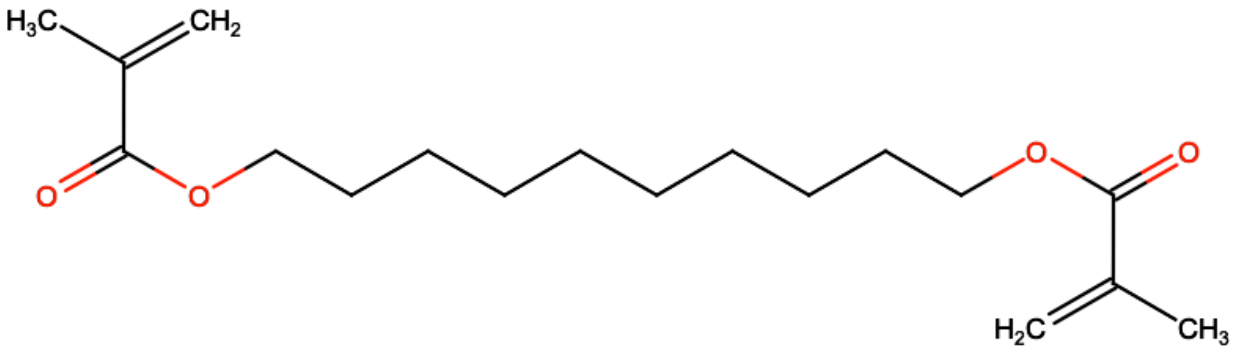

D3MA

Figure 9: Chemical structure of common composite monomers

Once initiated, the chemical reaction of these dimethacrylate monomers produces a rigid, heavily cross-linked polymer network around the numerous fillers and thus, the hardening of the dental composite occurs (Ferracane, 2011). Due to the formation of covalent bonds, the polymerization reaction results in volumetric polymerization shrinkage, which clinically, can result in catastrophic negative consequences if not managed correctly. There is a direct relationship between the amount of polymerization shrinkage and the amount/type of the various monomers used in the formulation. Typically, TEGDMA is used, most ideally in a 1:1 ratio, as a diluent monomer for both UEDMA based composites and BisGMA based composites due to its lower viscosity and copolymerization characteristics (Ferracane, 1995). Another important consideration is the degree of conversion (DC), defined as the percentage of consumed carbon-carbon double bonds that occurs during polymerization and is represented by the expression DC = (1 – R) X 100 % whereby R is the ratio of unreacted methacrylate groups before and after polymerization (Annusavice, 2008).

It has been postulated that resin strength is related to the monomer composition and it has been shown to be greatest when both BisGMA is used and the degree of conversion is maximized (Ferracane, 1989). Some evidence purports the advantages of UEDMA, namely lower viscosity and greater flexibility of the urethane linkage, which is then claimed to improve the toughness of resin composites (Indrani et al, 1995). However, establishing a general difference between different resin composites based on the monomer compositions is very difficult if not impossible to deduce due to the masking effect of the other variables (e.g. type and amount of filler, type and amount of initiators, and silanization of the filler particles) which may be more impactful on the mechanical properties than the nature of the copolymer (Asmussen and Peutzfeldt, 1998). Even so, a large part of the current experimental research is

focused on attempting to improve the polymeric matrix, specifically in the realm of reducing polymerization shrinkage and minimizing polymerization shrinkage stress (Ferracane, 2011).

1.2.2.1.1 Improved Polymerization Polymer Matrices

Polymerization shrinkage has been an Achilles heel of resin composites. Combine this undesirable side effect with inefficient and/or careless clinical handling by the clinician and the results prove to be disastrous. The margin of error, especially with posterior restorations, is simply much narrower than that that exists for amalgam. An initial attempt to overcome this issue occurred years ago with the introduction of ormocers (organically modified ceramics) but negative handling properties limited their use (Zimmerli et al, 2009), however, a recent comeback has been initiated with new ormocers that have improved handling properties.

Ormocers are three-dimensional cross-linked organic-inorganic copolymers that fundamentally have a silicon dioxide backbone functionalized with polymerizable organic units to produce three-dimensional compound polymers (Kalra et al, 2012). Essentially, as a result, the ormocer is already a polymer prior to the light curing reaction and due to the sheer abundance of polymerization opportunities in these materials, it minimizes/eliminates the residual monomers that remain post curing (Kalra et al, 2012).

Another matrix modification that has been investigated is to use molecules that polymerize through ring-opening polymerization. Tilbrook found that resins generally shrink less by ring-opening polymerization, due to the increase in excluded free-volume associated with the ring-opening process (Tilbrook, 2000). Silorane is one such molecule and nanocomposites containing Silorane have been shown to exhibit low shrinkage and comparable mechanical properties when tested in vitro (Weinmann et al, 2005).

1.2.2.2 Inorganic Fillers

The initial fillers used in the first dental composites were fused crystalline quartz or lithium aluminosilicate glasses ground and/or milled into particles of various sizes (Peutzfeldt, 1997). The two main drawbacks of these glasses were the radiolucent appearance on radiographs and the surface hardness mismatch of the fillers and the polymer matrix causing uneven wear. These drawbacks when considered together necessitated the development of more clinically friendly options. Amorphous silica; particles based on oxides of barium, strontium, zinc, aluminum or zirconium; colloidal silica; and ceramics are now more prevalently used (Klapdohr and Moszner, 2005). Generally, by weight, the concentration of filler is in the range of 70-80 %. By volume, the concentration is in the range of 40-70 % (Ilie and Hickel, 2009).

In general, filler volume percentage is a more important and pertinent parameter, since it is directly related to the mechanical properties of resin composite. It is the volume of exposed resin matrix to abrasion and the volume of matrix resin that has to polymerize that are important and as a result, only quoting the percentage weight is misleading (Jones, 1998).

The shape of the filler has additionally been subject to much research with commercial attempts utilizing branched fibres, nano-porous fibres, nano-agglomerates and ceramic whiskers (Ilie and Hickel, 2011).

In general, as resin composite development has progressed, filler size has decreased. The progression of resin composite technology has evolved from initially large particle size inorganic fillers towards smaller particle size configurations with modified, unique fillers. Important in this relationship is not only the filler size but the filler content, morphology and distribution of filler particles as the interplay of all these variables truly impact the mechanical properties and thus, ideally, the clinical success (Kahler et al, 2008).

Much like rebar previously, and small glass fibre more recently, have been used successfully in reinforcing concrete to improve its structural integrity, the use of nanofibers, embedded in the polymer matrix, has shown to have composite reinforcement properties (Fong, 2004). Tian et al electorspun nylon 6 nanocomposite nanofibers, containing highly aligned fibrillar silicate single crystals, into a BisGMA/TEGDA matrix, cured them and then ground them to be added as filler in another BisGMA/TEGDA matrix. They found that when small mass fractions of these impregnated nanofibres (1-2 %) were used, the mechanical properties of fracture toughness and flexural strength were substantially improved, however, when greater proportions of these mass fractions (4 % and 8 %) were used, it had the opposite effect (Tian et al, 2007). This shows that the utilization of reinforced fillers can be a double-edged sword whereby small variations in their usage amount can bring forth opposing effects on the mechanical properties of the material as a whole.

Ultimately, both the correlational impact of filler size on the resin composites' mechanical properties and the easily discernable dimensional differences have elicited filler size as often the basis for the many composite resin classification systems that exist today.

1.2.2.3 Organosilane Coupling Agents

The organic matrix and inorganic fillers are bonded covalently and this strong union is essential in order to not only realize the desired mechanical properties but to have a clinically usable/predictable resin composite restorative material. A silane-coupling agent that has functional groups that bond to the hydroxyl groups of the silica filler particles and copolymerize into the polymer methacrylate matrix is therefore used (Chen, 2010). A typical bifunctional

coupling agent is 3-methacryloxypropyltrimethoxysilane (MPTS) and its chemical formula is given in Figure 10.

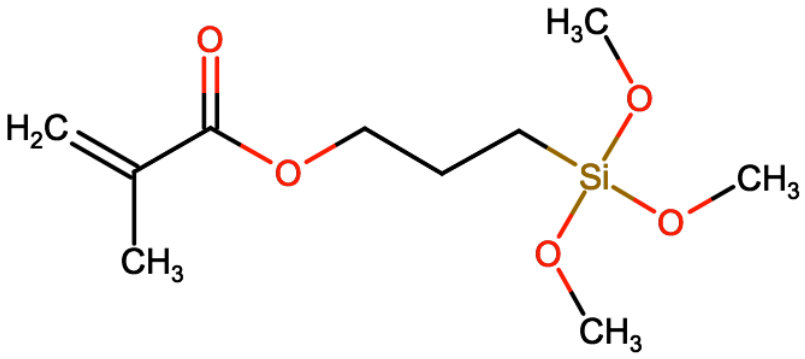

Figure 10: Silane (MPTS) chemical structure

1.2.2.4 Initiator Systems

The polymerization hardening reaction of resin composites can be activated chemically, via light or via a combination of these two methods. Typically, in a chemically activated resin composite, benzoyl peroxide activated by tertiary amines is the source of the free radicals that drive the polymerization. In light activated resin composite, camphoroquinone, a diketone photoactivator, is typically used (Azzopardi et al, 2009). Inhibitors are also added to prevent spontaneous polymerization during storage.

1.2.3 Recent Modifications

As clinical composite use has clearly overtaken amalgam use, innovative modifications have been introduced and/or are being investigated that improve the clinical performance in many different regards.

1.2.3.1 Adhesive Resin Composites

The addition of acidic monomers such as glycerolphosphate dimethacrylate (GPDM), commonly found in dentin bonding agents, may be capable of generating adhesion of resin composite to tooth structure (Ferracane, 2010). With the development of newer generational bonding agents, the so-called self-adhesives have become more clinically relevant even in the face of decreased bond strength, self-adhesive composites have begun to be investigated. If bonding is achieved and proved successful, it may just become more than a niche product.

1.2.3.2 Caries Prevention Fillers

Ferracane stated that "perhaps the most promising work in composites with modified fillers for both enhanced mechanical properties and remineralizing potential, by virtue of calcium and phosphate release, has been the work of fused silica whiskers and dicalcium anhydrous (DCPA) or tetracalcium phosphate (TTCP) nanoparticles" (Ferracane, 2010). Previous studies have showed that when Ca and PO_4 ions were released from composite restorations, they reformed as hydroxyapatite, significantly increasing the mineral content of the lesion and thus, promoted remineralization (Skrtic et al, 2000; Dickens et al, 2003). Using this principle, Xu et al confirmed this caries-inhibiting capability both using DCPA and TTCP whiskers, but also found that the whisker reinforcement more than doubled the composite's strength and significantly increased the elastic modulus (Xu et al 2007). Similar to the purported benefits of fluoride release in glass ionomers, resin composites that either follow the same fluoride release principles already deemed clinically relevant and/or this aforementioned hard tissue regenerative route should combat the commonly cited resin composite problem of secondary caries generation.

Additionally, the improved mechanical properties may further combat another commonly encountered problem, premature fracture.

1.2.4 Classification

Numerous authors have attempted to develop an appropriate classification system of resin composites. Some generalize the classification based on the method of polymerization; others tend to base the classification on use or specialized use; some advocate the matrix composition as being the basis for classification; while the vast majority tend to use filler size (with our without consideration of filler volume) as the foundation of the classification system (Lutz and Philips, 1983; Hosoda et al, 1990; Willems et al, 1992; Lang et al, 1992; Mount et al, 2009).

One of the original and still most popular classifications is the one proposed by Lutz and Philips in 1983. Their rationale was based around the fact that a correlation was made between wear and the components of the material whereby, if classified accordingly, clinical performance conclusions (and predictions) could be made for each established category of resin composite (Lutz and Philips, 1983). Four main groups of resin composites, as shown in Figure 11, were established from their work and has often served as the foundation of many subsequent classification systems.

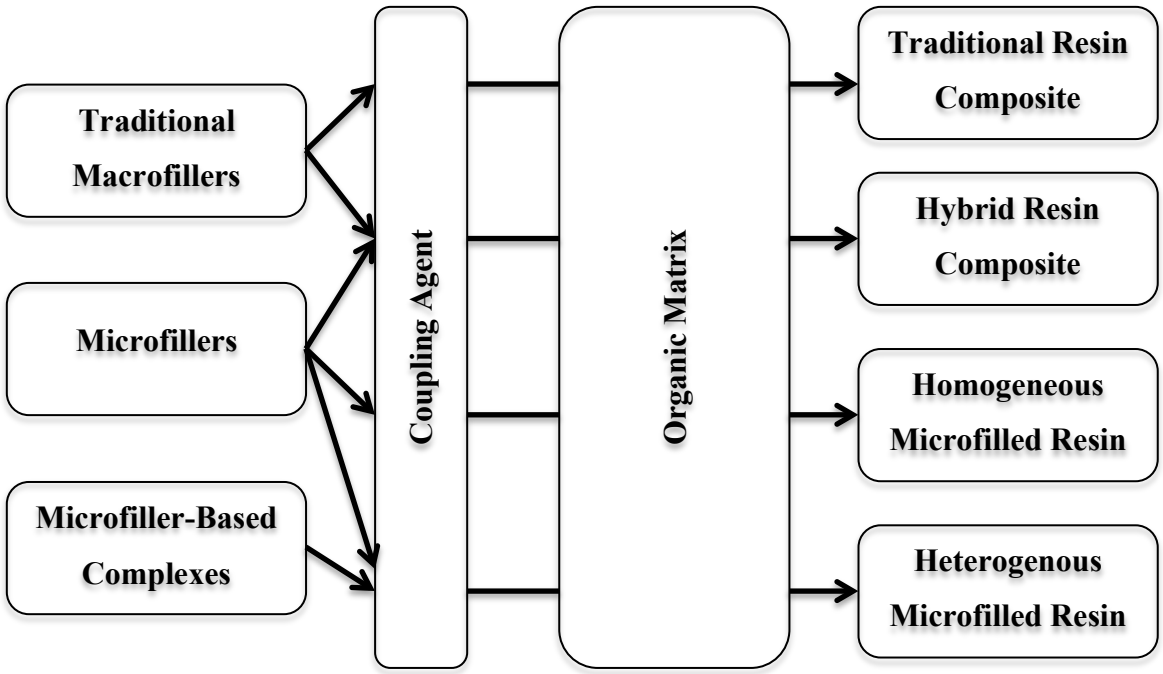

Figure 11: Lutz and Philips (1983) resin composite classification system

Willems et al espoused another, more advanced/detailed classification system in 1992. They "ranked" most/all the commercially available resin composite products at that time as a function of their mean particle size, filler size distribution, filler content, Young's modulus, surface roughness, surface hardness, compressive strength and scanning electron microscope (SEM) appearance (Willems et al, 1992). Although the interplay of the aforementioned properties were considered, the main determining factor of their classification system was volume fraction filler and thus, it is ultimately based on materials science properties. This massive undertaking aimed to both provide clinically relevant classifications and therefore provide solid recommendations of use, but also, based on a few mechanical properties, be easy to reclassify new materials as they appeared on the market (Willems et al, 1992). A summary of their classification is given in Table 2.

Composite Type	Filler
1. Densified composites a. Midway-filled i. Ultrafine ii. Fine b. Compact-filled i. Ultrafine ii. Fine	 < 60 % by volume Particles < 3 μm Particle > 3 μm > 60 % by volume Particles < 3 μm Particles > 3 μm
2. Microfine composites a. Homogeneous b. Heterogeneous i. Prepolymerized ii. Sintered	Average particle size (for all) = 0.04 μm
3. Miscellaneous composites	Blends of densified and microfine composites
4. Traditional composites	Equivalent to what are termed macrofill composites in other classifications
5. Fiber-reinforced composites	Industrial-use composites

Table 2: Willems et al (1992) resin composite classification system

The relationship then between the volume occupied by the filler and both the amount and penetrability of the organic resin matrix into and around these fillers, directly impacts the mechanical and clinical properties of resin composites. As the size of the particles decrease, and their resultant surface area increase, the polymer matrix is required to "cover" a larger are and as a result, a negative effect is seen in the mechanical properties of the material (Hosseinalipour et al, 2010; Ilie and Hickel, 2009). However, increasing the volume filler fraction has also allowed a reduction in the monomer content which consequently minimizes the polymerization shrinkage, optimizes wear and improves the polishability and thus, the aesthetics of the final restoration (Ilie and Hickel, 2009). Managing this balance has been the challenge of resin

composite manufacturers but has also led to the general improvements in the mechanical and clinical properties of resin composites over the past twenty years (Oliveira et al, 2012).

Specifically, the relationship of the volume fraction of both the fillers and the organic matrixes to the modulus of elasticity of the resin composite as a whole, is given in Equation 1.

$E_c = \frac{1}{\left(V_f / E_f\right) + \left(V_m / E_m\right)}$	E_c = Elastic modulus, composite E_m = Elastic modulus, resin E_f = Elastic modulus, filler V_m = Volume fraction resin V_f = Volume fraction filler

Equation 1: Formula for elastic modulus of resin composite (Callister and Rethwisch, 2012)

When the elastic modulus is plotted versus the specific volume fraction of the filler, the improvements in the elastic modulus are clearly seen in the resultant graph. Furthermore, the obvious transition zone in the curve of this plot provides an important division between the types of resin composites available for clinical use. This observation formed the basis of Willems et al (1992) classification system and as a result, is a more clinically appropriate classification system when determining the intended use/intraoral location of a selected resin composite. Figure 12 gives the elastic modulus to volume fraction filler graphical relationship.

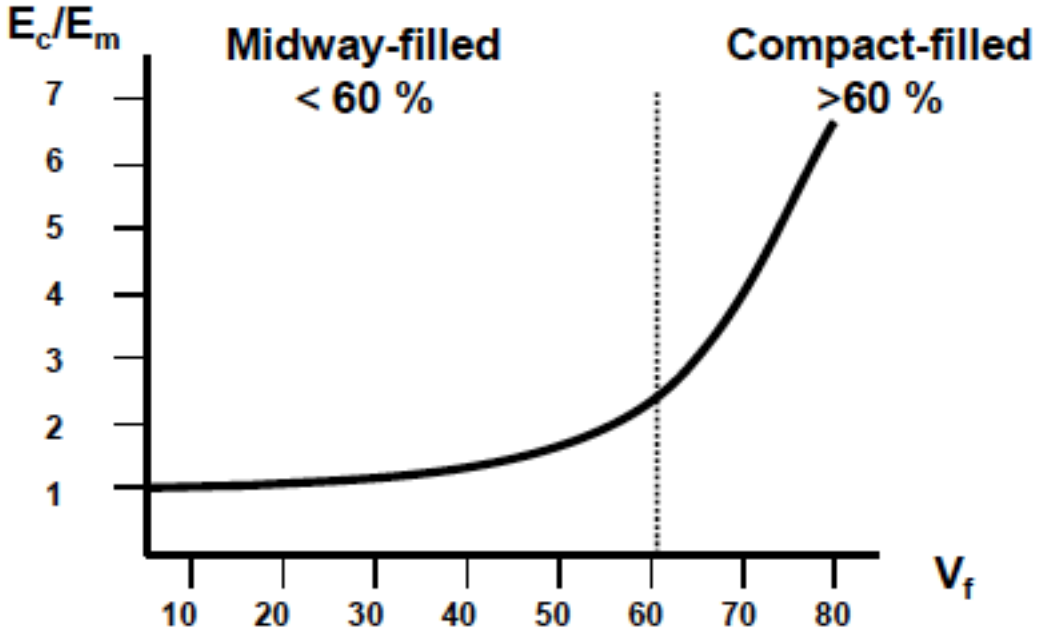

Figure 12: Relationship between volume fraction filler and elastic modulus (Willems et al, 1992)

The introduction of nano-sized particles has caused the need for expansion on both these popular classification systems. Although not a classification per se, Ferracane summarizes the "old" and the "new" categories of resin composites in his 2010 review. He stated that, through further milling and grinding, techniques have resulted in the development of particles that were sub-micron in size (0.4-1.0 μm) and initially termed "minifill" but later became known as "microhybrid" (Ferracane, 2010). The further development of nanoscale particles have yielded two new sub-groups, namely nanofill, whereby all the particles are of nanoscale, and nanohybrid, whereby the manufacturers have modified their formulations of microhybrids to include both nano-sized particles and larger pre-polymerized resin fillers (Ferracane, 2010). Figure 13 outlines the "old" and "new" classification as put forth by Ferracane in 2010.

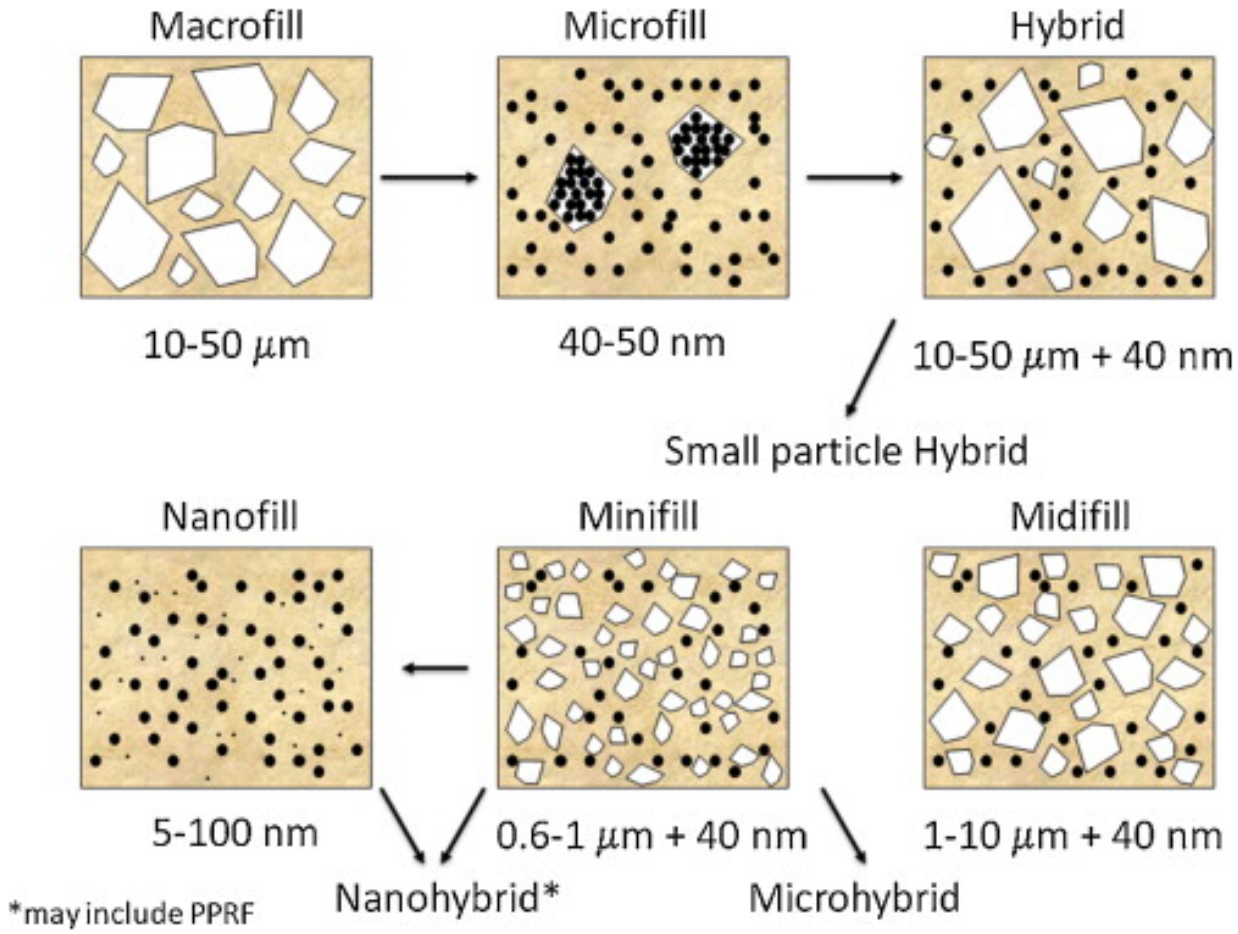

Figure 13: Composite groups based on particle size (Ferracane, 2010)

In summary, the macrofilled resin fillers tended to be quartz based while the microfilled tended to be colloidal silica. Although smaller, the surface area of the microfillers limited the filler volume that could be incorporated into the composite, which then resulted in a higher volume of resin and concomitantly, decreased mechanical properties (Ferracane, 2010). Both the original hybrid composites and the more modern hybrids (micro and nano) aim to solve the inherent weaknesses of each of their individual primary components. Much like the definition of a composite, the conglomeration of both particles together yields a new material that has improved mechanical properties than the individual components themselves.

In the newer small particle hybrids, some nanomers are grouped together as agglomerates and termed "nanoclusters" (Mitra et al, 2003). Currently, there are conflicting opinions on the effects that nanoparticles and nanoclusters have on the mechanical and clinical properties of the resin composite (Atai and Watts, 2006; Curtis et al, 2009; Ilie and Hickel, 2009; Chen et al, 2010).

1.2.5 Clinical Performance

Much in-vitro and in-vivo research has been done on resin composites. Some consistent limitations are seen that have yet to be overcome clinically.

1.2.5.1 Polymerization Shrinkage

Polymerization shrinkage has been called the "greatest limitation" of using resin composite as the negative sequelae that stems from this shrinkage are poor marginal seal, marginal staining leading to possible esthetic concerns and recurrent caries (Karthick et al, 2011). As the material shrinks, tensile forces pull the material away from the tooth surfaces, which can lead to marginal degradation, enamel crazing/cracking, restoration debonding and/or material fracture. It has been estimated that resin composites undergo 2.9 – 7.1 vol % shrinking during polymerization (Feilzer et al, 1987).

The amount of polymerization shrinkage is directly linked to the degree of conversion and reducing the degree of conversion would have terrible consequences on the resin composite restoration. Many factors affect the degree of conversion of the monomers into polymers (and thus the polymerization shrinkage) and these include: curing time; temperature; resin thickness; type of filler; curing distance; amount of organic material (Chen, 2006). Monomer conversion is

never 100 % and as such, the resin composites' physical and mechanical properties are directly related to the extent to which monomers react to form the polymer during polymerization (Chung et al, 1990). Modifying the material constituents in form, percentage (volume) and/or size to maximize the materials' degree of conversion will ideally minimize the associated polymerization shrinkage.

1.2.5.2 Wear

The life expectancy of any restorative material is directly related to the wear resistance of that material. Functional, parafunctional and abrasive activity all act upon the resin composite and the ability to withstand these deleterious actions is desirable. Much clinical research has centered on alterations of filler particle size as this intrinsic quality is directly related to wear resistance (Ruddell et al, 2002; Turssi et al, 2005). It has been found that the finer the particle size, the less interparticle spacing occurs which shields the softer resin matrix and leads to enhanced wear resistance of the material (Drummond et al, 2008; Turssi et al, 2005).

Ferracane stated that wear today is less of a concern than in the materials of a decade ago due to the refinement of reinforcing fillers. However, care must be undertaken when placing resin composites into large preparations and/or when used to replace functional cusps (Ferracane, 2010). As is evident in most things in dentistry, when considering potential restorative wear, proper case selection and material selection are paramount. Some investigators have attempted to utilize and correlate other in-vitro laboratory mechanical tests to predict potential clinical wear (Peutzfeldt and Asmussen, 1992; Truong and Tyas, 1988). Ferracane concluded, following investigation of thirteen hybrid dental composites, that the best correlations for clinical wear were between wear and fracture toughness and wear and flexural strength (Ferracane, 2013).

Although new technology has diminished the day-to-day clinical wear concern, it remains important to assess wear in clinical studies, to predict wear for new materials based on in-vitro test methods (both with wear tests and through the positive correlation with other mechanical properties) and to refine the methods for quantifying wear (Ferracane, 2006).

1.2.5.3 Success/Survival Studies

Depending on the study, the reasons for reduced success values for resin composites were either fracture or secondary caries. Analyzing these results even further, it is difficult to blanketly accept these conclusions as fact due to the interplay of other factors. Resin composite placement is known to be more technique sensitive and operator error could negatively impact success values. The prevalence of recurrent caries as a reason for restoration failure are also influenced by the general caries risk status of the study population and it is well established that the caries risk of the patient also plays a significant role in restoration longevity (Köhler et al, 2000; Opdam et al, 2007). Accepting that other contributing factors may have an impact on restoration success, both secondary caries and fracture must remain a clinical concern nonetheless.

Resin composite use, especially in posterior teeth, has continued to increase concomitantly as amalgam use has continued to decline. Annual failure rates of both materials have been documented in a prospective study as being equal (Manhart et al, 2004), however, when looking at endurance, three studies reported better longevity of amalgam restorations when compared to composite restorations (Van Nieuwenhuysen et al, 2003; Bernardo et al, 2007; Soncini et al, 2007). These results confirm the results of a 1999 Cochrane review whereby

amalgam was always superior in studies with unpaired design, and still superior, but less statistically significant, in studies with paired design (NHS Centre for Reviews, 1999).

As resin composite is becoming the universal restorative material of choice in many clinics/nations, many larger, long-term studies have been published. Overall clinical performance rates have been generally good and non-comparative studies are showing 75 % 17-year success rates and 64 % 22-year success rates respectively (Da Rosa et al, 2006, 2011). Comparatively, in an insurance database evaluation of 200000 amalgams and 100000 resin composites, 7-year success rates were shown to be 94 % and 93 % for amalgam and resin composite respectively (Bogacki et al, 2002). In a 12-year retrospective study comparing amalgam and composite, the authors concluded that in high-risk patients, composite and amalgam restorations were comparable, with amalgam performing better in smaller restorations. However, with low risk patients exclusively, composite restorations exhibited better survival (Opdam et al, 2010). Although these recent studies are beginning to challenge the long-held consensus that amalgam longevity is higher than resin composite, it may only be a matter of time (if not there already) that the recent advancements made in composite resin material development begin to level and tilt this playing field further.

1.3 Biomaterials Testing

Ultimately, dental materials that satisfy the aesthetic demands of the patient, withstand the biomechanical forces placed upon during normal function/parafunction and that are easy to fabricate, use, and manipulate are few and far between. Guazzato et al (2004) stated “the lack of sufficient clinical studies regarding the latest generation of materials has led manufacturers and

dental operators to place great emphasis on mechanical properties to define the clinical indications of these materials."

Mechanical properties are evaluated based on the results of in-vitro testing. As early as the 1920s, dental materials testing was identified as a program "having health-saving importance" and as a result, by 1927, the American Dental Association (ADA) formalized a cooperative research program that led to the formation of the International Standards Organization, Technical Committee 106 (Dentistry) (Kelly, 2012). Utilizing sound research protocols and standardized testing methods then allowed material comparisons to be made thus eliminating the era of manufacturers' unfounded and spurious claims of material superiority. Stanford summarized the necessity of dental standards as the provision of a basis for product comparison, establishment of consistent terminologies, assurance of desired qualities and performance levels, identification of products that are sub-par and an increased buyer/consumer confidence (Stanford, 1987). Development of test results databases then further opened the door to the powerful process of predicting dental materials clinical success based on this data and greatly reduced the number of clinical studies needed to summarize a prosthetic material (Anusavice et al, 2007).

1.3.1 Mechanical Properties of Materials

The laws of mechanics, and specifically those areas that deal with effects of energies and forces on bodies, govern the mechanical properties of materials (Anusavice, 2003). Because dental materials are static entities, all mechanical properties of these materials are measures of the resistance of the material to either deformation and/or fracture under an applied load (Anusavice, 2003).

It is essential that every component of any machine (or composite material) be able withstand the forces applied to it for it to perform maximally. With dental materials and or fixed restorations, the "components" are the material itself and/or the mechanism by which it is attached to the remaining tooth structure/implant. Accordingly, the "forces applied to it" are those forces that are encountered during function and/or parafunction and coupling the knowledge of these forces with the mechanical properties of materials could allow the clinician to best design the restoration/prosthesis for long-term clinical success.

The main forces that can act upon a material can be grouped as tensile, compressive, shearing and torsional. Tensile forces elongate a material, compressive forces shorten a material, shear forces deform a material around a central axis and torsion forces twist a material around a central axis. Additionally, bending forces, a compilation of tension, compression and shear forces, (sometimes called the combination stress) can also be seen. When evaluating those stresses that a dental restorative material is subjected to intraorally, bending forces are commonplace. Visual representation of these forces is given in Figure 14.

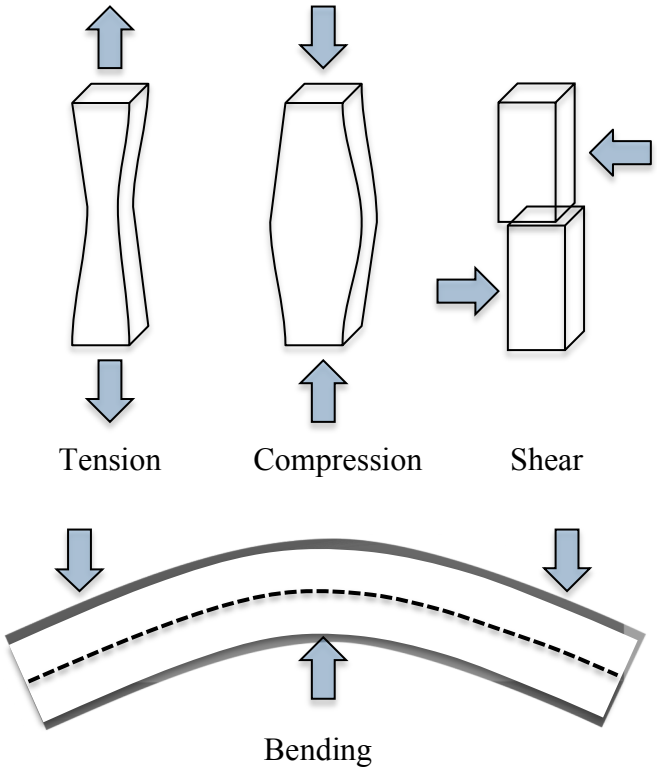

Figure 14: Types of forces

Stress (σ) is defined as the force per unit area (Anusavice, 2003). In dental applications, depending on the applied force and object shape, these stresses tend to be limited to tensile stresses (produced by a tensile force), compressive stresses (produced by a compressive force) and shear stresses (produced by a shear force). There is some interplay between these stresses as evidenced during flexural loading (e.g. on a bridge - occlusal load between two fixed abutments) and in such cases, brittle dental materials tend to fail due to the generated tensile stress.

Stress levels that cause elastic deformation in materials do not cause permanent deformation whereas stress levels that cause plastic deformation (non-elastic deformation) do cause some degree of permanent deformation and, if high enough, may cause material fracture (Anusavice, 2003). In brittle materials that only exhibit elastic deformation, stresses at or

beyond this elastic limit will result in catastrophic failure (Anusvavice, 2003). Therefore, it is paramount that material specific mechanical properties are understood before designing a restoration or prosthesis.

Strain (ε) is the deformation in a material when subjected to stress and it may either be elastic or plastic. By definition, the strain is the change in length (Δl) per original length (l_o). These entities, and the manner in which they are calculated are shown in Equation 2.

$$\text{Stress } (\sigma) = \frac{\text{Force (F)}}{\text{Area (A)}}$$

and

$$\text{Strain } (\varepsilon) = \frac{\Delta l}{l_0}$$

Equation 2: Stress and strain formulas

The relationship between stress and strain for each material is unique and can be displayed graphically in the form of a stress-strain curve. This curve also provides us with the measures of many other important mechanical properties. The slope of the elastic region of the stress-strain curve is the elastic modulus, E (also known as Young's modulus of elasticity) and is a representation of the stiffness or rigidity of a material. Other mechanical properties that can be gleaned from this graph include (Anusavice, 2003):

a) Proportional limit (σ_p) – maximum stress at which stress is proportional to strain and above which, plastic deformation occurs

b) Yield strength (σ_y) – the stress at which a test specimen exhibits a specific amount of plastic strain (usually 0.2 %)

c) Ultimate (tensile) strength (σ_u) – tensile stress at the point of fracture

d) Resilience – the amount of elastic energy per unit volume released on unloading of a test specimen. It is represented by the area under the elastic region of the stress-strain curve

e) Toughness – ability of a material to absorb elastic energy and to deform plastically before fracturing. It is measured as the total area under the stress-strain curve

The graphical representation of the stress-strain curve and the associated aforementioned properties are shown in Figure 15.

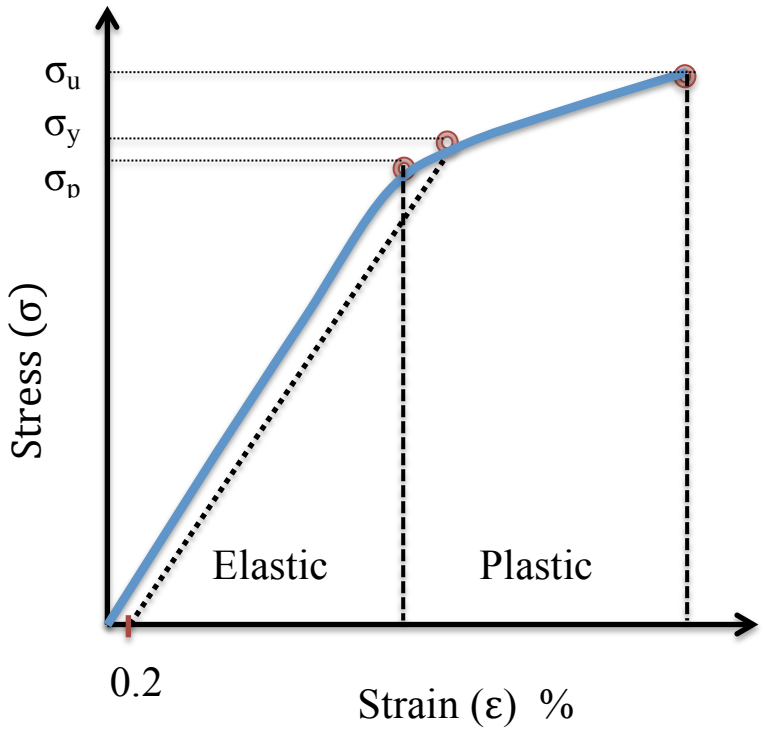

Figure 15: Stress-strain curve and properties associated with this graph

Brittleness is the relative inability of a material to undergo plastic deformation prior to fracture (Anusavice, 2003). Dental restorative materials as a group tend to be classified as brittle but that does not necessarily imply that these materials are weak, and often, quite the contrary. The mechanical properties of a brittle material are especially affected by intrinsic or process-induced microstructural defects/flaws. Whereas a ductile material has the ability to deform plastically and thus overcome the potential negative consequences of these flaws, a brittle material, devoid of the ability to plastically deform, is especially prone to premature failure when tensile forces are applied to it (Anusavice, 2003).

Two important aspects of these flaws are: (1) the stress intensity increases with the length of the flaw, especially when it is orientated perpendicular to the direction of the tensile stress,

and (2) flaws on the surface are associated with higher stresses than are flaws of the same size in interior regions (Anusavice, 2003). These factors belay the necessity to exhibit maximum care and caution during the mechanical adjustment of dental materials and the need to reduce as much as possible the inclusion and flaws that occur during material processing.

Due to their susceptibility to surface flaws and internal defects, when tensile stresses are present, combined with their inability to undergo plastic deformation to reduce these stress concentrations, brittle materials possess tensile strengths far lower than their compressive strengths (Anusavice, 2003). The tensile strength of a material can be derived from a three-point bend test, designed to measure the flexural strength. The flexural strength then represents the greatest stress experienced by the material at the time of failure and is represented by the symbol, σ_f. In studying dental materials that can be used for indirect restorations, a high σ_f is a desired property as once these materials are under the forces of mastication, the ability to withstand these forces without fracture is required. A three-point bend test is accomplished via supporting a predetermined sized bar on both ends and subjecting the material to a centralized static load. Figure 16 gives this test and the associated formula used to calculate σ_f.

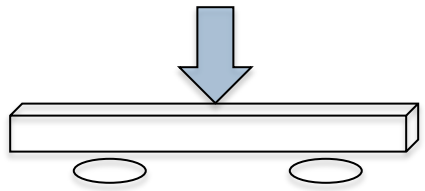	$\sigma_f = \frac{3Pl}{2bd^2}$	P = maximum load at the point of fracture l = distance between the supports b = width of the bar d = thickness of the bar

Figure 16: Flexural strength (σ_f)

A purported advantage of the three-point bend test is that it also allows one to simultaneously calculate E_f without the need for a second test. This mechanical property is given by the slope of the stress-strain curve obtained in a flexural strength test such as the three-point bend test. Along with the "ease" of sample preparation, these factors have led to the development of the three-point bend test as the ISO standard for calculating flexural strength of brittle dental materials. The formula for flexural modulus is given in Figure 17.

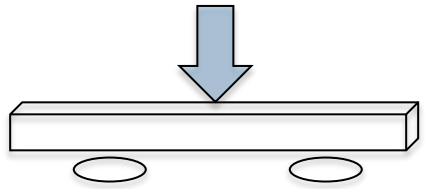	$E_f = \frac{L^3 m}{4bd^3}$	L = distance between the supports m = slope of the deflection curve b = width of the bar d = thickness of the bar

Figure 17: Flexural modulus (E_f)

1.3.2 Fracture Mechanics

The presence of production/machining flaws in all brittle dental materials leads to a mismatch of clinical success/survival with what might have been expected. Furthermore, the large variations in mechanical properties of similar materials as a result of these randomly distributed flaws renders the calculated absolute strength values less reliable. Premature, unexpected failure of restorative materials when subjected to normal functional loads has been problematic for restorative dentistry. Fracture mechanics aims to study and quantify the influence of factors such as stress level, presence of extrinsic and/or intrinsic flaws, inherent

material properties, and mechanisms of catastrophic propagation of a flaw to failure, in order to determine the fracture behavior of a material in aiding future designs (Hertzberg, 1996).

1.3.2.1 Fracture Toughness, K_{IC}

Inglis, in 1913, identified that the stress-concentration factor, K_I, around a crack tip, is directly related to the geometry (length and radius) of the crack itself (Hertzberg, 1996). As the K_I increases, the maximum stress-strain level that the cracked material can tolerate before failure decreases. Surrounding the crack tip, however, is a zone of plastic deformation that "absorbs" some of the stress being magnified at the crack tip and prevents the propagation of the crack and failure of the material. When the applied stress remains low, failure does not occur because concentration of stress at the stress tip does not reach the level necessary for failure.

In 1920, Griffith built upon Inglis' work when he determined that a crack-weakened material could be treated as an equilibrium problem in which the reduction in strain energy in the body containing the crack equated to the increase in surface energy due to an increase in surface area (Ceriolo and Di Tommasco, 1998). Griffith developed a relationship between the crack length (denoted as a), the surface energy on the crack-free surfaces (denoted as 2γ) and the applied stress (σ) and this is given in Equation 3.

$$\sigma = \sqrt{\frac{2E\gamma_s}{\pi a}}$$

Equation 3: Griffith's (1920) fracture mechanics formula

Although extremely important, an oversight in Griffith's work in that he did not factor the plastic deformation that occurs around the crack tip in many materials, resulted in predictions of strength values whereby compressive strength is eight times greater than its tensile strength, which cannot be valid for any material (Ceriolo and Di Tommasco, 1998).

Orowan suggested that the energy of plastic deformation needed to be added to Griffiths' formula and his proposed correction is illustrated in Equation 4 below.

$$\sigma = \sqrt{\frac{2E(\gamma_s + \gamma_p)}{\pi a}} = \sqrt{\frac{2E\gamma_s}{\pi a}(1 + \frac{\gamma_p}{\gamma_s})}$$

Equation 4: Orowan's (1950) fracture mechanics formula modification

In 1957, Irwin also built upon Griffith's work but introduced an idea of a "flat crack" as opposed to an elliptical crack and that a consideration must be added that considers the frictional force that develops between the cracked surfaces. From this, Irwin postulated that crack growth occurs when the strain energy release rate (annotated as G) is larger than the critical work required in creating two new surfaces via crack propagation (annotated as G_c) (Dowling, 1993).

He further found that the stress field around a sharp crack could be uniquely defined by a parameter named the stress intensity factor, annotated K (Soderholm, 2010). From this, once K equals and surpasses some critical value, labeled K_c, fracture will occur. Using his modification to Griffith's equation where he used the energy source term (elastic energy per unit crack length) as opposed to the surface energy on the crack surfaces, he rewrote the formula as in Equation 5 below.

$$\sigma = \sqrt{\frac{EG}{\pi a}}$$

Equation 5: Irwin's (1957) fracture mechanics formula modification

By equating his formula to Orowan's modification, Irwin deduced that at the point of instability, the elastic energy release rate reaches a critical value at which point fracture occurs and that this value is a material property that can be measured in the laboratory with sharply notched test specimens (Hertzberg, 1996). Equation 6 gives this seminal formula.

$$G = 2(\gamma_s + \gamma_p)$$

Equation 6: Irwin's (1957) strain energy release rate formula

Cracks can propagate as a result of three different loading conditions. Denoted as modes I, II and III, they specifically relate to:

a. Mode I: opening or tensile mode, where crack surfaces move directly apart;
b. Mode II: sliding or in plane shear mode, where the crack surfaces slide over one another perpendicularly to the leading edge of the crack;
c. Mode III: Tearing mode, where the crack surfaces move parallel to one another and parallel to the leading edge of the crack.

The different modes of loading are shown in Figure 18.

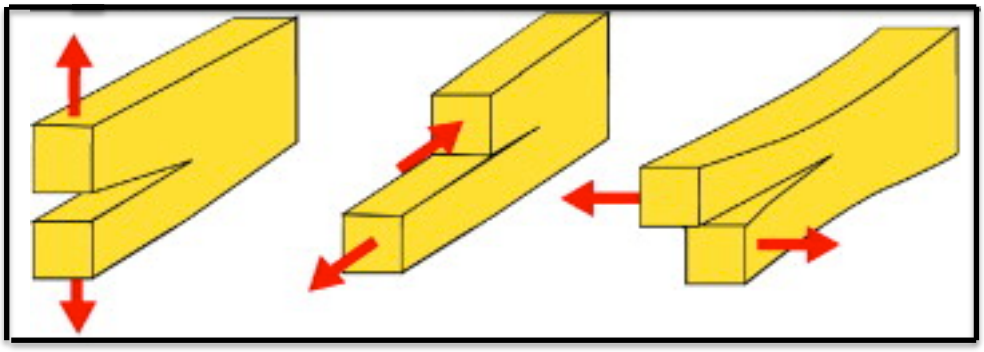

Figure 18: Modes of loading according to Irwin (Soderholm, 2010)

The stress intensity factor that Irwin introduced was calculated differently for each mode of loading. Again K relates to the magnitude of the stress intensity locally adjacent to the crack tip in terms of the applied loading and geometry of the structure where the crack is located (Soderholm, 2010). The equations in Equation 7 give the stress intensity factor formulas for each of these modes of loading.

$$K_I = (\sigma_{yy})_L a\pi^{1/2}$$

$$K_{II} = (\sigma_{xy})_L a\pi^{1/2}$$

$$K_{III} = (\sigma_{zy})_L a\pi^{1/2}$$

Equation 7: Stress intensity factor formulas for the different types of loading

Irwin determined that in mode I failure, the applied stress alone does not make the local fracture progress and that the stress distribution around any crack is similar (Hertzberg, 1996). As such, Irwin concluded that, for mode I failure, $K_I \geq K_{IC}$ and thus, K_{IC} is the critical stress intensity fracture value for crack growth (Hertzberg, 1996). Soderholm emphasized that K_{IC} reflects the intensity of the stress field ahead of a crack triggered by a mode I failure (Soderholm, 2010). He further outlines the power of the stress intensity factor approach, when crack propagation occurs. K_{IC} can be expressed as in Equation 8 where σ_o is the applied stress at crack growth and Q is a geometry constant (this geometry constant becomes important when determining the sample shape being tested, and thus provides the necessary modifications to the formula):

$$K_{IC} = Q\sigma_0 a^{1/2}$$

Equation 8: Irwin's (1957) plane strain K_{IC} formula

When a sample is thin enough, there is a minimal zone of plastic deformation surrounding the crack tip. This results in a situation whereby plane-stress conditions prevail and the material exhibits its maximum toughness, however, when thickness increases, the plastic zone of deformation is constrained and plane strain conditions increase. Plane strain fracture toughness, K_{IC}, occurs as a result, and this represents the minimum value needed for a crack to propagate. In other words, once a certain thickness is reached, specimen geometry no longer has an impact on the calculation of K_{IC} and it becomes solely an intrinsic property of the material itself.

Guazzato et al stated, “fracture toughness, which is independent of flaw distribution, is believed to be a more consistent property” and ultimately, this test determines the ability of a material to resist crack propagation (Guazzato et al, 2004). Yoshimura et al (2012) summarized this test as “the measure of a material's ability to absorb energy from elastic deformation, in relation to the level of tensile stress that can be achieved near the crack tip before the initiation of catastrophic fracture” (Yoshimura et al, 2012). Since brittle dental materials (especially ceramics) are unable to absorb appreciable quantities of elastic strain energy prior to fracture, the value of fracture toughness (K_{IC}) then becomes a measure of the strain-energy absorbing ability of the particular material (Yoshimura et al, 2012).

1.3.2.2 Methods of Measuring Fracture Toughness

As aforementioned, once modifications to the fracture toughness formula are made, known as the stress intensity calibration, many different shapes of material samples can be tested and compared.

Some commonly used test methods include:

a. Single edged notched beam (SENB)
b. Single edged precracked beam (SEPB)
c. Chevron notched short rod/Chevron notched short bar (CNSR/CNSB)
d. Surface crack in flexure (CT)
e. Indentation fracture (IF)
f. Indentation strength (IS)

Many studies have been initiated comparing identical materials using different test methods and unfortunately, many of these methods do not produce the same results, nor do they produce the same rankings for different materials, which is then a clear indication that some of these test methods are not accurate (Wang et al, 2007). Furthermore, conventional fracture mechanics testing methods as outlined above are wrought with inherent difficulties in their respective methodologies. These include difficulty minimizing the notch tip width in SENB, detecting stable crack growth (CNSR, CNSB, CT), controlling and measuring the length of the pre-crack (CT, SEPB), mastering specimen preparation (CT, IF, IS), sample preparation (all methods) and controlling the environment (Scherrer et al, 1998).

A popular, well-tested method for determining K_{IC} is the chevron notched short rod or bar (CNSR or CNSB) fracture toughness test. Pioneered by Barker in 1977, it allowed the preparation of specimens without the need for a pre-cracking procedure, the source of numerous problems in other test methods (Barker, 1977). Crack development happens at the tip of the chevron notch early in the loading and, based on their formula, allows easy calculation of K_{IC} (Bubsey et al, 1982). This formula and sample test specimen arrangement is given in Figure 19.

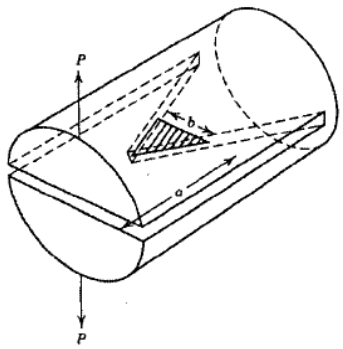

$$K_I = \frac{P}{D\sqrt{W}}Y$$

D = specimen diameter

W = specimen length

Y = dimensionless stress intensity factor coefficient

Figure 19: Chevron notch short rod (CNSR) test method (figure from Bubsey et al, 1982)

Bubsey et al performed compliance calibration calculations to determine the stress intensity factor for various short rod specimen proportions with a straight through crack (Bubsey, 1982). In performing the compliance calibrations, they found that for a brittle material, maximum load occurs when Y (the stress intensity factor coefficient) is at a minimum (Y^*_{min}) and catastrophic failure then occurs at K_{IC} as given in Equation 9.

$$K_{IC} = \frac{P}{D\sqrt{W}} Y^*_M$$

Equation 9: CNSR K_{IC} formula (Bubsey et al, 1982)

Although well accepted and well used, this test method is still limited by the cumbersome process and subsequent inherent difficulties in sample preparation. Building upon the "intrinsic shape" in the chevron notch test, Ruse et al developed a new method, the notchless triangular prism (NTP) specimen K_{IC} test, whereby a triangular prism of 6x6x6x12 mm is held in a split metal cylinder in order to achieve a configuration similar to that of the CNSR specimen (Ruse et al, 1996). In this fashion, the values for K_{IC} can be calculated using the standard CNSR formula proposed by Bubsey et al (Ruse et al, 1996). Figure 20 shows the test apparatus in the NTP test method.

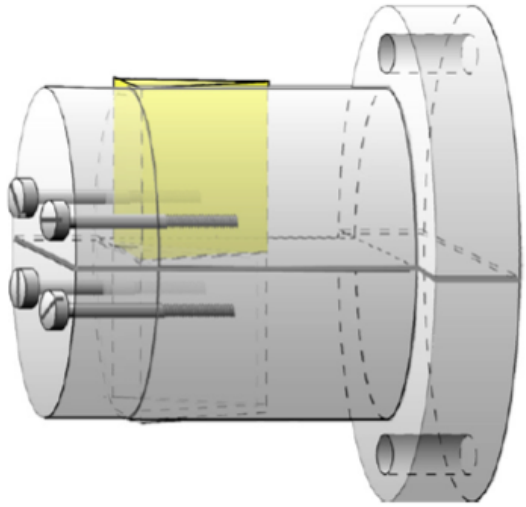

Figure 20: NTP test apparatus (Soderholm, 2010)

Via linear extrapolation and based upon the work done by Bubsey, Ruse et al calculated a Y^*_{min} to be 28 and that the test results, when compared to results of similarly tested materials with other test methods, showed excellent correlation (Ruse et al, 1996). According to Ruse et al, the NTP test has the following advantages (Ruse et al, 1998):

a. Ease of specimen fabrication;
b. Use of small enough samples to approximate actual clinical situations;
c. Avoidance of the need of cutting chevron notches into samples thereby eliminating the introduction of surface flaws;
d. Enabling of testing of very brittle materials with very small K_{1C} (as no notches need to be cut into the sample);
e. Avoidance of embedding tooth tissues for interfacial adhesive tests;
f. Reproducibility of test conditions by means of a specimen holder.

Soderholm, in his review on fracture mechanics testing, stated that "of the different chevron notch tests, Ruse et al's approach stands out when it comes to simplicity in sample preparation…and that of all the different test approaches, the one proposed by Ruse et al might have the most potential because of its simplicity in comparison to most other approaches (Soderholm, 2010).

The formula for calculating the K_{IC} utilizing the notchless triangular prism method is given in Equation 10.

$$K_{IC} = Y^*_{min} \frac{P_{max}}{DW^{1/2}}$$

Equation 10: K_{IC} formula

1.3.3 Clinical Relevance of Materials Testing

In 1969, Bjorn Hedegard stated that "with sound clinical research on a larger and more penetrating scale, data and information may be obtained, that will make it possible to set up more meaningful test procedures in the laboratory. And that is the goal: to be able to characterize the dental material in the laboratory and correctly predict its clinical performance" (Hedegard, 1969). The difficulty in realizing this statement is at minimum threefold. Firstly, the harsh oral environment that dental biomaterials are subjected to is difficult if not impossible to replicate in-vitro and although attempts are made with thermocycling, fatigue testing and aligning applied loads at various angles, these likely only scratch the surface of replicating the in-vivo

environment. Secondly, in order for a dental material to be used, it must be done so via the clinician. The skills of the clinician and the assurance that all necessary clinical steps are undertaken and adhered to in the correct application and use of a material, are paramount for material survival and success, but cannot be assured. Small clinical procedural errors can lead to magnified and catastrophic material responses/failures. Thirdly, dental biomaterials have intrinsic and randomly dispersed flaws and inclusions that directly affect their mechanical properties. Although analyses such as Weibull statistics are used to ascertain probability values instead of absolute values, these also can be nothing more than informed and educated estimations.

Although the common mode of failure of a dental material is tensile, any force applied to a restoration is more likely a combination of compressive, tensile and shear forces in action. Therefore, flexural strength testing (via a three-point bend test), which results in tensile, compressive and shear stresses in the same specimen, best "replicates" the manner in which many materials are stressed intraorally (Manhart et al, 2000). This test provides the investigator with a range of stress values for a given material, however, the found value is affected by flaw distribution, testing conditions, specimen size, elastic limitations and failure mode (Kelly, 1995).

Kelly further stated that correlation of strength data to clinical behavior is dependent on the following four factors (Kelly, 1995):

a. Critical flaws in test specimens replicate those involved with clinical failure;
b. Environmental factors are replicated in the lab;
c. Failure parameters regarding flaw size distribution and crack growth rates are known;
d. Stress distributions in clinical situation are well characterized.

However, even if those conditions are met, strength values by themselves do not provide enough information to decide whether or not a treatment process has improved the resistance to fast fracture (Mecholsky, 1995).

Measurement of the elastic modulus of a material is important in relation to anticipated longevity of a restoration and it is important for restorative materials to have moduli similar to the tooth tissues they replace (Burke, 2002). A material with low elastic modulus undergoes significant deformation, could fail at low stresses and could lead to marginal gaps (and thus marginal degradation and microleakage) thus causing premature failure (Tyas, 1990).

The fracture toughness, which measures the resistance of a material to the propagation of a crack, is an intrinsic property of a material (Burke, 2002). Because K_{IC} is an inherent property of all materials (and relates to crack propagation as opposed to crack initiation), in vitro K_{IC} testing of any new dental material is imperative prior to use in the oral environment as this property is material specific and not environment specific. The results of this specific test will ideally predict how any dental material desired for indirect restorations will resist crack propagation intraorally.

Although each of these tests is important within their own right, analyzing these results collectively provides a more accurate picture. De Groot et al, using a three-point bend test, found that the combination of elastic modulus, flexural strength and fracture toughness provided the best prediction for deflection and load at failure as opposed to each property by itself (De Groot et al, 1988). Similarly, Lewis found that the best predictor of wear requires consideration of these same factors in addition to resilience (Lewis, 1993).

Ultimately, dental biomaterials that satisfy the aesthetic demands of the patient, withstand the biomechanical forces placed upon during normal function/parafunction and that are easy to fabricate, use, and manipulate are few and far between. In advance of long-term clinical trials, biomechanical testing of any new restorative product is required to initially validate the manufacturer's claims. As aforementioned, K_{IC}, σ_f and E_f are critical mechanical properties that help predict how a biomaterial will respond intraorally and thus, an understanding of these properties is integral to be able to satisfy the demands of adhering to evidence based dentistry when one elects to use this material for a patient's restorative needs. However, even with these best predictions, waiting for results from long-term clinical trials is still more applicable and accurate when it comes to the intraoral restorative performance of dental biomaterials.

Chapter 2: Rationale

2.1 Specific Aims

The goal of this study was to determine the flexural strength (σ_f), flexural modulus (E_f) and fracture toughness (K_{IC}) of two new commercially available nano-ceramic resin composite CAD/CAM blocks (Lava Ultimate CAD and Enamic CAD) and compare them to those of a widely-used ceramic CAD/CAM block (IPS e.max CAD), that served as a control, in order to evaluate the clinical suitability of the former.

2.2 Null Hypotheses

Specifically, the following null hypotheses were tested:

a. There is no difference between the tested mechanical properties (namely σ_f, E_f, and K_{IC}) of non-aged Lava Ultimate or Enamic when compared to IPS e.max CAD;

b. There is no effect of aging Lava Ultimate and Enamic samples in 37 °C water for 30 days on the tested mechanical properties;

c. There are no differences between Enamic and Lava Ultimate with regards to the tested mechanical properties.

Chapter 3: Materials and Methods

3.1 Tested Materials

IPS e.max CAD, a lithium disilicate ceramic, was tested as a control group. Lava Ultimate and Enamic, the two new NCRCs on the market were then tested and compared.

The initial group of Enamic samples that was obtained directly from the inventor of this material has been classified as the experimental Enamic and was not available for consumer use. Although verbal assurances were obtained that indicated that these samples only possessed colour deficiencies that prevented them from being suitable for commercial use, sample specific testing problems occurred that demanded that commercial samples be obtained. Once obtained, this group was then categorized as commercial Enamic.

3.2 Flexural Strength and Flexural Modulus

In order to assess flexural strength and flexural modulus, σ_f and E_f respectively, a three-point bend test was employed according to ISO 6872.

3.2.1 Samples/Groups

Twenty-five bar samples of the following groups/sizes were fabricated for three-point bend testing:

a. Non-Aged Lava Ultimate (4 X 2 X 20 – tested on a 20 mm span);

b. Aged Lava Ultimate (4 X 2 X 20 – tested on a 20 mm span);

c. Non-Aged Experimental Enamic (4 X 1.2 X 16 – tested on a 12 mm span);

d. Aged Experimental Enamic (4 X 1.2 X 16 – tested on a 12 mm span);

e. Non-Aged Commercial Enamic (4 X 1.2 X 16 – tested on a 12 mm span);

f. Aged Commercial Enamic (4 X 1.2 X 16 – tested on a 12 mm span);

g. Non-Aged e.max CAD (4 X 1.2 X 16 – tested on a 12 mm span).

The varying specimen sizes were due to limitation imposed by the initial size of the blocks themselves. The test protocols set forth in ISO 6872 firmly state that the thickness of the sample should be no more than $1/10^{th}$ the distance between the supports, hence, the varying sample dimensions to ensure adherence to the ISO specifications.

Aging of the resin composite samples was accomplished via storage in water at 37°C for 30 days. The ceramic samples were not aged.

3.2.2 Sample Preparation

Lava Ultimate CAD (3M ESPE, St. Paul, MN, USA) samples were separated from their plastic housings and any adhesive residue was peeled away. The metal handles on the IPS e.max CAD (Ivoclar, Schaan, Liechtenstein) blocks and the Vita Enamic CAD (Vident, Bad Sackingen, Germany) blocks were removed leaving simply the blocks themselves. Utilizing sticky wax (Kerr, Romulus, MI, USA), each block was adhered to a metal housing (single saddle chuck) and placed on a low speed Isomet saw (Buehler, Lake Bluff, IL, USA). Under constant water irrigation, pre-measured precision cuts were made utilizing a diamond-wafering blade (UKAM, Valencia, CA, USA) to obtain the aforementioned predetermined sized samples. Each sample was then polished using 600 grit abrasive disks (Beuhler, Lake Bluff, IL, USA) mounted onto a Buehler Metaserv wheel grinder (Beuhler, Lake Bluff, IL, USA) to render them ready for testing.

IPS e.max bars were then crystallized at 850°C in a Programat CS ceramic and crystallization furnace, according to the preset IPS e.max conditions programmed into the furnace by the manufacturer.

Precise determination of the dimensions of each sample was made and recorded using digital calipers (Mitutoyo, Kawasaki, Japan).

Figure 21 shows a prepared sample ready for testing.

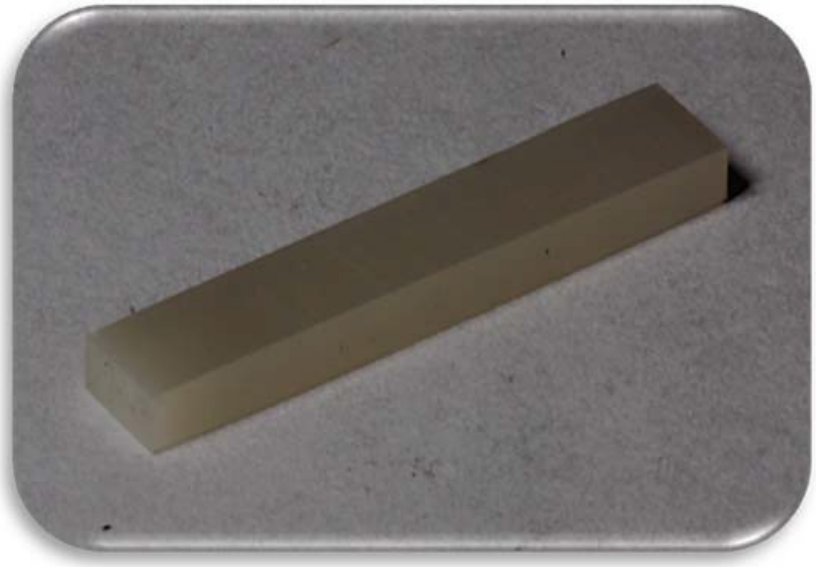

Figure 21: Three-point bending test bar sample

Figure 22 show the Isomet low speed saw and the Metaserv wheel grinder used to prepare the samples.

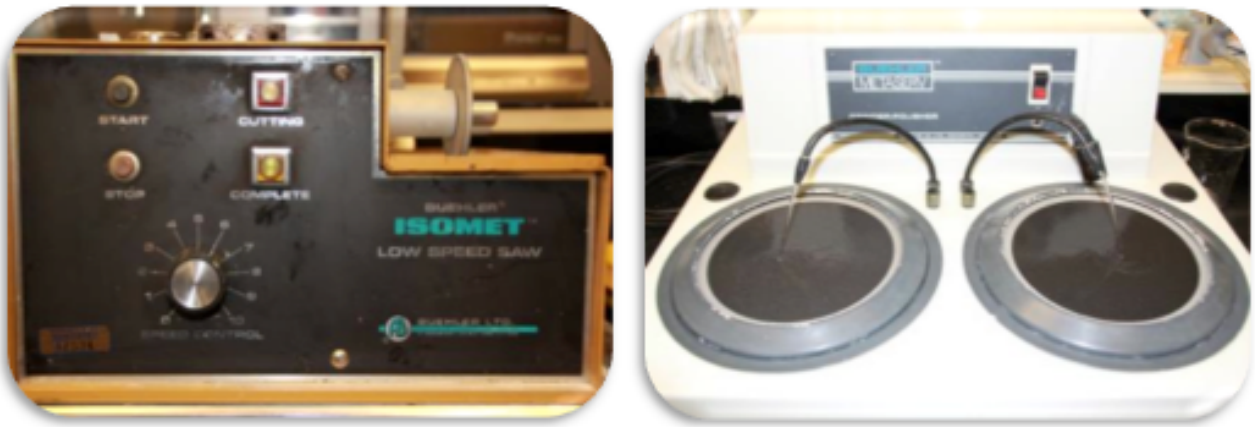

Figure 22: Isomet low speed saw and Metaserv wheel grinder

3.2.3 Three Point Bending Test

A computer-controlled Instron 4301 universal testing machine, with a 1 kN Instron load cell, was used for three-point bend testing. Specifically, the samples were placed on a precision milled custom jig (UBC Engineering Department, Vancouver BC, Canada) that supported the entire width of the bars on 2 mm diameter roller pins such that the pins were equidistant from the length edges of the beam. As aforementioned, the specific dimensions of the bars (depth, width, span length) were precisely measured with digital calipers and inputted individually into the controlling software prior to testing. A central force was applied at a constant crosshead speed of 1 mm/min until failure. The results for σ_f and E_f were calculated, based on the test data, by Bluehill 2 software (Instron USA, Norwood, MA, USA).

Figure 23 shows the test arrangement with a bar arranged on the custom jig/rollers prior to application of the central force.

Figure 23: Three-point bend test set-up

The maximum load recorded at failure was used to calculate $\sigma_{f,}$ in MPa, using equation 11 where P = maximum load; L = span between supports; b = specimen width; and t = specimen thickness.

$$\sigma_f = \frac{3PL}{2bt^2}$$

Equation 11: Flexural strength formula from a three-point bend test

The slope ($\delta P/\delta d$) of the straight portion of the load-displacement curve obtained during the three-point bend test was used to calculate the E_f in GPa using Equation 12 where again, P = maximum load; L = span between supports; b = specimen width; t = specimen thickness; and d = the displacement.

$$E_f = \frac{L^3}{4bt^3}\frac{\delta P}{\delta d}$$

Equation 12: Flexural modulus formula from a three-point bend test

3.3 Fracture Toughness

In order to assess fracture toughness, K_{IC}, the notchless triangular prism (NTP) specimen K_{IC} test (Ruse et al, 1996) was used and adhered to the principles of ISO 18756.

3.3.1 Samples/Groups

Fifteen 6X6X6X12 equilateral triangular prisms of the following groups (except where indicated) were fabricated for the NTP specimen K_{IC} test for the following groups:

a. Non-Aged Lava Ultimate;

b. Aged Lava Ultimate;

c. Non-Aged Experimental Enamic;

d. Aged Experimental Enamic;

e. Non-Aged Commercial Enamic (8 samples);

f. Aged Commercial Enamic (8 samples);

g. Non-Aged e.max CAD.

Aging of the samples was accomplished via storage in water at 37°C for thirty days.

3.3.2 Sample Preparation

Lava Ultimate samples were separated from their plastic housings and any adhesive residue was peeled away. The metal handles on the IPS e.max CAD blocks and the Vita Enamic blocks were removed leaving simply the blocks themselves. Utilizing sticky wax each block was adhered to a metal housing (single saddle chuck) and placed on a low speed Isomet saw. The blocks were cut into four roughly equal sized blocks using the same grit diamond-wafering blade under constant water irrigation. Each sample was then mounted in a custom jig (UBC Engineering Department, Vancouver BC, Canada) that when rotated and polished using 240, 400 and 600 grit abrasive disks mounted onto a Buehler Metaserv wheel grinder under constant water irrigation, 6X6X6X12 mm equilateral triangular prisms resulted that were ready for testing.

IPS e.max prisms were then crystallized at 850°C in a Programat CS ceramic and crystallization furnace, according to the preset IPS e.max conditions programmed into the furnace by the manufacturer.

Figures 24 and 25 shows the custom jig used to prepare the equilateral prism samples.

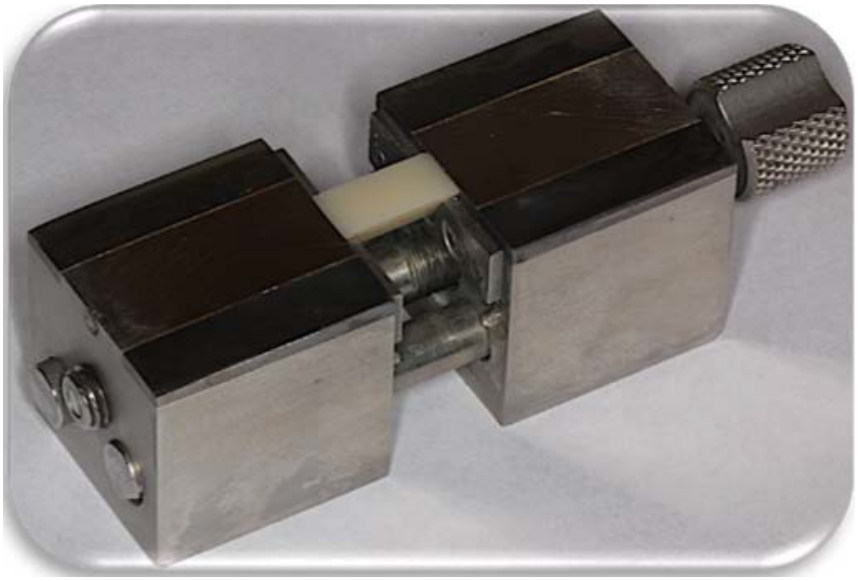

Figure 24: Custom jig for NTP specimen preparation

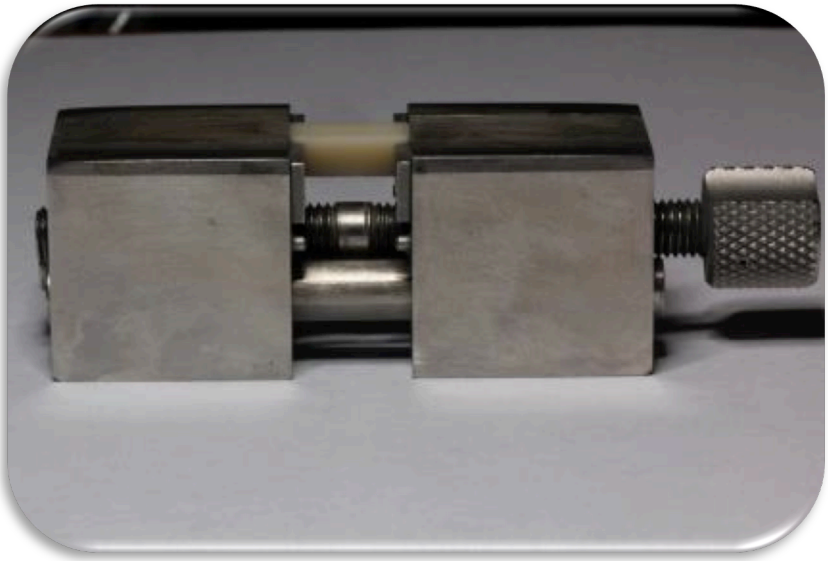

Figure 25: Custom jig for NTP specimen preparation

Figure 26 shows a sample of the equilateral triangle ready for testing according to the NTP specimen K_{IC} test protocol.

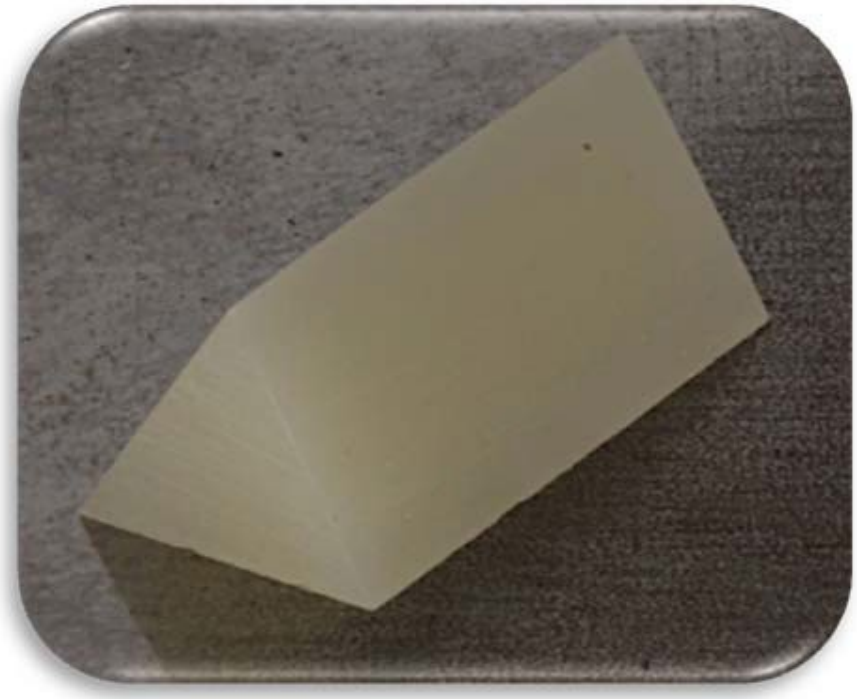

Figure 26: Equilateral NTP specimen

3.3.3 Fracture Toughness Test

The assembly of the NTP specimen and the specimen holder achieves a final configuration similar to the one present in a CNSR test. The prism, when fitted into the holder, reproduces the chevron shape of the area to be fractured during the test.

Figure 27 shows these comparable test shapes.

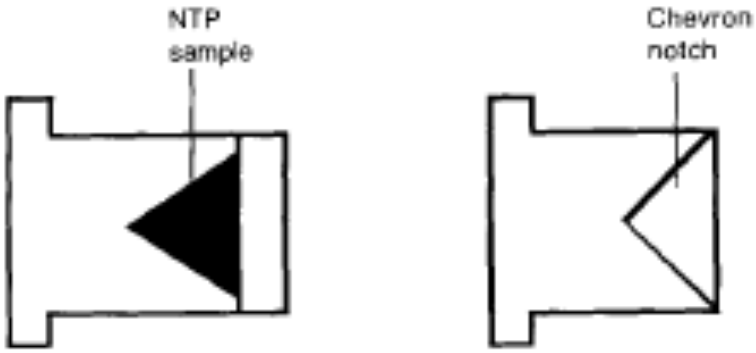

Figure 27: Similarity of NTP sample and CNSR sample (Ruse et al, 1996)

The holder has four components: two symmetrical half cylinders (ϕ = 12 mm, h = 9 mm) with a loading collar (ϕ = 18 mm, h = 3 mm) at one end and a triangular prismatic groove (6x6x6x6 mm) at the other form the base into which the NTP specimen is placed; two symmetrical half-disks (ϕ = 12 mm, h = 3 mm), fastened with screws across the triangular grooves of the corresponding half-cylinders of the base, restrain the NTP specimen. The split circular opening (ϕ = 18 mm, h = 5 mm) in the center of the upper mounting block can accommodate the two symmetrical half-cylinders of the holder. One half of the upper part of the mounting block slides horizontally, allowing the placement of a spacer (200 μm) between the two halves.

Figures 28 and 29 show this custom NTP specimen holder with a specimen in place.

Figure 28: NTP specimen holder

Figure 29: NTP specimen holder

The specimen holder halves were placed into the mounting jig and kept apart by a 200 μm thick spacer. A sharp razor blade was used to create a ~0.1 mm deep crack initiation point midway along one of the edges of the NTP specimen. The specimen was then placed into the groove with the crack initiation point aligned with split line of the holder and was secured in place by the two-screw-tightened lids. Figure 30 shows the specimen holder in the mounting with the spacer in place.

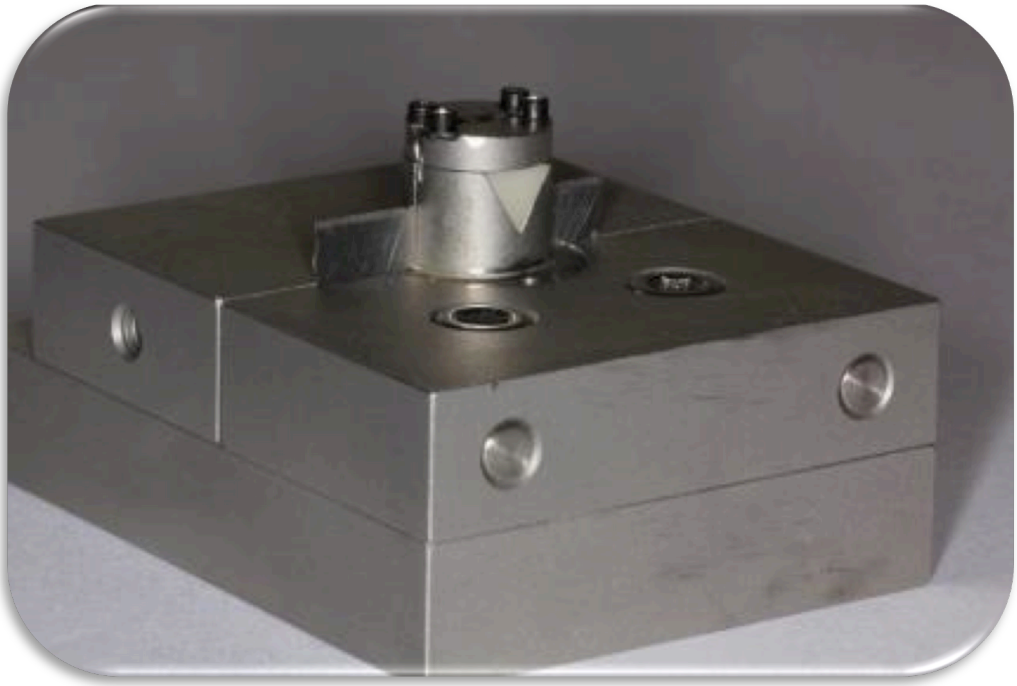

Figure 30: NTP specimen holder in mounting with spacer

The test assembly was then secured in the custom designed grips attached to a computer-controlled Instron 4301 universal testing machine, with a 1 kN Instron load cell. The assembly was loaded in tension at a crosshead speed of 0.1 mm/min, and the load and the displacement were constantly monitored and recorded until crack propagation or crack failure.

Figure 31 shows the NTP specimen test assembly loaded in the Instron machine.

Figure 31: NTP specimen loaded for testing

The maximum load recorded before crack arrest or complete failure was used to calculate K_{IC} using Equation 13 where P_{max} = maximum load recorded during testing; D = specimen diameter (12 mm); W = specimen length; Y^*_{min} = dimensionless stress intensity factor coefficient minimum (equal to 28 for the NTP test) (Ruse et al, 1996).

$$K_{IC} = Y^{*}_{min} \frac{P_{max}}{DW^{1/2}}$$

Equation 13: Fracture toughness formula using NTP specimen test

3.4 Scanning Electron Microscopy

One of the aims of fractographic examination is to determine the cause of failure by studying the features of a fractured surface. Surface characteristics due to crack growth can be evident, which then aid in determining the mode of failure. Often, this analysis must be carried out a resolution level much finer than produced by an optical microscope thus rendering a scanning electron microscope (SEM) a necessity. The SEM uses a focused beam of electrons whose wavelength is much lower than that of light thus allowing for the resolution of an image of a surface at the nanoscale level. Visualizing fractured material surfaces and their characteristics at this detail then allows for material structural analysis and for characterization of fracture paths.

Following K_{IC} testing, selected samples closest to the mean of each group and selected samples that fractured prematurely were selected for SEM observation. The specimen halves were mounted, labeled and subsequently gold coated with an Edwards S150A sputter coater (Edwards Vacuum, Crawley, UK). The specimens were then observed under a scanning electron microscope (Cambridge Stereoscan 260, Cambridge Instruments, England). Photomicrographs were taken at various magnifications.

Figure 32 shows the mounted samples prior to gold coating.

Figure 32: SEM samples

3.5 Statistical Analysis

The results were subjected to statistical analysis using SSPS (IBM, Armonk, NY, USA). Student t-tests were first used to determine if the groups, especially the experimental and commercial Enamic, were significantly different from each other. Additionally, a two-way ANOVA followed by post-hoc modified Scheffé procedure were used to search for significance of the impact of each independent variable on the results.

Weibull statistics (Weibull, 1951) were then used because for brittle materials, the maximum stress that a sample can withstand before failure is unpredictable and varies from specimen to specimen, even under identical testing conditions, due to inherent flaws present in the material from manufacturing and manipulation (Nohut and Lu, 2012). Weibull statistics are used to estimate the cumulative probability that a given brittle sample will fail under a given load and is essentially a measure of the variability of the strength of a material (McCabe and Carrick, 1986). Weibull statistics offer more clinically relevant parameters and enable the evaluation of

the dependability of a material. Specifically, the characteristic strength, σ_θ (or scale parameter) is the value whereby 63.2 % of the tested samples would have failed/fractured and the Weibull modulus, m (or shape parameter) is the slope of the Weibull plot. The probability of a given sample fracturing below a tensile stress (σ) is given by Equation 14, whereby P_f = probability of failure; m = Weibull modulus; σ_θ = characteristic strength; and σ_u = minimum stress under which a specimen will not break.

$$P_f = 1 - \exp\left(\frac{\sigma - \sigma_u}{\sigma_\theta}\right)^m$$

Equation 14: Probability of failure formula for Weibull statistics

For my analysis, the characteristic strength and Weibull modulus were determined and compared between the respective groups. A high Weibull modulus indicated that the determined characteristic strength served as a good description of the sample-to-sample performance and that physical flaws, whether inherent to the material itself or resulting from the manufacturing process, were distributed uniformly throughout the material.

Chapter 4: Results

4.1 Flexural Strength (σ_f)

The means, standard deviations, Weibull modulus and characteristic strength for all groups are given in Table 3. Outliers, one to four per group, having a value over two standard deviations below the mean (due to sample preparation defects) were excluded from the calculations.

Material	σ_f	Weibull Modulus (m)	Weibull characteristic strength (σ_θ)
e.max CAD	359.87 ± 30.93 MPa (n = 22)	13.75	383.22 MPa
Non-Aged Lava Ultimate	155.31 ± 17.28 MPa (n = 22)	10.62	166.43 MPa
Aged Lava Ultimate	114.81 ± 12.94 MPa (n = 21)	10.46	122.96 MPa
Non-Aged Commercial Enamic	145.64 ± 6.52 MPa (n = 23)	26.99	151.84 MPa
Aged Commercial Enamic	128.03 ± 7.95 MPa (n = 21)	19.49	134.32 MPa
Non-Aged Experimental Enamic	139.90 ± 8.49 MPa (n = 24)	19.73	146.80 MPa
Aged Experimental Enamic	123.84 ± 8.48 MPa (n = 24)	17.50	130.32 MPa

Table 3: Flexural strength results

This data clearly shows that the strength of NCRC groups was significantly below that of e.max CAD. With the NCRCs, the following observations were made:

- Lava Ultimate was statistically significantly different than both the commercial and experimental Enamic groups in both the aged and non-aged groups;
- Non-aged commercial and experimental Enamic were statistically significantly different, however, the aged samples were not statistically significantly different;
- The aging effect was statistically significant in all groups and more pronounced in Lava Ultimate compared to either Enamic group (27 % vs 12 %);
- The Weibull modulus of all the Enamic groups was noticeably higher than either the e.max CAD or Lava Ultimate groups – attributed to the consistent method of production.

Figure 33 shows a boxplot of the absolute σ_f values of all the commercially available groups. This graph clearly shows the substantial difference between the control ceramic e.max CAD and the two NCRCs. It also readily shows the decrease of σ_f that occurred as a result of aging the samples in 37 °C water for thirty days.

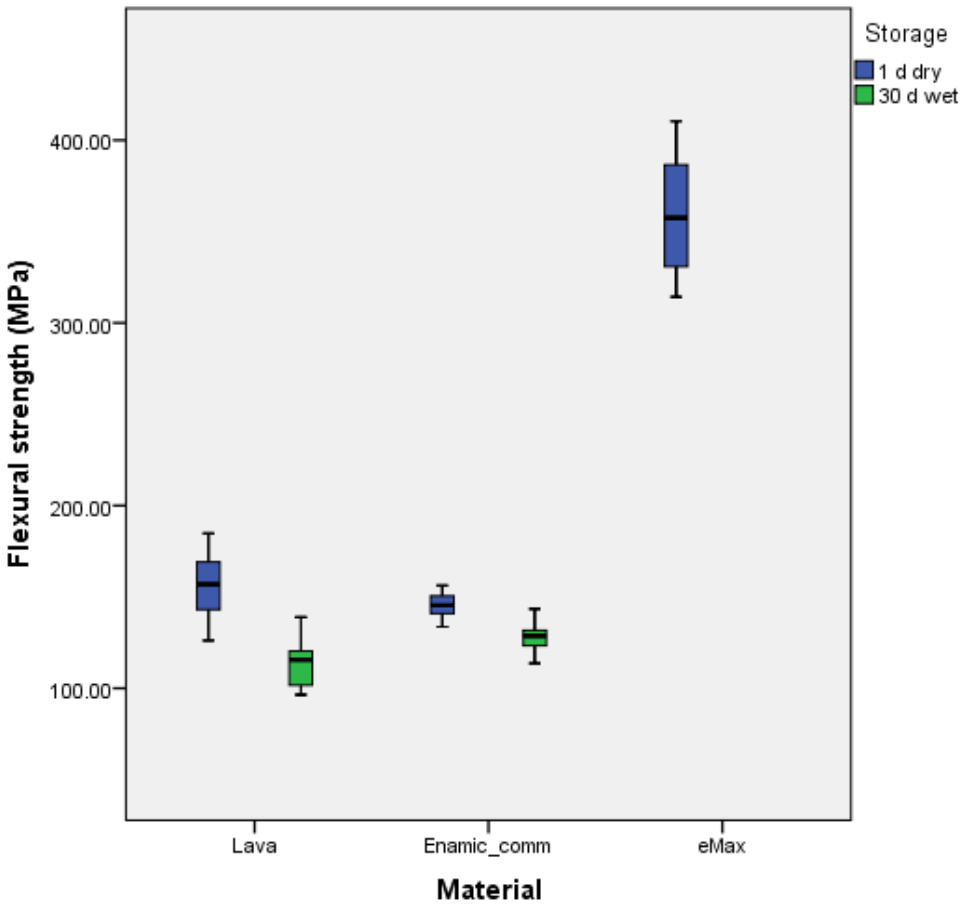

Figure 33: Flexural strength boxplot

Table 4 shows the results of the ANOVA for σ_f when examining all Lava Ultimate and Enamic samples together; when examining just the non-aged samples in isolation; and when examining just the aged samples in isolation.

Groups	Type III Sum of Squares	df	Mean Square	F	Sig
All samples	24281.486	5	4964.297	42.322	0.00
Non-aged samples	2765.219	2	1382.609	10.924	0.00
Aged samples	1924.666	2	962.333	9.674	0.00
Material * Storage	4124.609	2	2062.304	17.582	0.00

Table 4: Flexural strength ANOVA

Table 5 summarizes the post-hoc Scheffé analysis where, when all samples are grouped together (aged and non-aged), it shows that only one subset exists (expressed in MPa). However, when broken down individually into aged and non-aged as separate groups, there is not a significant difference between the commercial and experimental Enamic groups however, there is a significant difference between these groups and the Lava Ultimate group.

Scheffe[a,b,c]

Material	N	Subset
		1
Enamic_exp	48	131.8696
Lava	43	135.5293
Enamic_comm	44	137.2352
Sig.		.067

Scheffe[a,b,c]

Material	N	Subset	
		1	2
Enamic_exp	24	139.9021	
Enamic_comm	23	145.6409	
Lava	22		155.3086
Sig.		.252	1.000

Scheffe[a,b,c]

Material	N	Subset	
		1	2
Lava	21	114.8081	
Enamic_exp	24		123.8371
Enamic_comm	21		128.0290
Sig.		1.000	.386

Table 5: Scheffé post-hoc σ_f analysis (all groups; non-aged; and aged respectively)

Figure 34 shows the Weibull distribution for σ_f whereby P_f is the probability of failure.

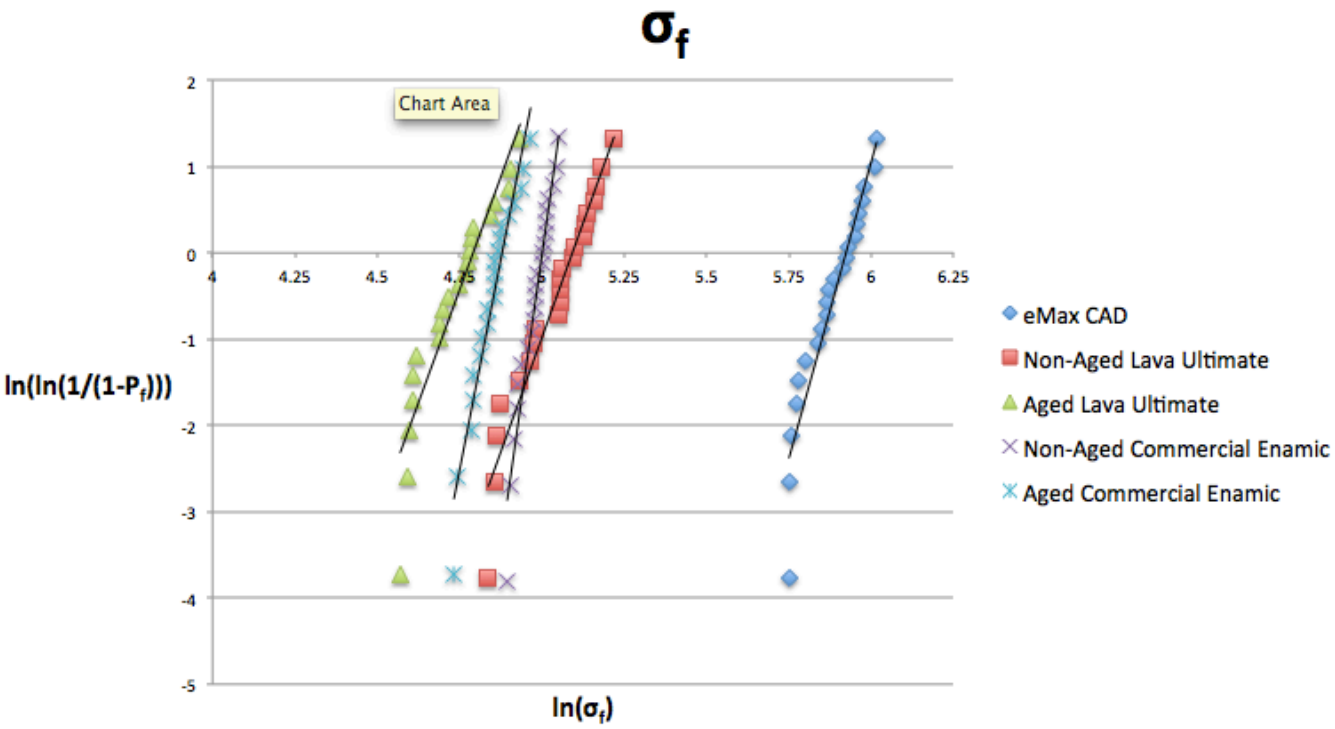

Figure 34: Weibull plot for flexural strength

This graphical representation shows that all the samples are appropriately fitted to the straight lines of the Weibull unimodal distribution. Furthermore, this graphically shows, via the more vertical trendlines, that the commercial Enamic, either aged or non-aged, behaved more predictably with regards to σ_f.

4.2 Flexural Modulus (E_f)

The means and standard deviations for all groups are given in Table 6. Outliers, one to three per group, having a value over two standard deviations below the mean (due to sample preparation defects) were excluded from the calculations.

Material	E_f
e.max CAD	69.29 ± 5.19 GPa (n = 22)
Non-Aged Lava Ultimate	14.21 ± 0.81 GPa (n = 22)
Aged Lava Ultimate	13.04 ± 0.91 GPa (n = 21)
Non-Aged Commercial Enamic	32.93 ± 2.78 GPa (n = 23)
Aged Commercial Enamic	31.09 ± 2.61 GPa (n = 21)
Non-Aged Experimental Enamic	29.20 ± 3.03 GPa (n = 24)
Aged Experimental Enamic	27.93 ± 1.86 GPa (n = 24)

Table 6: Flexural modulus results

This data clearly shows that the NCRC groups have values much below that of e.max CAD. For the NCRCs, the following observations were made:

- The effect of aging was statistically significant in Lava Ultimate and the commercial Enamic group but not in the experimental Enamic group;
- The mean E_f value for the commercial Enamic groups were statistically significantly higher than that seen in both the corresponding experimental Enamic and Lava Ultimate groups;
- The three groups were statistically significantly different from each other in both the aged and the non-aged groups.

Figure 35 shows a boxplot of E_f values of all the commercially available groups. This graph clearly shows the substantial difference between the control ceramic e.max CAD and the two NCRCs. Although not statistically significant, it also shows the decrease in E_f that occurred as a result of aging the samples in 37 °C water for thirty days.

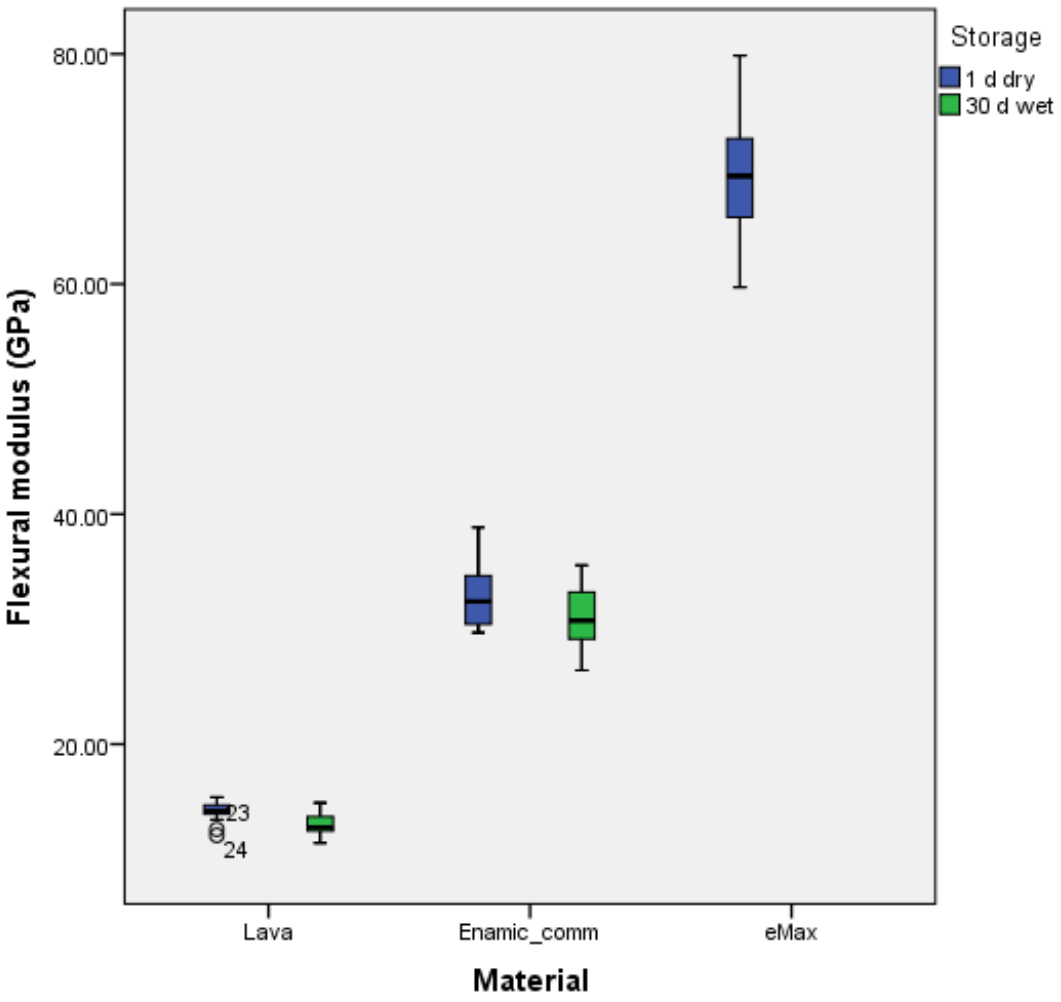

Figure 35: Flexural modulus boxplot

Table 7 shows the results of the ANOVA for E_f when examining all Lava Ultimate and Enamic samples together; when examining just the non-aged samples in isolation; and when examining just the aged samples in isolation.

Groups	Type III Sum of Squares	df	Mean Square	F	Sig
All samples	8957.369	5	1791.474	377.361	0.00
Non-aged samples	4472.233	2	2236.116	380.715	0.00
Aged samples	4409.117	2	2204.558	603.259	0.00
Material * Storage	3.055	2	1.528	0.322	0.725

Table 7: Flexural modulus ANOVA

Table 8 summarizes the post-hoc Scheffé analysis where, when all samples are grouped together (aged and non-aged), it shows that three subsets exist (expressed in GPa). Even when broken down individually into aged and non-aged as separate groups, there were differences between the commercial and experimental Enamic groups and differences between these groups and the Lava Ultimate group.

Scheffe[a,b,c]

Material	N	Subset		
		1	2	3
Lava	47	13.6143		
Enamic_exp	48		28.5656	
Enamic_comm	45			31.9889
Sig.		1.000	1.000	1.000

Scheffe[a,b,c]

Material	N	Subset		
		1	2	3
Lava	23	14.2143		
Enamic_exp	24		29.1971	
Enamic_comm	22			32.9332
Sig.		1.000	1.000	1.000

Scheffe[a,b,c]

Material	N	Subset		
		1	2	3
Lava	24	13.0392		
Enamic_exp	24		27.9342	
Enamic_comm	23			31.0857
Sig.		1.000	1.000	1.000

Table 8: Scheffé post-hoc E_f analysis (all groups; non-aged; and aged respectively)

4.3 Fracture Toughness (K_{IC})

In testing to determine $K_{IC,}$ a small number of samples were excluded if they were not of ideal equilateral triangular prismatic shape and thus could not be held firmly in the custom jig to be tested, failed/prematurely fractured during mounting or exhibited unusual load-deflection curves. The majority of these samples belonged to one of two groups. Firstly, six samples of the IPS e.max CAD group had to be excluded as the preparation of the samples was more difficult and resulted in a few samples being too small for the specimen holder. Secondly, more than four samples of the non-aged experimental Enamic group fractured post-crack initiation as the specimen holder was being closed prior to testing. As a result, the number of samples that failed prematurely resulted in less than sixteen samples being analyzed.

As a result of these pre-test Enamic failures, commercial Enamic samples were obtained to both see if these testing failures continued to occur and to validate the results of those samples that were successfully tested. However, as aforementioned, only a limited number of commercial Enamic CAD blocks were available thus limiting the number of triangular prism samples that could be prepared.

The means and standard deviations for all groups are given in Table 9.

Material	K_{IC}
e.max CAD	1.88 ± 0.24 MPa·m^{½} (n = 9)
Non-Aged Lava Ultimate	0.91 ± 0.15 MPa·m^{½} (n = 14)
Aged Lava Ultimate	0.99 ± 0.23 MPa·m^{½} (n = 15)
Non-Aged Commercial Enamic	0.93 ± 0.10 MPa·m^{½} (n = 6)
Aged Commercial Enamic	1.30 ± 0.25 MPa·m^{½} (n = 6)
Non-Aged Experimental Enamic	0.88 ± 0.30 MPa·m^{½} (n = 11)
Aged Experimental Enamic	1.00 ± 0.09 MPa·m^{½} (n = 8)

Table 9: Fracture toughness results

This data clearly shows that the NCRCs have values much below that of e.max CAD. Within the NCRCs, the following observations were made:

- The effect of aging was more pronounced in Enamic (statistically significant in the commercial Enamic) as opposed to the Lava Ultimate group;
- Aging caused the K_{IC} to increase in all groups (only significant in the aforementioned commercial Enamic groups).

Figure 36 shows a boxplot of the K_{IC} values of all the commercially available groups. This graph clearly shows the substantial difference between the control ceramic e.max CAD and the two NCRCs. It also readily shows the increase effect on K_{IC} that occurred as a result of aging the samples in 37 °C water for 30 days, especially in the Enamic group.

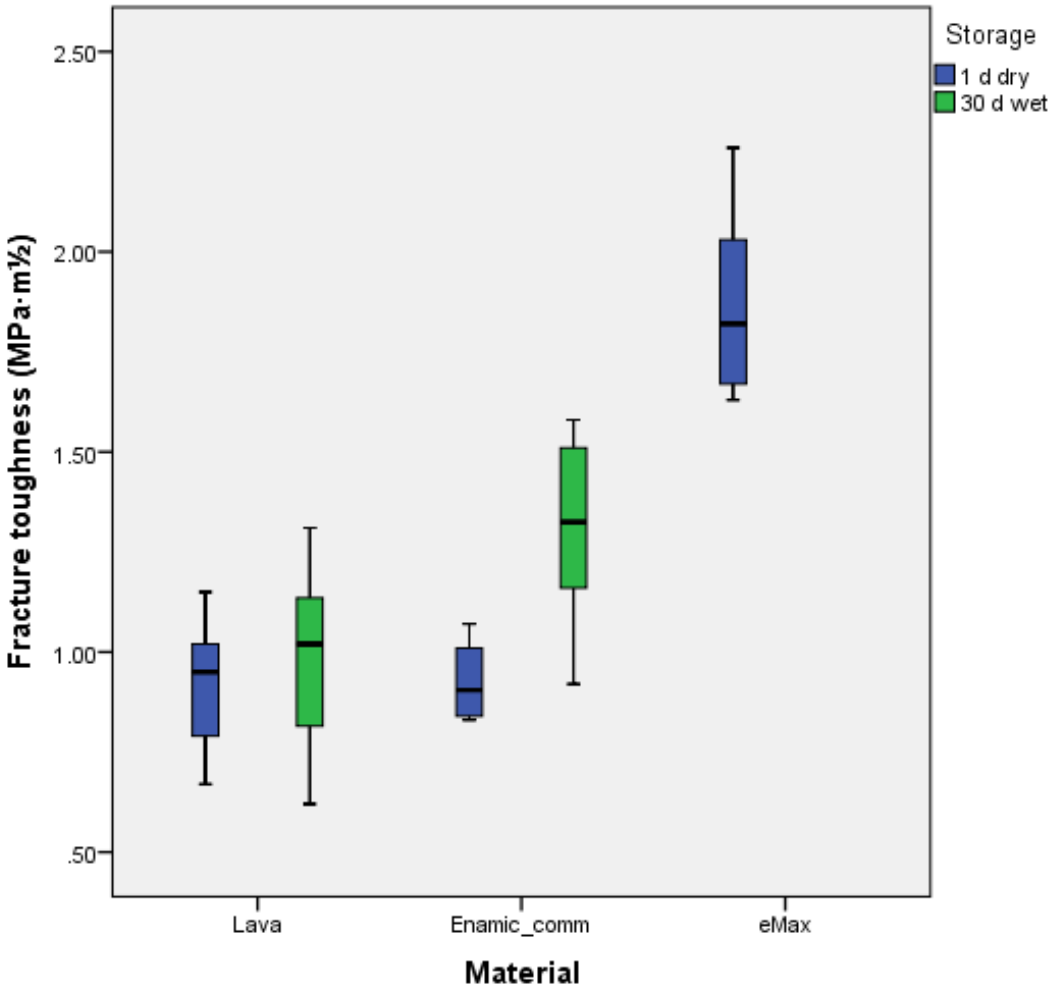

Figure 36: Fracture toughness boxplot

Table 10 shows the results of the ANOVA for K_{IC} when examining all Lava Ultimate and Enamic samples together; when examining just the non-aged samples in isolation; and when examining just the aged samples in isolation.

Groups	Type III Sum of Squares	df	Mean Square	F	Sig
All samples	0.811	5	0.162	3.689	0.06
Non-aged samples	0.009	2	0.005	0.102	0.903
Aged samples	0.463	2	0.232	5.296	0.012
Material * Storage	0.203	2	0.101	2.307	0.109

Table 10: Fracture toughness ANOVA

Table 11 summarizes the post-hoc Scheffé analysis where, when all samples are grouped together (aged and non-aged), it shows that two subsets exist, with Lava Ultimate fitting into both subsets (expressed in $MPa \cdot m^{1/2}$). In other words, the commercial and the experimental Enamic groups behaved differently to be classified into different subsets and the Lava Ultimate bridged these groups. When broken down individually into aged and non-aged as separate groups, the non-aged groups behaved collectively as one subset however, the commercial Enamic group had a significantly higher result than the other two groups.

Scheffe[a,b,c]

Material	N	Subset	
		1	2
Enamic_exp	19	.9337	
Lava	29	.9514	.9514
Enamic_comm	12		1.1150
Sig.		.969	.078

Scheffe[a,b,c]

Material	N	Subset
		1
Enamic_exp	11	.8836
Lava	14	.9143
Enamic_comm	6	.9267
Sig.		.909

Scheffe[a,b,c]

Material	N	Subset	
		1	2
Lava	15	.9860	
Enamic_exp	8	1.0025	
Enamic_comm	6		1.3033
Sig.		.987	1.000

Table 11: Scheffé post-hoc K_{IC} analysis (all groups; non-aged; and aged respectively)

4.4 Commercial vs. Experimental Enamic

The experimental Enamic samples were described as only having colour deficiencies that prevented them from being suitable for commercial use. However, with the advent of sample

failures, some commercial samples were obtained to both verify the initial results and, if similar, increase the number of samples per group. Table 12 shows the results of a student t-test (same tested samples) used to determine if the experimental and commercial Enamic samples could be grouped together into one group and the significance of the results of this test.

		Non-Aged Enamic		Aged Enamic	
		Experimental	**Commercial**	**Experimental**	**Commercial**
Flexural Strength	**Mean**	139.90 MPa	145.64 MPa	123.84 MPa	128.03 MPa
	Significance	0.013		0.096	
Flexural Modulus	**Mean**	29.20 GPa	31.99 GPa	27.93 GPa	31.09 GPa
	Significance	0.00		0.00	
Fracture Toughness	**Mean**	0.88 MPa · $m^{½}$	0.93 MPa · $m^{½}$	1.00 MPa · $m^{½}$	1.30 MPa · $m^{½}$
	Significance	0.742		0.00	

Table 12: Student t-test comparing experimental and commercial Enamic

The following observations were made:

- When examining flexural modulus, in both the aged and non-aged samples, the experimental and commercial groups were statistically significantly different and could not be grouped together;

- When examining flexural strength, the non-aged samples were statistically significantly different and could not be grouped together, however, the aged samples were not statistically different and could be grouped together;
- When examining fracture toughness, the non-aged samples were not statistically significantly different and could be grouped together however, the aged samples were different and could not be grouped.

Due to these inconsistencies both between tests and within tests, the experimental Enamic group and the commercial Enamic group were evaluated and discussed as completely separate entities for all tests.

4.5 SEM Analysis

SEM analysis was conducted on both randomly selected average samples in addition to some samples that failed prematurely in the hopes of viewing the causes of this failure and/or the plane of crack propagation.

As outlined in the methodology, once the triangular prisms were first placed into the specimen holder, a defect was initiated into the leading edge using a sharp razor blade. Figures 37 and 38 show this initiation on a randomly selected non-aged experimental Enamic sample and a randomly selected non-aged Lava Ultimate sample, at 60x magnification.

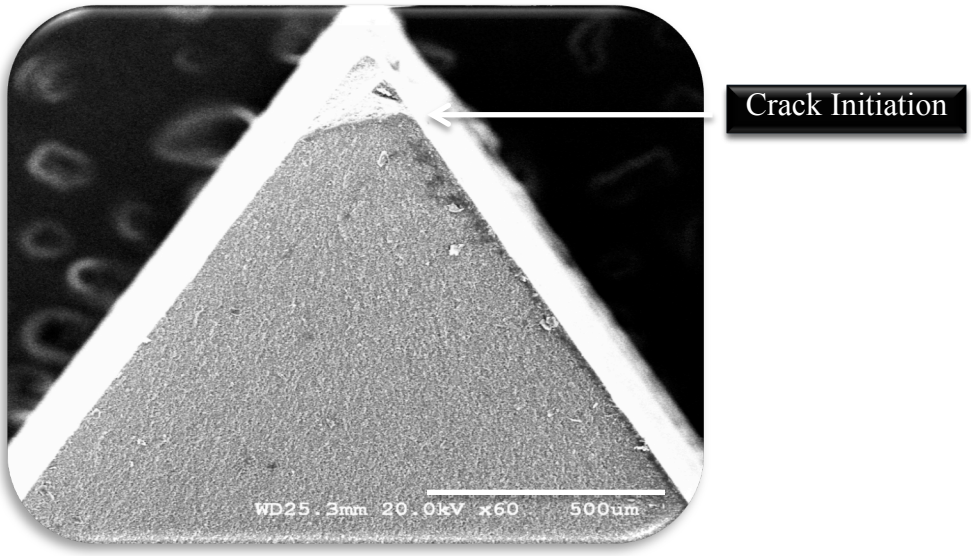

Figure 37: SEM image - Lava Ultimate initiation (bar = 500 µm)

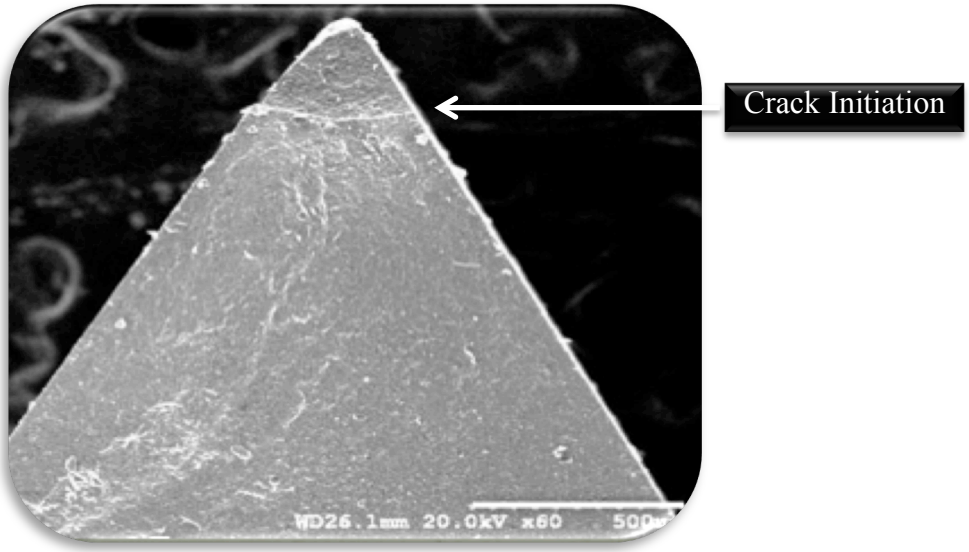

Figure 38: SEM image- experimental Enamic initiation (bar = 500 µm)

As is evident, the size of the initiation remains relatively constant, although, in reality, the size of the initiation does not truly have an impact in determining the fracture toughness of a material as this property is an intrinsic property irrespective of the iatrogenically induced flaw.

Figures 39 and 40, at 1500x magnification, show the effects of aging on a randomly selected, average Lava Ultimate sample.

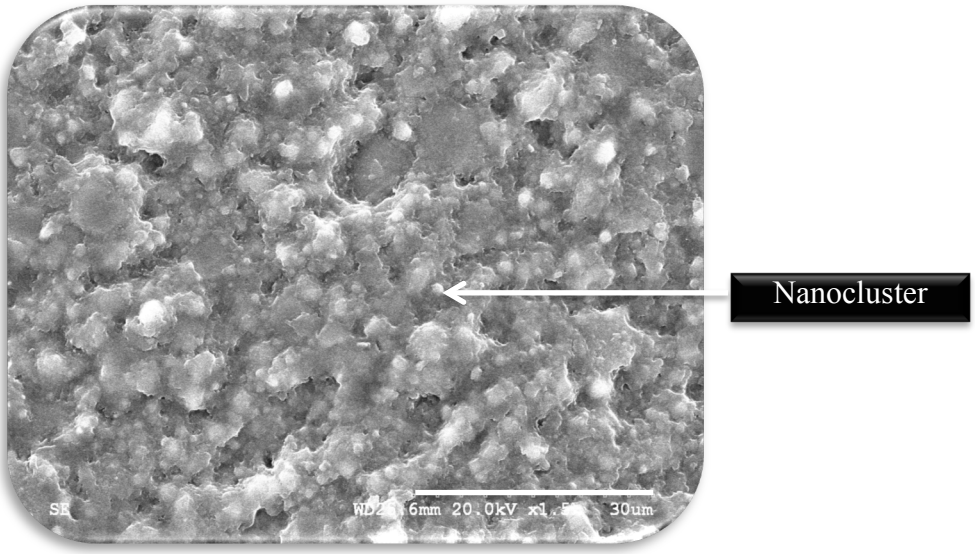

Figure 39: SEM image - non-aged Lava Ulimate (bar = 30 µm)

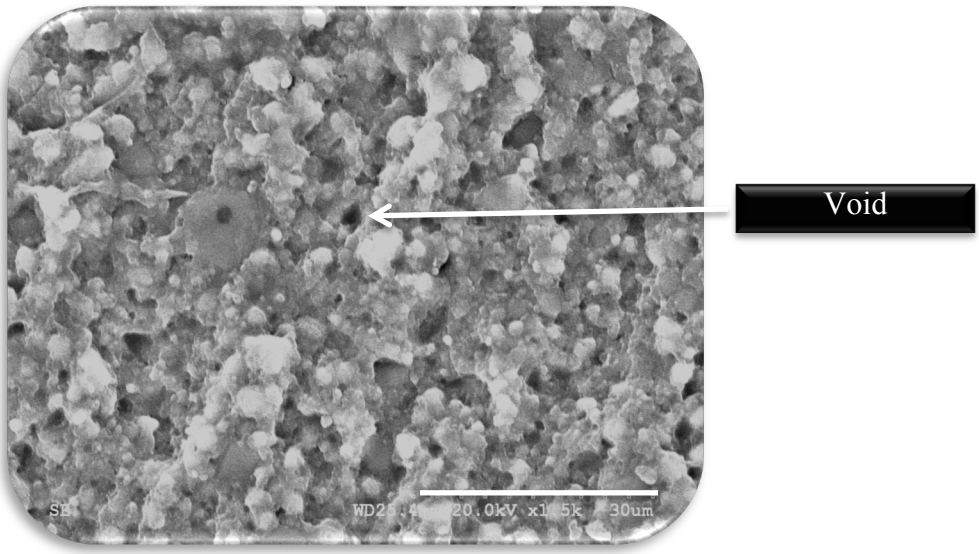

Figure 40: SEM image - aged Lava Ultimate (bar = 30 µm)

Readily visible are the ceramic nanoclusters surrounded by a resin matrix. Also evident are what appear to be some voids, which could lead to the propagation of a crack and premature failure of the material.

Figures 41 and 42, also at 1500x magnification, show the double interpenetrating network of Enamic. The porous ceramic latticework framework is evident and surrounded again by a resin matrix. However, the presence of voids within this network in this experimental Enamic sample seems to show that the interpenetration of these networks is not complete. The aged sample in figure 42 appears to not have the same "lines" that are visible in the non-aged sample in figure 41. This disappearance could be a visual representation of the material undergoing stress relaxation from being submerged in water and thus explains the decrease σ_f and E_f but the increase in K_{IC}

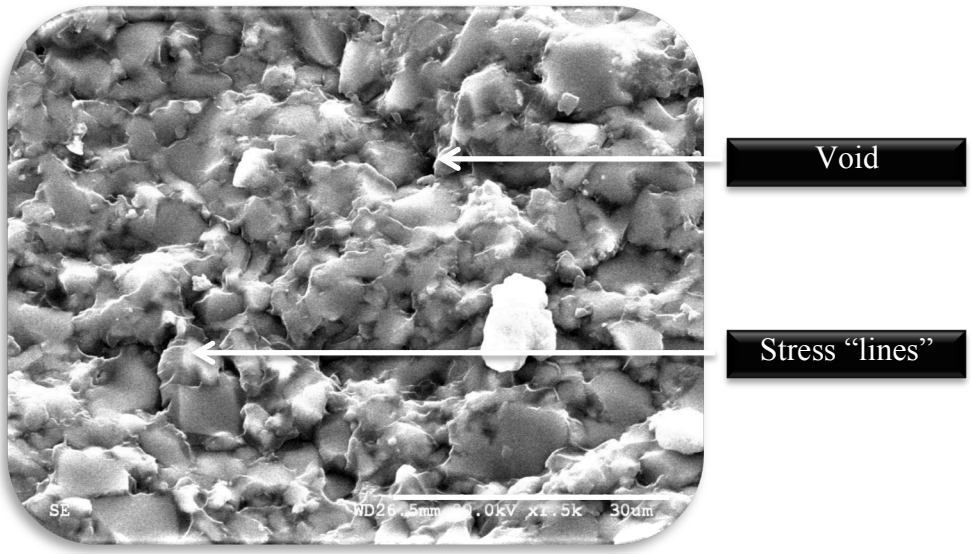

Figure 41: SEM image - non-aged experimental Enamic (bar = 30 µm)

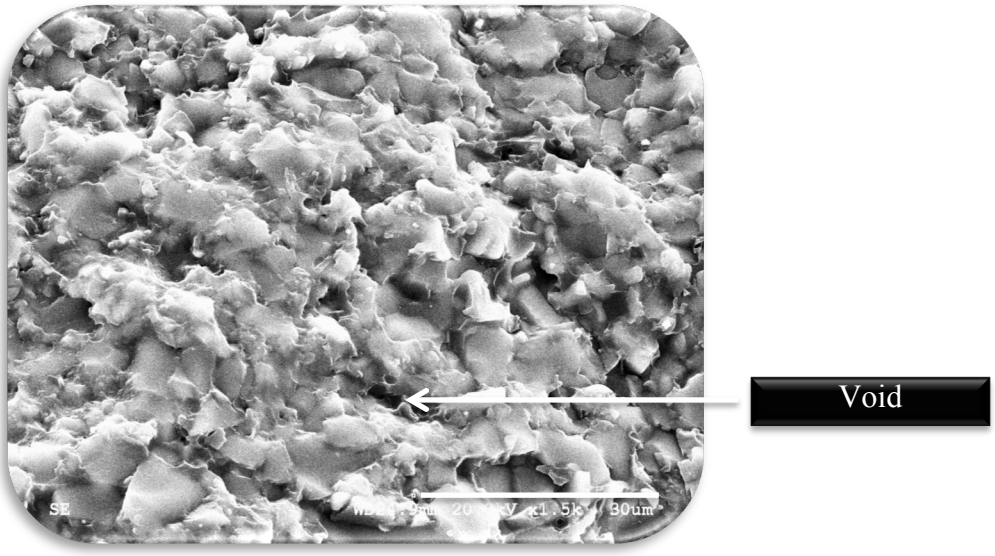

Figure 42: SEM image - aged experimental Enamic (bar = 30 µm)

Figure 43 is a 5000x magnification of a non-aged average experimental sample whereby both the aforementioned stress lines and the voids are more evident.

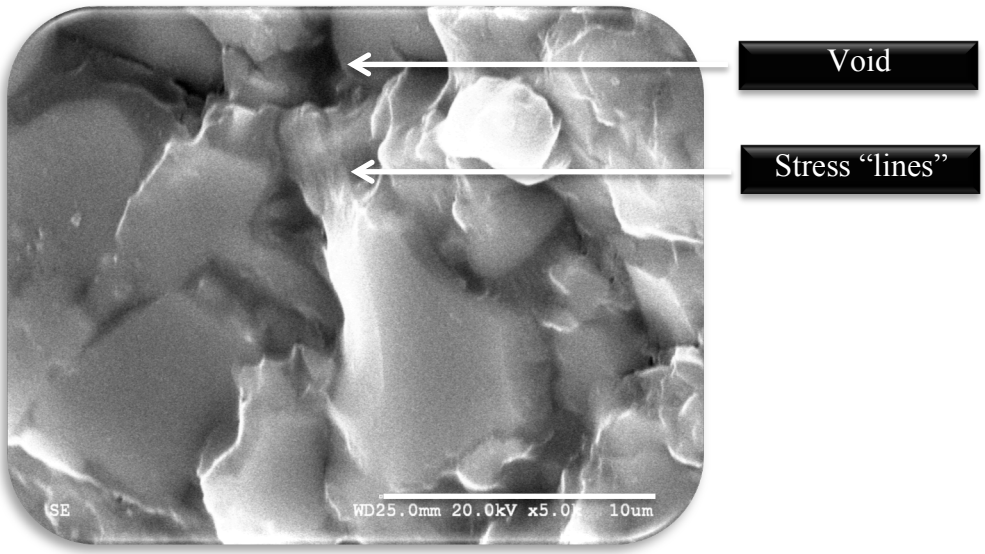

Figure 43: SEM image - experimental Enamic (bar = 10 µm)

No commercial Enamic samples were examined under SEM to see if there are general manufacturing deficiencies or whether they were isolated to those experimental samples previously identified as only having colour issues.

Chapter 5: Discussion

5.1 Validity of Test Methods

5.1.1 Three-point Bend Test

The three-point bend test is one of three standard tests used to determine σ_f and E_f of dental materials (with the others being biaxial flexure test and the four-point bend test). Although there are limitations with all these methods, the ISO standard test to determine the strength of polymer based restorative materials remains the three-point bend test. Accordingly, the utilization of this method to test these new materials allows for easy comparative analysis with other previously published results employing the same standard test methods. Some degree of caution is required nonetheless as non-standardized test sample sizes as outlined in the ISO standard have been used in other published data that will directly impact the analysis (Seghi and Sorensen, 1995; Cattell et al, 1997; Tinschert et al, 2000)

The presence of flaws, in particular edge flaws, accounts for some of the variation between different test samples of an identical material (Sadighpour et al, 2006). With a three-point bend test, the concentration of the tensile force is located on the opposing side of the specimen, directly under the applied force. Some authors contend that by using a four-point bend test, the specimen, now subjected to two applied forces, the applied stresses are exposed to a higher flaw containing area of the material and thus represents a more accurate result (Ritter, 1995; Quinn, 2003). As a result of these fundamental differences between the testing, three-point bending tests tend to produce higher apparent values than those of four-point bending tests (Rodrigues et al, 2008). However, given that a dental restorative material used intraorally is

subjected more similarly to the test conditions of a three-point bend test, it remains a more clinically relevant test.

Weibull size scaling analysis has been employed to determine the equivalent strengths between different test methods (Rodrigues et al, 2008). Typically, a 15 % higher strength is expected for the three-point bend test (Chithchumnong et al, 1989; Jin et al, 2004). This size scaling analysis is accomplished by using Equation 15.

$\sigma_3/\sigma_4 = (A_4/A_3)^{1/m}$	σ_3 = flexural strength measured in three-point bend test σ_4 = flexural strength measured in four-point bend test A_3 and A_4 = effective areas of the test configurations m = Weibull modulus

Equation 15: Weibull size scaling analysis between three and four-point bend tests

Kelly identifies a further limitation of any bar specimen bend test in that the structure of a crown is not represented well. Specifically, whereby the tensile stresses leading to fracture in a bar specimen are governed by the simple mathematic relationship using the geometry of the bar/test apparatus only, the clinical crown are uniformly supported on/bonded to a relatively elastic foundation that, when testing a bar specimen, ultimately leads to an oversimplification of this calculation (Kelly, 1999). Understanding that the nature of failure of clinical crowns (or dental materials intraorally) is complex and multifactorial, nonetheless, the absolute value of flexural strength and flexural modulus plays an integral role in failure and predicting failure. The sheer impossibility of testing every plausible shape/configuration for any material (i.e.

crown prep/crown shape/occlusion) renders the need for a simplistic, repeatable shape to which inferences and predictions on clinical performance can be made. The three-point bend test provides this possibility.

5.1.2 Notchless Triangular Prism Specimen Fracture Toughness Test

Ruse and colleagues introduced the NTP specimen K_{IC} test in 1996 but it has yet to garner universal acceptance as a standard ATSM test. Although Soderholm purported its benefits and accuracy in 2010, it is still not widely used (Soderholm, 2010). In using this test method and to be able to make relevant conclusions, it is important to reexamine the precision, accuracy and validity of the NTP specimen K_{IC} test (Ruse et al, 1996).

When compared to its widely accepted counterpart, the CNSR, initial confirmation of the validity of the NTP was accomplished via comparative finite element analysis whereby it was shown that the maximum stress was indeed concentrating at a point on the edge of the prism that is similar to the tip of the chevron notch (Ruse et al, 1996). Clinical testing of polymethyl methacrylate samples both yielded comparable results to those previously published and the observation that crack arrest occurred signifying stable and reliable crack growth (Ruse et al, 1996). Follow-up testing of subsequent materials (Durelon, Vitremer, Panavia and Z-100) using this method and comparing the results previously obtained in other CNSR studies confirmed the accuracy and validity of this test method (Ruse et al, 1996). The dimensionless stress intensity coefficient of 28 to be used in the K_{IC} calculations from the NTP test was extrapolated from compliance calibration work done by Bubsey et al (1982) done on different specimen geometries of CNSR samples. The simple application of this Y^*_{min} value into the NTP calculations without measuring each sample in this thesis could bring about some degree of error in the results (for all

samples), however, understanding these limitations, valid comparisons and conclusions could still be made.

When looking at published results for e.max CAD, it is seen in Table 13 that they are comparable to the results of this thesis thus further confirming the NTP as a valid K_{IC} test method.

	Thornton ID (unpublished)	Coldea et al (2014)	Wang et al (2013)	Charlton et al (2007)
K_{IC} Results (in MPa·$m^{½}$)	1.79 ± 0.29	2.27 ± 0.16	1.87 ± 0.2	2.13 ± 0.30

Table 13: Verification of the NTP specimen test method for e.max CAD

Although these results were obtained using indentation test methods and it has been shown that varying the test methods when testing K_{IC} will impact the results (Scherrer et al, 1998; Wang et al, 2007) and that indentation tests can be difficult to perform, when looking at the values and the standard deviations, these all fall within the same experimental range. Although our results had a larger standard deviation than typically seen in the NTP test method, this can be attributed to the difficulty in the crack initiation process with this harder material. Previous NTP testing has been done on materials whereby the crack initiation was relatively straightforward and easy due to the "softer" nature of the material itself. IPS e.max CAD is a harder ceramic and the difficulty initiating the pre-crack both caused in an increased variability of the results, it also likely produced some small degree of systematic error in the mean and caused the necessity of some samples to be excluded from the analysis.

5.2 Relevance of Test Methods

There are limitations of any laboratory test attempting to correlate to clinical results. The strength of resin composites is directly related to its component parts and increasing the volume of the reinforcing filler increases strength, however, it does not predict clinical success (Bayne, 2012). The same author recommends harvesting and testing previously placed intraoral restorations in teeth destined for extraction and then testing the material/restoration in the laboratory (Bayne, 2012). Although this may offer better insight into the effects that the harsh oral environment has on a dental biomaterial, the actual process is fraught with difficulties and the conclusions drawn are still limited due to the individual effects of saliva properties, age/time in use, operator skill and occlusion amongst other factors. In another review of the relevance of in-vitro testing of resin composite dental materials, the authors stated, "in-vitro tests are important for providing initial predictors for the success of a material but by no means replace clinical tests in patients" (Heintze and Zimmerli, 2010). With new materials such as these NCRCs, in-vitro testing is important, as these authors outline, to provide initial predictors of clinical success. In terms of the recommended tests to realize this prediction, σ_f, E_f and K_{IC}, along with wear, are the most clinically relevant laboratory tests (Ilie and Hickel, 2009; Ferracane, 2013).

5.3 Nano-ceramic Resin Composites vs. IPS e.max CAD

The only previous mechanical properties testing results for Enamic and Lava Ultimate are those found within the manufacturer's product information sheets. Although some implicit trust and validity must be applied to these results, they are neither held to the same standard of scrutiny as those found in the published literature nor are the requirements outlining the testing

methodology, to allow for reproducibility of results, as exacting. Additionally, implied "best interests of the company" are obvious sources of bias for manufacturer "published" data.

The only published study on comparing Lava Ultimate to Paradigm MZ-100 was a load-to-failure test. Although not a clinically relevant test, some relevance can still be garnered when comparing the results exclusively. The authors found that Lava Ultimate fractured at slightly higher loads at the three tested thicknesses (Johnson et al, 2014). This confirms that the manufacturing process between Paradigm MZ-100 and Lava Ultimate changed with only minimal improvements to the material. This same opinion was reached in a study of the wear characteristics of CAD/CAM restorative materials (including both Enamic and Lava Ultimate) whereby the authors concluded that the physical properties of resin composites "are not improved structurally by block fabrication for CAD/CAM" (Mormann et al, 2013).

When looking at the spectrum of resin composite – ceramic, it becomes clear that the new NCRCs do not behave similarly to the tested control, a lithium disilicate ceramic, IPS e.max CAD, and actually behave as resin composites.

5.3.1 Flexural Strength and Flexural Modulus

The mean σ_f of e.max CAD was 359.87 MPa whereby Lava Ultimate and Enamic were 155.31 and 145.64 MPa respectively. The mean E_f of e.max CAD was 69.29 GPa whereby Lava Ultimate and Enamic were 14.21 and 32.93 GPa respectively. This amounts to substantial differences whereby, when extrapolated clinically, IPS e.max may withstand larger loads until failure. Although this facet is clinically beneficial, the selection of a dental restorative material is dependent on more factors than simply the ability to withstand occlusal load. It has been stated that CAD/CAM crowns fabricated from Paradigm MZ-100 are a superior option in many

regards to all-ceramic crowns (Ramirez-Sebastia et al, 2013). Interestingly though, Vanoorbeek et al started a prospective study comparing the clinical success of composite CAD/CAM crowns to InCeram CAD/CAM crowns and had to stop the study after 120 delivered crowns "when it became apparent that the resin-based crowns were not functioning well and from then on, only ceramic crowns were delivered" (Vanoorbeek et al, 2010). Fasbinder had better success with CAD/CAM composite inlays where forty resin inlays performed as well as forty porcelain inlays with regards to margin adaptation, post-operative sensitivity and clinical complications (Fasbinder et al, 2005). Nonetheless, it has been postulated that the low E_f of resin composites contribute to premature loosening of composite crowns that is not seen in ceramics with higher E_f values (Mormann et al, 2013).

Nguyen et al found σ_f values for Paradigm MZ-100 of 131.85 ± 36.38 MPa and 138.2 ± 24.3 MPa (Nguyen et al, 2012; Nguyen et al, 2013). Vichi et al found σ_f values of 109.14 ± 10.10 MPa (Vichi et al, 2014). It appears, based on these data and the results obtained in this thesis that the modified structure of both Lava Ultimate and Enamic resulted in some improvements in σ_f. However, given the posted standard deviations, the results actually fall within the same experimental range rendering the improvements in σ_f questionable.

The internal data for Lava Ultimate claimed σ_f and E_f of 204 MPa and 12.8 GPa. The internal data for Enamic claimed a σ_f of between 150 and 160 MPa and E_f of 30 GPa. With the exception of σ_f for Lava Ultimate, the results obtained in this thesis were consistently close to all these posted values.

The obvious categorization of these materials as resin composites becomes strengthened when one examines the in-vitro results of direct resin composites. Ilie and Hickel tested 72 clinically available direct restorative resin composites and found that σ_f values ranged from 62.9

– 160.8 MPa and E_f ranged from 2.4 – 12.5 GPa (Ilie and Hickel, 2009). When specifically looking at Z-100, the "parent" direct restorative resin composite of Paradigm MZ-100, the results were 134.5 MPa and 11.3 GPa respectively (Ilie and Hickel, 2009), results which are similar to the results obtained in this thesis for the NCRC Lava Ultimate. With exception of E_f of Enamic, σ_f values for Enamic and Lava Ultimate are extremely comparable. The small differences between Lava Ultimate and Paradigm-MZ100 makes one question how much an improvement the latter material is over the former that it replaced on the consumer market. Figure 44 shows the σ_f, E_f and K_{IC} of commercially available resin composites to further illustrate how Enamic and Lava Ultimate compare.

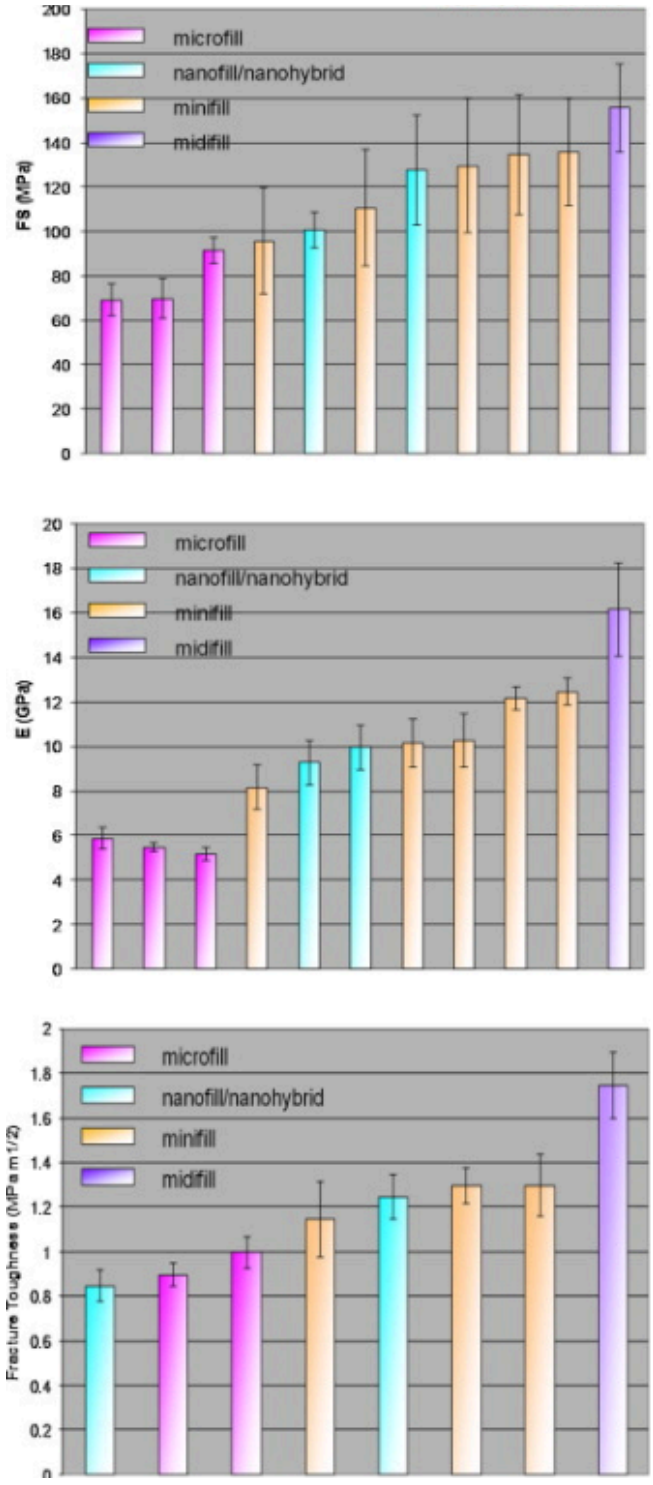

Figure 44: Flexural strength, flexural modulus and fracture toughness of resin composites (Ferracane, 2011)

5.3.2 Fracture Toughness

The mean K_{IC} of e.max CAD was 1.88 MPa•$m^{1/2}$ whereby Lava Ultimate and Enamic were 0.91 and 0.93 MPa•$m^{1/2}$ respectively. The internal data for Lava Ultimate claimed a K_{IC} of 2.02 MPa•$m^{1/2}$ (3M ESPE internal data, 2012). The K_{IC} of Enamic was not listed on the company's internal data. However, a recent study using novel polymer infiltrated ceramic networks made by Vita found, using the single v-notch edged beam, the K_{IC} of this material was 1.0 MPa•$m^{1/2}$ (Coldea et al, 2013). Utilizing the same test methods, Della Bonna et al additionally found a K_{IC} of 1.09 MPa•$m^{1/2}$ (Della Bonna et al, 2014). The results obtained in this thesis were consistently close to all these values for Enamic, further validating the test method. However, for Lava Ultimate, the results obtained in this thesis did not confirm the data put forth by the manufacturer.

5.3.3 Other Tests

Comparative studies on fatigue resistance of CAD/CAM ceramic crowns versus Paradigm MZ-100 resin composite crowns yielded interesting results. In two studies where samples were cycled and repeatedly loaded with varying forces, the resin composite crowns yielded 100 % survival whereby the ceramic crowns performed considerably worse, surviving from 0 – 30 % of the time, depending on the material (Magne et al, 2010; Kassem et al, 2012). One study comparing the wear on the material and the wear of the opposing enamel found that Paradigm MZ-100 exhibited a significantly higher wear than all the tested ceramic materials but also showed significantly smaller wear of antagonistic enamel (Kunzelmann et al, 2001). Although the aforementioned tests were not related to the mechanical properties investigated in the present study, it does allow one to correlate that if these same experiments were conducted

with Lava Ultimate and Enamic, being essentially resin composite CAD/CAM blocks, they would perform similarly to the published results of Paradigm MZ-100.

5.4 Enamic vs. Lava Ultimate

As stated previously, Lava Ultimate contains a blend of aggregated clusters of silica/zirconia nano-particles and individually bonded nano-particles, all embedded in a highly cross-linked polymer matrix while Enamic is a double penetrating polymer infiltrated ceramic network. Nonetheless, based on their composition of a ceramic framework/particles surrounded by/bonded to a polymer matrix, these materials are classified together as an NCRC, a proposed new class of dental CAD/CAM restorative material.

The σ_f of these materials, following a two-way ANOVA and post-hoc modified Scheffé analysis, showed that when grouping both the aged and non-aged samples of both Enamic groups (commercial and experimental) and Lava Ultimate, they belonged to one subset. However, when only considering the aged samples of all three groups and/or all the non-aged samples of all three groups, the commercial Enamic and Lava Ultimate belonged to two different subsets. The reason for this disparity is that the effect of aging on Lava Ultimate samples was more pronounced than on Enamic. Thus when averaging the non-aged and aged Lava Ultimate samples, the results were similar to the average of the more consistent Enamic aged and non-aged groups.

For E_f, there were significant differences between the two Enamic groups in addition to differences with Lava Ultimate. The three groups behaved as three different subsets when analyzed via two-way ANOVA and post-hoc Scheffé analysis. Although the manufacturing process can be attributed to the differences between the Enamic groups and Lava Ultimate, it was

nonetheless surprising that the commercial and the experimental Enamic groups behaved differently. The experimental Enamic groups had supposed only colour deficiencies that limited their commercial use, however based on these results, perhaps there were also more manufacturing deficiencies present as well. Nevertheless, the high value of E_f determined for Enamic sets it apart from any direct/indirect restorative resin composite currently on the market. This finding, coupled with a non-significant effect of ageing identified in this study, renders this material as having the most clinical potential and the most interesting for further in-vivo evaluation.

For K_{IC}, following a two-way ANOVA and modified post-hoc Scheffé analysis, the only significant difference that resulted in the materials being separated into different subsets occurred between the aged commercial Enamic samples and the aged Lava Ultimate samples. But considering sample size limitations as a result of testing problems and/or material acquisition problems, the number of the samples within each group limits the conclusions that can be drawn from these data.

5.4.1 Weibull Analysis

Weibull statistics are used to analyze brittle dental materials, as the test results for identical samples of the same material will vary as a result of the random flaw distribution. The Weibull modulus is the shape parameter of the Weibull distribution and represents the reliability of the results/material. Furthermore, when looking at a mechanical property like $\sigma_{f,}$, the characteristic strength value represents the point at which 63.2 % of the samples will fail.

For σ_f, the Weibull modulus for both aged and non-aged Lava Ultimate were significantly lower than those of both the experimental and commercial Enamic groups. At ranges between

17.50 and 26.99, the Weibull moduli of the Enamic groups were quite reliable and this can be attributed to the method of fabrication of the material. The polymer infiltrated ceramic double interpenetrating network in Enamic results in a more consistent fabrication with likely fewer flaws than the incorporation and dispersion of the nanoclusters in Lava Ultimate. The three-point bending test method then magnifies this circumstance and if a four-point bend test were used, although the values would be lower, it is predicted that the Weibull modulus of Lava Ultimate would increase.

Figure 45, from internal VITA research and development data, shows the Weibull modulus of CAD, Enamic and Lava Ultimate and shows strong similarities to the Weibull modulus for these same materials calculated in this study.

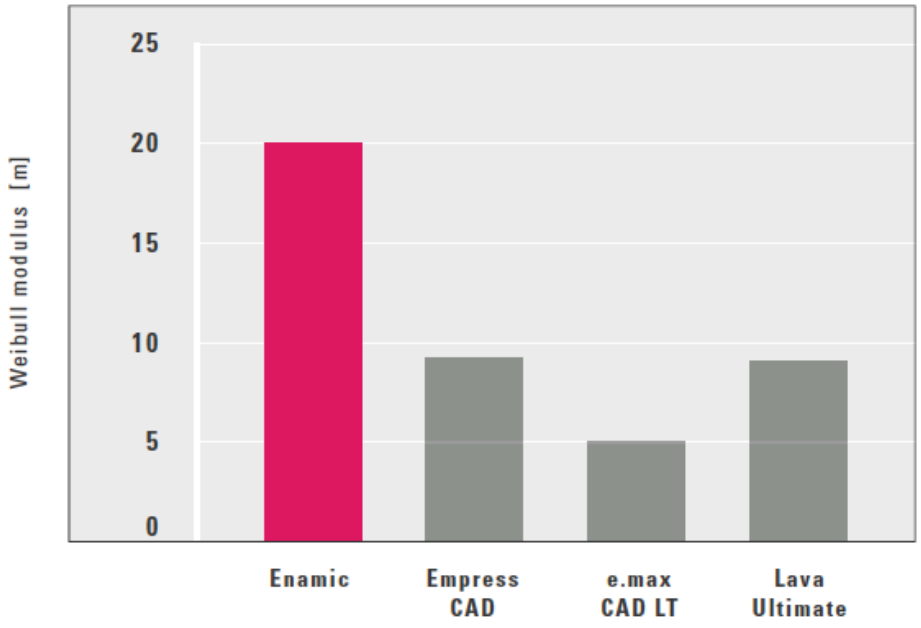

Figure 45: Weibull modulus of CAD/CAM restorative options (VITA internal data, 2013)

5.5 Polymer Infiltrated Ceramic Networks

Dental material scientists have long attempted to develop a material with similar mechanical behavior to that of natural human tooth structure and based on preliminary results in the literature, the polymer infiltrated ceramic network material (PICN), like Enamic, is possibly a successful step toward such a goal (He and Swain, 2011). In this He and Swain study, the authors looked at the elastic modulus, hardness and fracture toughness of experimental polymer infiltrated ceramic networks of various concentrations and had positive initial results whereby the material behaved mechanically like enamel and dentin (He and Swain, 2011). Della Bonna tested Enamic and found that the elastic modulus, density and fracture toughness were between resin based composites and porcelains (Della Bonna et al, 2014). These authors concluded that this material holds potential as having biomimetic properties that have not really been seen before and require further evaluation based on this potential (Della Bonna et al, 2014).

Other studies have tested the K_{IC} of PICNs and found higher results ranging from 1.46 to 1.84 $MPa \bullet m^{1/2}$ (He and Swain, 2011; Coldea et al, 2013; Nguyen et al, 2014). These authors tested novel PICNs of varying ceramic densities and/or polymerized under different pressures to obtain the effects that the varying compositions had on the tested mechanical properties. They found that, in general, higher initial density of the pre-infiltrated ceramic and higher infiltration pressure gave increased general mechanical properties (hardness, K_{IC} and σ_f) but concomitantly had decreased elastic modulus (He and Swain, 2013; Coldea et al, 2013; Nguyen et al, 2014). Ultimately, although the initial results are promising, ongoing in-vitro and in-vivo testing to determine the best balance of the ease of manufacturing, desired mechanical properties and clinical usability is paramount for the success of PICN restorative materials.

Figure 46, based on internal data, shows the elastic modulus of Enamic, Lava Ultimate and IPS e.max CAD and illustrates the fact that previously, no other resin-based restorative dental material has had elastic modulus in the range of dentin.

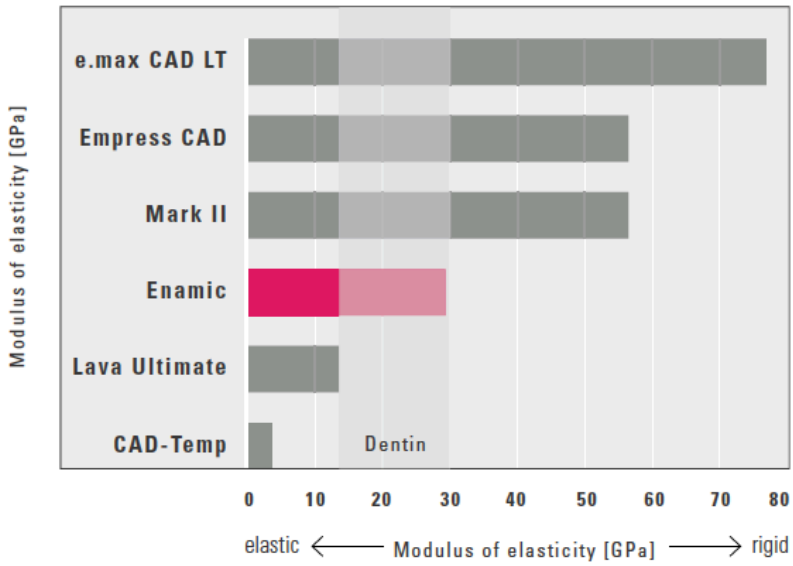

Figure 46: Elastic modulus of CAD/CAM restorative materials (VITA internal data, 2013)

The above data show E_f of 76 GPa for IPS e.max CAD, 30 GPa for Enamic and 15 GPa for Lava Ultimate. The results obtained in this thesis were 70 GPa for IPS e.max CAD, 32 GPa for Enamic and 14 GPa for Lava Ultimate and therefore show good overall consistency for all tested materials with this published data.

The great advantage of having a material with a modulus similar to dentin is that when bonded to dentin as a crown/onlay/inlay it will be better suited to share occlusal forces that could directly impact both the success and survivability of the restoration and remaining tooth structure. Based on this unique property, He and Swain stated that "more equivalent mechanical properties to enamel and dentin make the material a highly appropriate choice for implant

supported denture teeth as well as phantom teeth for simulation and dental education purposes" (He and Swain, 2011).

5.6 Effects of Aging

Intraoral degradation of resin composite restorations due to water sorption has been an issue in general for all resin composites (Bastioli et al, 1990). In their review on the mechanical properties of resin composites available on the consumer market, Ilie and Hickel commented that the recent trend in miniaturization of fillers has caused an enlargement of the surface area to volume ratio of the fillers resulting in increased water uptake and degradation of the filler/matrix interface (Ilie and Hickel, 2009). Many researchers have shown specifically that the σ_f of composite decreases with aging the test material in water for periods longer than twenty-four hours (Ferracane et al, 1998; Yoshida et al, 2004; Curtis et al, 2009; Stawarczyk et al, 2011).

Thirty day aging of our resin composite samples also yielded similar statistically significant results whereby after aging, Lava Ultimate σ_f values decreased by almost 27 % and Enamic decreased by 12 %. Additionally statistically significant, small concomitant reductions in E_f in both materials were also seen and this is similar to the only 5-10 % change seen in a previous study (Ferracane, 1998). In the only two published studies investigating the wear of a resin composite CAD/CAM test sample, one group of authors found a slight increase in σ_f of Paradigm MZ-100 while another found an almost 25 % reduction in the σ_f values of an experimental material (Peampring and Sanohkan, 2013; Yoshida et al, 2004). However, the variability of these results could be attributed to the different materials being tested with one being on an experimental resin composite that never made it to commercial production.

Our results showed a 10 % and 40 % increase in K_{IC} for Lava Ultimate and Enamic respectively following aging. This disagrees with the decrease in K_{IC} that Ferracane saw following aging in his study involving Z-100 and four other experimental composites (Ferracane et al, 1995). These differences can be attributed to the varying K_{IC} test methods and the confirmed impact that the different methodologies had on the variation of the results (Scherrer, 1998; Wang et al, 2007).

Soaking resin composite in water causes first a rapid elution of unbound filler particles followed by a slow diffusion of the water into the polymer matrix (Soderholm et al, 1984). This slow diffusion has resulted in the hypothesis that a plasticizing effect or softening of the polymer resin matrix via swelling of the network occurs and thus results in a reduction of the frictional forces between the polymer chains (Ferracane, 1998). This plasticization and reduction of the inherent manufacturing internal stresses explains the results of ageing obtained in this thesis, namely a reduction in σ_f, and E_f and an increase K_{IC} of the two tested NCRCs, Enamic and Lava Ultimate.

5.7 Future Recommendations

As a new class of dental material with limited in-vitro and in-vivo results, it is obvious that additional laboratory and clinical testing of these materials is required. Specifically, future tests on wear, biocompatibility, brittleness index during machining, fatigue resistance, colour stability are recommended. Additionally, validation studies testing similar mechanical properties as tested in this thesis are important before any distinct definitive restorative clinical recommendation can be made.

Prospective clinical trials assessing complications, microleakage, success and survivability are warranted. Previous studies with previous iterations of CAD/CAM resin restorative indirect restorations have had mixed results. Specifically, good esthetics, decreased wear of the opposing enamel and improved fatigue resistance have been the advantages previously reported (Kunzelmann et al, 2001; Behr et al, 2003; Kassem et al, 2012). Increased wear of the material itself, deterioration of surface finish, fractures and colour instability were the listed disadvantages (Behr et al, 2003; Attia et al, 2006; Venoorbeek et al, 2010). Utilizing these studies as benchmarks for new clinical trials with NCRCs will provide a definitive conclusion as to whether or not these materials are anything other than a resin composite and therefore should be used as anything but such. A previous strong correlation between K_{IC}, σ_f and E_f with bulk fracture in class IV restorations has been established (Tyas, 1990) in addition to an inverse correlation between K_{IC} and marginal breakdown of composite denture teeth after two years (Ferracane and Condon, 1999). If then, like in this study, future results confirm that the NCRCs are nothing more than resin composites, clinical predictions should be able to be made based on these mechanical properties.

Presently, in my opinion, the use of these materials should be limited to long-term provisional restorations (especially during treatment planning) and, as He and Swain mentioned, as simulation for dental education purposes (He and Swain, 2011). Potential future use as a definitive restoration on implants exists based on the unique mechanical properties, specifically in regards to the E_f of Enamic, as the stress absorbing nature of E_f may prevent the unwanted transmission of occlusal forces to the implant itself and minimize occlusion mediated implant complications.

Further research is needed to continue with the manufacturing process. Although the industrial standardized manufacturing process of CAD/CAM blocks minimizes flaws and yields better and more consistent mechanical properties (Tinschert et al, 2000; Mormann et al, 2013), refinement of this process to further improve the mechanical properties is recommended. Specifically, the positive results gleaned from utilizing high pressure and high temperature during resin composite polymerization vastly improved the mechanical properties in numerous tested materials (Nguyen et al, 2012, 2013, 2014). If the manufacturing process used in these studies can be applied to commercially available CAD/CAM materials and produce similar improvements while maintaining both the desirable properties and the clinical/milling usability of the current materials, then truly we may have a material that bridges the gap between resin composites and ceramics. This best of both worlds new material could be the elusive universal dental restorative material that researchers and clinicians crave. Based on the results of this study, Enamic and Lava Ultimate do not meet this claim.

Chapter 6: Conclusion

All the null hypotheses were rejected. Specifically:

1. σ_f, E_f, and K_{IC} were significantly lower for Lava Ultimate and Enamic when compared with IPS e.max CAD;
2. Aging in water did cause changes in the mechanical properties of Lava Ultimate and Enamic, whereby σ_f, E_f were lowered and K_{IC} was increased (for σ_f, E_f, aging had a more pronounced effect on samples of Lava Ultimate than it did on samples of Enamic, while the opposite was true for K_{IC});
3. There were differences between the NCRCs themselves, specifically in that σ_f and K_{IC} of Lava Ultimate was higher than that of Enamic, and E_f of Enamic was higher than that of Lava Ultimate.

Although E_f of Enamic surpasses that of dentin, the unpredictability of these samples, as evidenced by the low Weibull modulus, limit the positives that can be gleaned from this data. Ultimately, when compared to known values of conventional resins (both CAD/CAM and direct restorative material), the addition of ceramic nano-particles to the composite resin matrices of both Lava Ultimate and Enamic does not greatly improve the mechanical properties of these materials, nor does it cause the approach the of the test values of σ_f, E_f and K_{IC} seen in ceramics such as the control in this thesis, IPS e.max CAD.

Therefore, based on the limitations of this study and the results found therein, their consideration and clinical use should be limited to and similar to that of a conventional CAD/CAM composite resin.

References

3M ESPE internal data (2012). Lava Ultimate CAD/CAM restorative technical profile. 1-23 http://multimedia.3m.com/mws/mediawebserver?mwsId=SSSSSufSevTsZxtUoYtUmY_ZevUqevTSevTSevTSeSSSSSS--&fn=Lava_Ult_TPP.pdf (accessed 11 July 2014)

Anusavice KJ, Kakar K, Ferree N (2007). Which mechanical and physical testing methods are relevant for predicting the clinical performance of ceramic-based dental prostheses? *Clin Oral Implants Res* **18 Suppl 3**:218-231.

Anusavice KJ, Santos Jd, Shen C, Phillips RW (2003). Phillips' science of dental materials. **11th ed**. St. Louis, Mo, Saunders.

Asmussen E, Peutzfeldt A (1998). Influence of UEDMA BisGMA and TEGDMA on selected mechanical properties of experimental resin composites. *Dent Mater* **14**:51-56.

Atai M, Watts DC (2006). A new kinetic model for the photopolymerization shrinkage-strain of dental composites and resin-monomers. *Dent Mater* **22**:785-791.

Attia A, Abdelaziz KM, Freitag S, Kern M (2006). Fracture load of composite resin and feldspathic all-ceramic CAD/CAM crowns. *J Prosthet Dent* **95**:117-123.

Azzopardi N, Moharamzadeh K, Wood DJ, Martin N, van Noort R (2009). Effect of resin matrix composition on the translucency of experimental dental composite resins. *Dent Mater* **25**:1564-1568.

Barker LM (1977). A simplified method for measuring plane strain fracture toughness. *Eng Fract Mech* **9**:361-369.

Barker LM (1979). Theory for determining KIc from small, non-LEFM specimens, supported by experiments on aluminum. *Int J Fracture* **15**:515-536.

Bastioli C, Romano G, Migliaresi C (1990). Water sorption and mechanical properties of dental composites. *Biomaterials* **11**:219-223.

Bayne SC (2012). Correlation of clinical performance with in vitro tests of restorative dental materials that use polymer-based matrices. *Dent Mater* **28**:52-71.

Behr M, Rosentritt M, Handel G (2003). Fiber-reinforced composite crowns and FPDs: a clinical report. *Int J Prosthodont* **16**:239-243.

Bernardo M, Luis H, Martin MD, Leroux BG, Rue T, Leitao J, DeRouen TA (2007). Survival and reasons for failure of amalgam versus composite posterior restorations placed in a randomized clinical trial. *J Am Dent Assoc* **138**:775-783.

Beuer F, Schweiger J, Edelhoff D (2008). Digital dentistry: an overview of recent developments for CAD/CAM generated restorations. *Br Dent J* **204**:505-511.

Bogacki RE, Hunt RJ, del AM, Smith WR (2002). Survival analysis of posterior restorations using an insurance claims database. *Oper Dent* **27**:488-492.

Bowen RL (1963). Properties of a silica-reinforced polymer for dental restorations. *J Am Dent Assoc* **66**:57-64.

Bubsey RT, Munz D, Pierce WS, Shannon JL, Jr. (1982). Compliance calibration of the short rod chevron-notch specimen for fracture toughness testing of brittle materials. *Int J Fracture* **18**:125-133.

Buonocore MG (1955). A simple method of increasing the adhesion of acrylic filling material to enamel surfaces. *J Dent Res* **34**:849-853.

Burke FJ, Shortall AC, Combe EC, Aitchison TC (2002). Assessing restorative dental materials: I. Test methods and assessment of results. *Dent Update* **29**:188-194.

Callister WD, Rethwisch DG (2010). Materials science and engineering an introduction. **8th ed**. Hoboken, NJ, John Wiley.

Cattell MJ, Clarke RL, Lynch EJR (1997). The transverse strength, reliability and microstructural features of four dental ceramics -- Part I. *J Dent* **25**:399-407.

Ceriolo L, Di Tommaso A (1998). Fracture mechanics of brittle materials: a historical point of view. In *2nd Symposium in Civil Engineerg, Budapest*.

Charlton DG, Roberts HW, Tiba A (2007). Measurement of select physical and mechanical properties of 3 machinable ceramic materials. *Quintessence Int* **39(7)**:573-579.

Chen MH (2010). Update on dental nanocomposites. *J Dent Res* **89**:549-560.

Chung KH, Greener EH (1990). Correlation between degree of conversion, filler concentration and mechanical properties of posterior composite resins. *J Oral Rehabil* **17**:487-494.

Coldea A, Swain MV, Thiel N (2014). Hertzian contact response and damage tolerance of dental ceramics. *J Mech Behav Biomed Mater* **34**:124-133.

Coldea A, Swain MV, Thiel N (2013a). In-vitro strength degradation of dental ceramics and novel PICN material by sharp indentation. *J Mech Behavior Biomed Mater* **26**:34-42.

Coldea A, Swain MV, Thiel N (2013b). Mechanical properties of polymer-infiltrated-ceramic-network materials. *Dent Mater* **29**:419-426.

Cramer NB, Stansbury JW, Bowman CN (2011). Recent advances and developments in composite dental restorative materials. *J Dent Res* **90**:402-416.

Curtis AR, Palin WM, Fleming GJP, Shortall ACC, Marquis PM (2009). The mechanical properties of nanofilled resin-based composites: The impact of dry and wet cyclic pre-loading on bi-axial flexure strength. *Dent Mater* **25**:188-197.

Da Rosa Rodolpho PA, Cenci MS, Donassollo TA, Loguercio AD, Demarco FF (2006). A clinical evaluation of posterior composite restorations: 17-year findings. *J Dent* **34**:427-435.

Da Rosa Rodolpho PA, Donassollo TA, Cenci MS, Loguercio AD, Moraes RR, Bronkhorst EM, Opdam NJ, Demarco FF (2011). 22-Year clinical evaluation of the performance of two posterior composites with different filler characteristics. *Dent Mater* **27**:955-963.

Davidowitz G, Kotick PG (2011). The use of CAD/CAM in dentistry. *Dent Clin North Am* **55**:559-570.

de Groot R, van Elst HC, Peters MC (1988). Fracture mechanics parameters for failure prediction of composite resins. *J Dent Res* **67**:919-924.

Della Bona A, Corazza PH, Zhang Y (2014). Characterization of a polymer-infiltrated ceramic-network material. *Dent Mater* **30**:564-569.

Denissen H, Dozic A, van der Zel J, van WM (2000). Marginal fit and short-term clinical performance of porcelain-veneered CICERO, CEREC, and Procera onlays. *J Prosthet Dent* **84**:506-513.

Denry I, Holloway JA (2010). Ceramics for Dental Applications: A Review. *Materials* **3**:351-368.

Denry I (2013). How and when does fabrication damage adversely affect the clinical performance of ceramic restorations? *Dent Mater* **29**:85-96.

Denry I, Kelly JR (2008). State of the art of zirconia for dental applications. *Dent Mater* **24**:299-307.

Dentca company website. http://www.dentca.com (accessed 11 July 2014)

De Sousa Muianga MI (2009). Data capture stabilising device. *Doctoral dissertation, Faculty of Health Sciences, University of the Witwatersrand*. http://wiredspace.wits.ac.za/handle/10539/7954 (accessed 11 July 2014)

Dickens SH, Flaim GM, Takagi S (2003). Mechanical properties and biochemical activity of remineralizing resin-based Ca-PO4 cements. *Dent Mater* **19**:558-566.

Dowling NE (1993). Mechanical behavior of materials: engineering methods for deformation, fracture, and fatigue. Englewood Cliffs, Prentice-Hall, Inc.

Drummond JL (2008). Degradation, fatigue, and failure of resin dental composite materials. *J Dent Res* **87**:710-719.

Ender A, Mehl A (2011). Full arch scans: conventional versus digital impressions--an in-vitro study. *Int J Comput Dent* **14**:11-21.

Ernst CP, Brandenbusch M, Meyer G, Canbek K, Gottschalk F, Willershausen B (2006). Two-year clinical performance of a nanofiller vs a fine-particle hybrid resin composite. *Clin Oral Investig* **10**:119-125.

Fasbinder DJ (2010a). Materials for chairside CAD/CAM restorations. *Compend Contin Educ Dent* **31**:702-709.

Fasbinder DJ (2010b). The CEREC system: 25 years of chairside CAD/CAM dentistry. *J Am Dent Assoc* **141 Suppl 2**:3S-4S.

Fasbinder DJ (2006). Clinical performance of chairside CAD/CAM restorations. *J Am Dent Assoc* **137**:22S-231.

Feilzer AJ, de Gee AJ, Davidson CL (1987). Setting stress in composite resin in relation to configuration of the restoration. *J Dent Res* **66**:1636-1639.

Ferracane JL (1995). Current trends in dental composites. *Crit Rev Oral Biol Med* **6**:302-318.

Ferracane JL (2006a). Is the wear of dental composites still a clinical concern? Is there still a need for in vitro wear simulating devices? *Dent Mater* **22**:689-692.

Ferracane JL (2011). Resin composite--state of the art. *Dent Mater* **27**:29-38.

Ferracane JL, Antonio RC, Matsumoto H (1987). Variables affecting the fracture toughness of dental composites. *J Dent Res* **66**:1140-1145.

Ferracane JL, Condon JR (1999). In vitro evaluation of the marginal degradation of dental composites under simulated occlusal loading. *Dent Mater* **15**:262-267.

Ferracane JL, Hopkin JK, Condon JR (1995). Properties of heat-treated composites after aging in water. *Dent Mater* **11**:354-358.

Ferracane JL (2006b). Hygroscopic and hydrolytic effects in dental polymer networks. *Dent Mater* **22**:211-222.

Ferracane JL (2013). Resin-based composite performance: Are there some things we can't predict? *Dent Mater* **29**:51-58.

Fong H, Chun I, Reneker DH (1999). Beaded nanofibers formed during electrospinning. *Polymer* **40**:4585-4592.

Frankenberger R, Sindel J, Kramer N, Petschelt A (1999). Dentin bond strength and marginal adaptation: direct composite resins vs ceramic inlays. *Oper Dent* **24**:147-155.

Galhano GA, Pellizzer EP, Mazaro JV (2012). Optical impression systems for CAD-CAM restorations. *J Craniofac Surg* **23**:e575-e579.

Giordano R (2006). Materials for chairside CAD/CAM-produced restorations. *J Am Dent Assoc* **137**:14S-21.

Goodacre CJ, Garbacea A, Naylor WP, Daher T, Marchack CB, Lowry J (2012). CAD/CAM fabricated complete dentures: concepts and clinical methods of obtaining required morphological data. *J Prosthet Dent* **107**:34-46.

Guazzato M, Albakry M, Ringer SP, Swain MV (2004). Strength, fracture toughness and microstructure of a selection of all-ceramic materials. Part I. Pressable and alumina glass-infiltrated ceramics. *Dent Mater* **20**:441-448.

Handelman SL, Shey Z (1996). Michael Buonocore and the Eastman Dental Center: a historic perspective on sealants. *J Dent Res* **75**:529-534.

He LH, Swain M (2011). A novel polymer infiltrated ceramic dental material. *Dent Mater* **27**:527-534.

Heintze SD, Zimmerli B (2011). Relevance of in vitro tests of adhesive and composite dental materials, a review in 3 parts. Part 1: Approval requirements and standardized testing of composite materials according to ISO specifications. *Schweiz Monatsschr Zahnmed* **121**:804-816.

Hertzberg RW (1996). Deformation and fracture mechanics of engineering materials. **4**. New York, J. Wiley & Sons.

Hervas-Garcia A, Martinez-Lozano MA, Cabanes-Vila J, Barjau-Escribano A, Fos-Galve P (2006). Composite resins. A review of the materials and clinical indications. *Med Oral Patol Oral Cir Bucal* **11**:E215-E220.

Hickel R, Manhart J (2001). Longevity of restorations in posterior teeth and reasons for failure. *J Adhes Dent* **3**:45-64.

Hosoda H, Yamada T, Inokoshi S (1990). SEM and elemental analysis of composite resins. *J Prosthet Dent* **64**:669-676.

Ho GW, Matinlinna JP (2011). Insights on ceramics as dental materials. Part I: ceramic material types in dentistry. *Silicon*, *3*(3), 109-115. http://link.springer.com/article/10.1007%2Fs12633-011-9078-7#page-1 (accessed 11 July 2014)

Hosseinalipour M, Javadpour J, Rezaie H, Dadras T, Hayati AN (2010). Investigation of mechanical properties of experimental Bis-GMA/TEGDMA dental composite resins containing various mass fractions of silica nanoparticles. *J Prosthodont* **19**:112-117.

Ilie N, Hickel R (2009a). Investigations on mechanical behaviour of dental composites. *Clin Oral Investig* **13**:427-438.

Ilie N, Hickel R (2009b). Macro-, micro- and nano-mechanical investigations on silorane and methacrylate-based composites. *Dent Mater* **25**:810-819.

Ilie N, Hickel R (2011). Resin composite restorative materials. *Aust Dent J* **56 Suppl 1**:59-66.

Ilie N, Hickel R, Valceanu A, Huth K (2012). Fracture toughness of dental restorative materials. *Clin Oral Invest* **16**:489-498.

Indrani DJ, Cook WD, Televantos F, Tyas MJ, Harcourt JK (1995). Fracture toughness of water-aged resin composite restorative materials. *Dent Mater* **11**:201-207.

Isenberg BP, Essig ME, Leinfelder KF (1992). Three-year clinical evaluation of CAD/CAM restorations. *J Esthet Dent* **4**:173-176.

Ivoclar Vivadent internal data (2005). IPS e.max CAD scientific documentation. 1-16. http://roedentallab.com/downloads/e.maxCADData.pdf (accessed 11 July 2014)

Jin J, Takahashi H, Iwasaki N (2004). Effect of test method on flexural strength of recent dental ceramics. *Dent Mater J* **23**:490-496.

Johnson AC, Versluis A, Tantbirojn D, Ahuja S (2014). Fracture strength of CAD/CAM composite and composite-ceramic occlusal veneers. *J Prosthodont Res* **58**:107-114.

Jones RM (1999). Mechanics of composite materials. **2nd ed**. Philadelphia, PA, Taylor & Francis.

Kahler B, Kotousov A, Swain MV (2008). On the design of dental resin-based composites: A micromechanical approach. *Acta Biomater* **4**:165-172.

Kalra S, Singh A, Gupta M, Chadha V (2012). Ormocer: An aesthetic direct restorative material; An in vitro study comparing the marginal sealing ability of organically modified ceramics and a hybrid composite using an ormocer-based bonding agent and a conventional fifth-generation bonding agent. *Contemp Clin Dent* **3**:48-53.

Kanazawa M, Inokoshi M, Minakuchi S, Ohbayashi N (2011). Trial of a CAD/CAM system for fabricating complete dentures. *Dent Mater J* **30**:93-96.

Karthick K, Kailasam S, Geetha Priya PR, Shankar S (2011). Polymerization shrinkage of composites–a review. *J Indian Acad Dent Specialists*, ***2*(2)**: 32-36. http://jiads.net/Archives/2011/9.pdf (accessed 11 July 2014)

Kassem AS, Atta O, El-Mowafy O (2012). Fatigue Resistance and Microleakage of CAD/CAM Ceramic and Composite Molar Crowns. *J Prosthodont* **21**:28-32.

Kelly JR (1995). Perspectives on strength. *Dent Mater* **11**:103-110.

Kelly JR (1999). Clinically relevant approach to failure testing of all-ceramic restorations. *J Prosthet Dent* **81**:652-661.

Kelly JR, Benetti P (2011). Ceramic materials in dentistry: historical evolution and current practice. *Aust Dent J* **56 Suppl 1**:84-96.

Kelly JR, Benetti P, Rungruanganunt P, Bona AD (2012). The slippery slope - Critical perspectives on in vitro research methodologies. *Dent Mater* **28**:41-51.

Khng KYK (2013). An in vitro evaluation of the marginal integrity of CAD/CAM interim crowns compared to conventional interim resin crowns. *Masters dissertation, Faculty of Oral Sciences, University of Iowa.* http://ir.uiowa.edu/cgi/viewcontent.cgi?article=4904&context=etd (accessed 11 July 2014)

Klapdohr S, Moszner N (2005). New inorganic components for dental filling composites. *Monatshefte fur Chemie* **136**:21-45.

Kohler B, Rasmusson CG, Odman P (2000). A five-year clinical evaluation of Class II composite resin restorations. *J Dent* **28**:111-116.

Kramer N, Reinelt C, Richter G, Petschelt A, Frankenberger R (2009). Nanohybrid vs. fine hybrid composite in Class II cavities: clinical results and margin analysis after four years. *Dent Mater* **25**:750-759.

Kunzelmann KH, Jelen B, Mehl A, Hickel R (2001). Wear evaluation of MZ100 compared to ceramic CAD/CAM materials. *Int J Comput Dent* **4**:171-184.

Lang BR, Jaarda M, Wang RF (1992). Filler particle size and composite resin classification systems. *J Oral Rehabil* **19**:569-584.

Lewis G (1993). Predictors of clinical wear of restorative dental composite materials. *Biomed Mater Eng* **3**:167-174.

Lutz F, Phillips RW (1983). A classification and evaluation of composite resin systems. *J Prosthet Dent* **50**:480-488.

Magne P, Schlichting LH, Maia HP, Baratieri LN (2010). In vitro fatigue resistance of CAD/CAM composite resin and ceramic posterior occlusal veneers. *J Prosthet Dent* **104**:149-157.

Manhart J, Chen H, Hamm G, Hickel R (2004). Buonocore Memorial Lecture. Review of the clinical survival of direct and indirect restorations in posterior teeth of the permanent dentition. *Oper Dent* **29**:481-508.

Manhart J, Kunzelmann KH, Chen HY, Hickel R (2000). Mechanical properties of new composite restorative materials. *J Biomed Mater Res* **53**:353-361.

Martin N, Jedynakiewicz NM (1999). Clinical performance of CEREC ceramic inlays: a systematic review. *Dent Mater* **15**:54-61.

McCabe JF, Carrick TE (1986). A statistical approach to the mechanical testing of dental materials. *Dent Mater* **2**:139-142.

McLaren EA, Cao PT (2009). Ceramics in Dentistry—Part I: Classes of Materials. *Inside Dentistry* **5(9)**:94-103. https://www.dentalaegis.com/id/2009/10/many-different-types-of-ceramic-systems-have-been-introduced-in-recent-years-for-all-types-of-indirect-restorations (accessed 11 July 2014)

McLaren EA (2011). CAD/CAM dental technology: a perspective on its evolution and status. *Compend Contin Educ Dent* **32(4)**:74-75. http://www.dentalaegis.com/cced/2011/05/cad-cam-dental-technology-a-perspective-on-its-evolution-and-status (accessed 11 July 2014)

Mecholsky JJ (1995). Fracture mechanics principles. *Dent Mater* **11**:111-112.

Mehl A, Ender A, Mormann W, Attin T (2009). Accuracy testing of a new intraoral 3D camera. *Int J Comput Dent* **12**:11-28.

Mitra SB, Wu D, Holmes BN (2003). An application of nanotechnology in advanced dental materials. *J Am Dent Assoc* **134**:1382-1390.

Miyazaki T, Hotta Y, Kunii J, Kuriyama S, Tamaki Y (2009). A review of dental CAD/CAM: current status and future perspectives from 20 years of experience. *Dent Mater J* **28**:44-56.

Mohsen C (2011). Corrosion effect on the flexural strength & micro-hardness of ips e-max ceramics. *Open Journal of Stomatology* **1**:29-35 http://file.scirp.org/Html/5700.html (accessed 11 July 2014)

Mormann WH, Brandestini M, Lutz F, Barbakow F (1989). Chairside computer-aided direct ceramic inlays. *Quintessence Int* **20**:329-339.

Mormann WH, Stawarczyk B, Ender A, Sener B, Attin T, Mehl A (2013). Wear characteristics of current aesthetic dental restorative CAD/CAM materials: two-body wear, gloss retention, roughness and Martens hardness. *J Mech Behav Biomed Mater* **20**:113-125.

Mormann WH (2006). The evolution of the CEREC system. *J Am Dent Assoc* **137**:7S-13.

Mount GJ, Tyas MJ, Ferracane JL, Nicholson JW, Berg JH, Simonsen RJ, Ngo HC (2009). A revised classification for direct tooth-colored restorative materials. *Quintessence Int* **40**:691-697.

Nakamura T, Dei N, Kojima T, Wakabayashi K (2003). Marginal and internal fit of Cerec 3 CAD/CAM all-ceramic crowns. *Int J Prosthodont* **16**:244-248.

Nguyen JF, Migonney V, Ruse ND, Sadoun M (2012). Resin composite blocks via high-pressure high-temperature polymerization. *Dent Mater* **28**:592-534.

Nguyen JF, Ruse D, Phan AC, Sadoun MJ (2014). High-temperature-pressure Polymerized Resin-infiltrated Ceramic Networks. *J Dent Res* **93**:62-67.

Nguyen JF, Migonney V, Ruse ND, Sadoun M (2013). Properties of experimental urethane dimethacrylate-based dental resin composite blocks obtained via thermo-polymerization under high pressure. *Dent Mater* **29**:535-541.

Nohut S, Lu CS (2012). Fracture statistics of dental ceramics: Discrimination of strength distributions. *Ceram Int* **38**:4979-4990.

Oliveira GU, Mondelli RF, Charantola RM, Franco EB, Ishikiriama SK, Wang L (2012). Impact of filler size and distribution on roughness and wear of composite resin after simulated toothbrushing. *J Appl Oral Sci* **20**:510-516.

Opdam NJ, Bronkhorst EM, Loomans BA, Huysmans MC (2010). 12-year survival of composite vs. amalgam restorations. *J Dent Res* **89**:1063-1067.

Opdam NJ, Bronkhorst EM, Roeters JM, Loomans BA (2007). Longevity and reasons for failure of sandwich and total-etch posterior composite resin restorations. *J Adhes Dent* **9**:469-475.

Peampring C, Sanohkan S (2013). Effect of thermocycling on flexural strength and Weibull statistics of machinable glass–ceramic and composite resin. *J Indian Prosthodont Soc* 1-5. http://link.springer.com/article/10.1007%2Fs13191-013-0335-x (accessed 11 July 2014)

Peutzfeldt A (1997). Resin composites in dentistry: the monomer systems. *Eur J Oral Sci* **105**:97-116.

Peutzfeldt A, Asmussen E (1992). Modulus of resilience as predictor for clinical wear of restorative resins. *Dent Mater* **8(3)**:146-148.

Posselt A, Kerschbaum T (2003). Longevity of 2328 chairside Cerec inlays and onlays. *Int J Comput Dent* **6**:231-248.

Quinn GD (2003). Weibull strength scaling for standardized rectangular flexure specimens. *J Am Ceram Soc* **86**:508-510.

Ramirez-Sebastia A, Bortolotto T, Roig M, Krejci I (2013). Composite vs ceramic computer-aided design/computer-assisted manufacturing crowns in endodontically treated teeth: analysis of marginal adaptation. *Oper Dent* **38**:663-673.

Rekow D, Thompson VP (2005). Near-surface damage--a persistent problem in crowns obtained by computer-aided design and manufacturing. *Proc Inst Mech Eng H* **219**:233-243.

Ritter JE (1995). Critique of test methods for lifetime predictions. *Dent Mater* **11**:147-151.

Rodrigues SA, Jr., Ferracane JL, Della BA (2008). Flexural strength and Weibull analysis of a microhybrid and a nanofill composite evaluated by 3- and 4-point bending tests. *Dent Mater* **24**:426-431.

Ruddell DE, Maloney MM, Thompson JY (2002). Effect of novel filler particles on the mechanical and wear properties of dental composites. *Dent Mater* **18**:72-80.

Rueggeberg FA (2002). From vulcanite to vinyl, a history of resins in restorative dentistry. *J Prosthet Dent* **87**:364-379.

Ruse ND, Troczynski T, MacEntee MI, Feduik D (1996). Novel fracture toughness test using a notchless triangular prism (NTP) specimen. *J Biomed Mater Res* **31**:457-463.

Sadighpour L, Geramipanah F, Raeesi B (2006). In vitro mechanical tests for modern dental ceramics. *J Dent (Tehran)* **3(3)**:143-152 http://jdt.tums.ac.ir/index.php/jdt/article/viewFile/114/108 (accessed 11 July 2014)

Santos GC, Jr., Santos MJ, Jr., Rizkalla AS, Madani DA, el-Mowafy O (2013). Overview of CEREC CAD/CAM chairside system. *Gen Dent* **61**:36-40.

Scherrer SS, Denry IL, Wiskott HW (1998). Comparison of three fracture toughness testing techniques using a dental glass and a dental ceramic. *Dent Mater* **14**:246-255.

Schulein TM (2005). Significant events in the history of operative dentistry. *J Hist Dent* **53**:63-72.

Seghi RR, Sorensen JA (1995). Relative flexural strength of six new ceramic materials. *Int J Prosthodont* **8**:239-246.

Shannon JL, Bubsey RT, Pierce WS, Munz D (1982). Extended Range Stress Intensity Factor Expressions for Chevron-Notched Short Bar and Short Rod Fracture-Toughness Specimens. *Int J Fracture* **19**:R55-R58.

Shearer AC, Heymann HO, Wilson NH (1993). Two ceramic materials compared for the production of CEREC inlays. *J Dent* **21**:302-304.

Sheldon T, Treasure E (1999). Dental restoration: what type of filling. *Effective Health Care (NHS Centre for Reviews and Dissemination)* **5(2)**:1-12. http://www.york.ac.uk/inst/crd/EHC/ehc52.pdf (accessed 11 July 2014)

Sirona internal data (2008). CEREC – CAD/CAM for dentist: from vision to reality. 1-30 http://www.dentalunion.nl/nieuw/PDF/CEREC_MCXL.pdf (accessed 11 July 2014)

Sjogren G (1995). Marginal and internal fit of four different types of ceramic inlays after luting. An in vitro study. *Acta Odontol Scand* **53**:24-28.

Skrtic D, Antonucci JM, Eanes ED, Eichmiller FC, Schumacher GE (2000). Physicochemical evaluation of bioactive polymeric composites based on hybrid amorphous calcium phosphates. *J Biomed Mater Res* **53**:381-391.

Soderholm KJ, Zigan M, Ragan M, Fischlschweiger W, Bergman M (1984). Hydrolytic degradation of dental composites. *J Dent Res* **63**:1248-1254.

Soderholm KJ (2010). Review of the fracture toughness approach. *Dent Mater* **26**:e63-e77.

Soncini JA, Maserejian NN, Trachtenberg F, Tavares M, Hayes C (2007). The longevity of amalgam versus compomer/composite restorations in posterior primary and permanent teeth: Findings From the New England Children's Amalgam Trial. *J Am Dent Assoc* **138**:763-772.

Spitznagel FA, Horvath SD, Guess PC, Blatz MB (2014). Resin Bond to Indirect Composite and New Ceramic/Polymer Materials: A Review of the Literature. *J Esthet Restor Dent* .

Stanford JW (1987). Importance of international standardization in dental products. *J Dent Res* **66**:1782.

Stawarczyk B, Egli R, Roos M, Ozcan M, Hammerle CH (2011). The impact of in vitro aging on the mechanical and optical properties of indirect veneering composite resins. *J Prosthet Dent* **106**:386-398.

Tian M, Gao Y, Liu Y, Liao YL, Xu RW, Hedin NE, Fong H (2007). Bis-GMA/TEGDMA dental composites reinforced with electrospun nylon 6 nanocomposite nanofibers containing highly aligned fibrillar silicate single crystals. *Polymer* **48**:2720-2728.

Tilbrook DA, Clarke RL, Howle NE, Braden M (2000). Photocurable epoxy-polyol matrices for use in dental composites I. *Biomaterials* **21**:1743-1753.

Tinschert J, Zwez D, Marx R, Anusavice KJ (2000). Structural reliability of alumina-, feldspar-, leucite-, mica- and zirconia-based ceramics. *J Dent* **28**:529-535.

Truong VT, Tyas MJ (1988). Prediction of in vivo wear in posterior composite resins: a fracture mechanics approach. *Dent Mater* **4(6)**:318-327.

Trustrum K, Jayatilaka ADS (1979). Estimating the Weibull modulus for a brittle material. *J Mater Sci* **14**:1080-1084.

Tsitrou EA, Northeast SE, van Noort R (2007). Brittleness index of machinable dental materials and its relation to the marginal chipping factor. *J Dent* **35**:897-902.

Turssi CP, Ferracane JL, Ferracane LL (2006). Wear and fatigue behavior of nano-structured dental resin composites. *J Biomed Mater Res B Appl Biomater* **78B**:196-203.

Turssi CP, Ferracane JL, Vogel K (2005). Filler features and their effects on wear and degree of conversion of particulate dental resin composites. *Biomaterials* **26**:4932-4937.

Tyas MJ (1990). Correlation between fracture properties and clinical performance of composite resins in Class IV cavities. *Aust Dent J* **35**:46-49.

Tysowsky GW (2009). The science behind lithium disilicate: a metal-free alternative. *Dent Today* **28**:112-113.

Van Nieuwenhuysen J-P, D'Hoore W, Carvalho J, Qvist V (2003). Long-term evaluation of extensive restorations in permanent teeth. *J Dent* **31**:395-405.

Vanoorbeek S, Vandamme K, Lijnen I, Naert I (2010). Computer-aided designed/computer-assisted manufactured composite resin versus ceramic single-tooth restorations: a 3-year clinical study. *Int J Prosthodont* **23**:223-230.

Vichi A, Sedda M, Del SF, Louca C, Ferrari M (2013). Flexural resistance of Cerec CAD/CAM system ceramic blocks. Part 1: Chairside materials. *Am J Dent* **26**:255-259.

VITA internal data (2013). Vita Enamic: the concept. 1-16 http://vident.com/wp-content/uploads/2013/01/Enamic-Concept-Brochure-L-10024E.pdf-8_13.pdf (accessed 11 July 2014)

Wang H, Pallav P, Isgro G, Feilzer AJ (2007). Fracture toughness comparison of three test methods with four dental porcelains. *Dent Mater* **23**:905-910.

Wang RR, Lu CL, Wang G, Zhang DS (2013). Influence of cyclic loading on the fracture toughness and load bearing capacities of all-ceramic crowns. *Int J Oral Sci*. **6**:99-104

Weibull W (1951). A statistical distribution function of wide applicability. *J Appl Mech* **18**:293-297.

Weinmann W, Thalacker C, Guggenberger R (2005). Siloranes in dental composites. *Dent Mater* **21**:68-74.

Willems G, Lambrechts P, Braem M, Celis JP, Vanherle G (1992). A classification of dental composites according to their morphological and mechanical characteristics. *Dent Mater* **8**:310-319.

Williams RJ, Bibb R, Eggbeer D, Collis J (2006). Use of CAD/CAM technology to fabricate a removable partial denture framework. *J Prosthet Dent* **96**:96-99.

Wittneben JG, Wright RF, Weber HP, Gallucci GO (2009). A systematic review of the clinical performance of CAD/CAM single-tooth restorations. *Int J Prosthodont* **22**:466-471.

Xu HH, Weir MD, Sun L, Takagi S, Chow LC (2007). Effects of calcium phosphate nanoparticles on Ca-PO4 composite. *J Dent Res* **86**:378-383.

Yin L, Song XF, Song YL, Huang T, Li J (2006). An overview of in vitro abrasive finishing & CAD/CAM of bioceramics in restorative dentistry. *Int J Mach Tool Manu* **46**:1013-1026.

Yoshida K, Morimoto N, Tsuo Y, Atsuta M (2004). Flexural fatigue behavior of machinable and light-activated hybrid composites for esthetic restorations. *J Biomed Mater Res B Appl Biomater* **70B**:218-222.

Yoshimura HN, Gonzaga CC, Cesar PF, Miranda WG (2012). Relationship between elastic and mechanical properties of dental ceramics and their index of brittleness. *Ceram Int* **38**:4715-4722.

Zimmerli B, Strub M, Jeger F, Stadler O, Lussi A (2010). Composite materials: composition, properties and clinical applications. A literature review. *Schweiz Monatsschr Zahnmed* **120**:972-986.